PB85-216554

Batch Pretreatment Process Technology for Abatement of Emissions and Conservation of Energy in Glass Melting Furnaces: Phase IIA Process Design Manual

Corning Glass Works, NY

Prepared for

Environmental Protection Agency, Cincinnati, OH

Jun 85

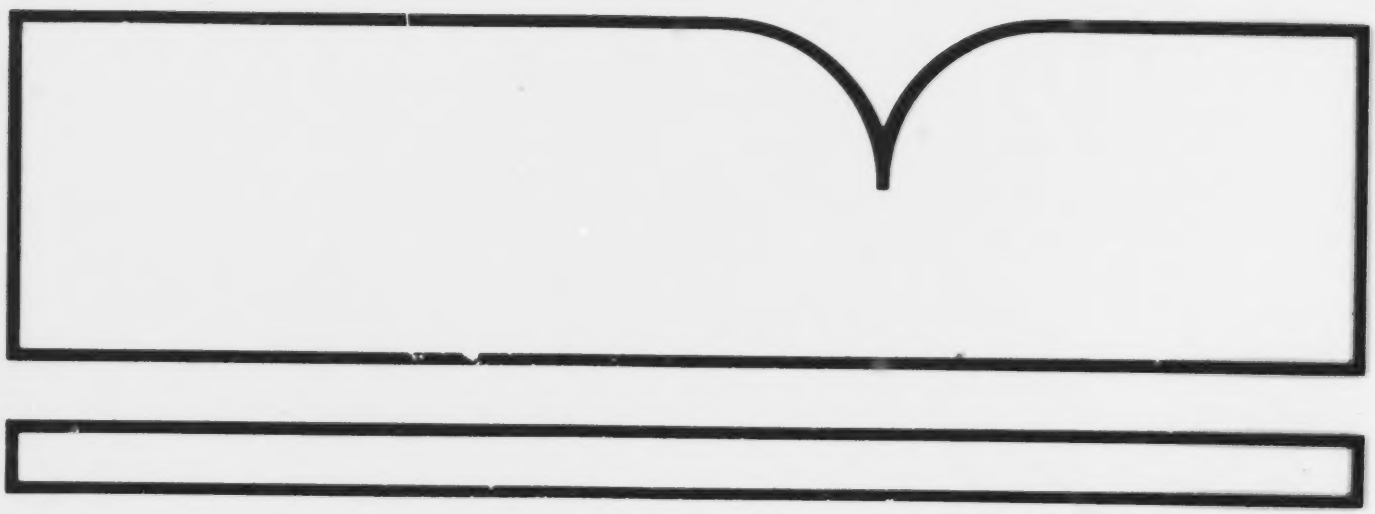

U.S. Department of Commerce
National Technical Information Service
NTIS

PB85-216554

EPA/600/2-85/073
June 1985

BATCH PRETREATMENT PROCESS TECHNOLOGY FOR ABATEMENT OF EMISSIONS AND CONSERVATION OF ENERGY IN GLASS MELTING FURNACES: PHASE IIA, PROCESS DESIGN MANUAL

by

R.E. Miller, R. Raghavan, and R.R. Thomas
Corning Glass Works
Corning, New York 14831

Contract No. 68-02-2640

Project Officer

Charles H. Darvin
Manufacturing and Service Industries Branch
Water Engineering Research Laboratory
Cincinnati, Ohio 45268

This study was conducted
in cooperation with the
U.S. Department of Energy

WATER ENGINEERING RESEARCH LABORATORY
OFFICE OF RESEARCH AND DEVELOPMENT
U.S. ENVIRONMENTAL PROTECTION AGENCY
CINCINNATI, OHIO 45268

REPRODUCED BY
NATIONAL TECHNICAL
INFORMATION SERVICE
U.S. DEPARTMENT OF COMMERCE
SPRINGFIELD, VA. 22161

TECHNICAL REPORT DATA
(Please read Instructions on the reverse before completing)

1. REPORT NO.	2.	3. RECIPIENT'S ACCESSION NO.
EPA/600/2-85/073		PB85-216554

4. TITLE AND SUBTITLE	5. REPORT DATE
Batch Pretreatment Process Technology for Abatement of Emissions and Conservation of Energy in Glass Melting Furnaces: Phase IIA, Process Design Manual	June 1985
	6. PERFORMING ORGANIZATION CODE
7. AUTHOR(S)	8. PERFORMING ORGANIZATION REPORT NO.
R.E. Miller, R. Raghaven, R.R. Thomas	
9. PERFORMING ORGANIZATION NAME AND ADDRESS	10. PROGRAM ELEMENT NO.
Corning Glass Works Corning, NY 14831	
	11. CONTRACT/GRANT NO.
	68-02-2640
12. SPONSORING AGENCY NAME AND ADDRESS	13. TYPE OF REPORT AND PERIOD COVERED
Water Engineering Research Laboratory--Cin., OH Office of Research and Development U.S. Environmental Protection Agency Cincinnati, Ohio 45268	Final
	14. SPONSORING AGENCY CODE
	EPA/600/14

15. SUPPLEMENTARY NOTES

Project Officer: Charles H. Darvin
Present Contact: Roger Wilmoth (513)684-7509

16. ABSTRACT

A jointly funded project was formally initiated in 1977 by the Department of Energy, Corning Glass Works, and the Environmental Protection Agency to develop and demonstrate the capability of glass batch preheating for controlling glass manufacturing pollution while reducing energy consumption. That project involved preliminary laboratory studies and developed a process design manual that defined only adequately energy conservation potential. The recommendation of that study indicated the need for additional research to define the pollution capture potential of the concept. This study carried out that recommendation by conducting pollution capture studies on an operating commercial regenerative furnace and packed bed using agglomerated batch pellets. Also included are results of the pollution capture potential of the bed when it is electrostatically enhanced. Conclusions were developed on particulate pollution capture potential of the packed bed with and without electrostatic enhancement, on SO_x capture efficiency, and on glass product quality.

The results of this study indicated that particulate capture capability ranges from 20 to 90 percent depending on gas stream parameters. The SO_x reduction efficiency was determined to range up to 95 percent. These results could provide the basis for a larger technology demonstration on a pilot glass furnace and will decrease energy costs and risks in developing a full-scale production system.

17. KEY WORDS AND DOCUMENT ANALYSIS

a. DESCRIPTORS	b. IDENTIFIERS/OPEN ENDED TERMS	c. COSATI Field/Group
Air Pollution Energy Conservation Glass Batch SO_x Control NO_x Control Particulate Control	Glass Manufacturing SO_x NO_x Particulate	

18. DISTRIBUTION STATEMENT	19. SECURITY CLASS (This Report)	21. NO. OF PAGES
Release to Public	Unclassified	122
	20. SECURITY CLASS (This page)	22. PRICE
	Unclassified	

EPA Form 2220-1 (Rev. 4-77) PREVIOUS EDITION IS OBSOLETE

DISCLAIMER

The information in this document has been funded wholly or in part by the United States Environmental Protection Agency under Contract No. 68-02-2640 to Corning Glass Works. It has been subject to the Agency's peer and administrative review, and it has been approved for publication as an EPA document. Mention of trade names or commercial products does not constitute endorsement or recommendation for use

FOREWORD

The U.S. Environmental Protection Agency is charged by Congress with protecting the Nation's land, air, and water systems. Under a mandate of national environmental laws, the agency strives to formulate and implement actions leading to a compatible balance between human activities and the ability of natural systems to support and nurture life. The Clean Water Act, the Safe Drinking Water Act, and the Toxics Substance Control Act are three of the major congressional laws that provide the framework for restoring and maintaining the integrity of our Nation's water, for preserving and enhancing the water we drink, and for protecting the environment from toxic substances. These laws direct the EPA to perform research to define our environmental problems measure the impacts, and search for solutions.

The Water Engineering Research Laboratory is that component of EPA's Research and Development program concerned with preventing, treating, and managing municipal and industrial wastewater discharges; establishing practices to control and remove contaminants from drinking water and to prevent its deterioration during storage and distribution; and assessing the nature and controllability of releases of toxic substances to the air, water, and land from manufacturing processes and substances to the uses. This publication is one of the products of that research and provides a vital communication link between the researcher and the user community.

This report contains results of pilot size studies for pelletizing and drying soda-lime glass batch materials, and for using the pellets as filter media in static packed beds to reduce actual furnace flue gas emissions. The purpose of this study was to confirm the pollution capture results of earlier laboratory tests. This work is a continuation of a project to develop a system for preheating glass batch agglomerates in a shaft preheater and filling hot agglomerated glass batch materials into a melting furnace using furnace waste heat to preheat and prereact the batch agglomerates. This report should be of value to manufacturers of glass and glass ceramic materials.

Francis T. Mayo, Director
Water Engineering Research Laboratory

ABSTRACT

In 1973 a study of glass manufacturing process concluded that batch preheating with furnace stack gases is a potential option for controlling glass manufacturing pollution while reducing energy consumption. The potential for faster glass melting with this process would compound the energy savings and return to the melting tank the materials normally lost from the stack as particulate pollution.

A jointly funded project was formally initiated in 1977 to develop and demonstrate the capability of glass batch preheating. The Department of Energy, Corning Glass Works, and the Environmental Protection Agency sponsored and funded this effort. That project involved preliminary laboratory studies and development of a process design manual. The project was completed in late 1981 and was documented in report number EPA -600/57-81-038, May 1981.

Since the laboratory experimentation defined adequately only the energy conservation potential of the concept, the report recommended that additional research be conducted to define the pollution capture potential of the concept. This project was designed to accomplish that recommendation and included conducting pollution capture studies on an operating commercial regenerative furnace and a packed bed using agglomerated glass batch pellets. Also included are results of the pollution capture potential of the bed when it was electrostatically enhanced. Conclusions were developed on the particulate pollution capture potential of the packed bed with and without electrical enhancement, on SO_x capture efficiency of the packed bed and on glass product quality. The results of this study indicated that the particulate capture capability ranges from 20 to 90 percent depending on the gas stream parameters. The SO_x reduction efficiency was determined to range up to 95 percent.

The study concluded that the packed bed can capture particulate and gaseous emissions from glass furnaces. Capture efficiency can be further enhanced with electrostatic charging of the bed. These results could provide the basis for a larger technology demonstration on a pilot glass furnace and will decrease costs and risks in developing a full-scale production system.

CONTENTS

Title Page
Disclaimer ii
Foreword iii
Abstract iv
Contents v
Figures vi
Tables viii
Abbreviations and Symbols x
SI Conversion Factors xiii
Acknowledgments xiv

1. Introduction 1
2. Conclusions 3
3. Recommendations 6
4. Laboratory Electrified Filter Bed Development 7

Historical Background 7
EFB Concept and Equipment 8
Test Setup and Test Procedures 12
EFB Collection Efficiency Results 15
Particle Size Distribution Sampling and Results 20

5. Pellet Development and Evaluation 25

Pelletizing and Drying System 25
Operation of the Pelletizing System 35
Pelletizing Development 37
Borosilicate Glass Batch 47

6. Packed Bed Testing 48

Background and Objectives 48
Test Setup and Equipment 49
Test Procedures 52
Sampling and Analytical Procedures 54
Testing Strategy and Experimental Conditions. 59
Results and Conclusions 62

7. Prototype Process 103

References 107

FIGURES

Number		Page
1	Electrified Filter Bed Schematic	9
2	Polarization of Bed Granules	10
3	Schematic Test Set-Up	13
4	Comparison of Sampling Methods Particle Concentration	14
5	Comparison of Theoretical and Actual Capture Efficiency for EFB	19
6	Comparison of Sampling Methods Particle Size Distribution	21
7	Pelletizing System Schematic	26
8	Pelletizer Pan - Plan View	30
9	Schematic View of Batch and Pellets in the Pelletizer Pan	31
10	Pellet Distribution Chute from Pelletizer to Belt Dryer	34
11	Pelletizing Rate Correlation	40
12	Pan Angle	41
13	Pellet Size as a Function of Pan Angle	42
14	Pellet Strength as Function of Size	44
15	Schematic Test Setup	50
16	Packed Bed Dimensions	51
17	Electrified Filter Bed Dimensions	53
18	Particulate Sampling Train	55
19	Method 5 Sampling Locations	56

FIGURES (Continued)

Number		Page
20	Packed Bed Captur Efficiency; Effect of Gas Velocity and Bed Depths	65
21	Packed Bed Inlet Particle Size Distribution - Aerodynamic Diameter	77
22	Packed Bed Inlet Particle Size Distribution - Physical Diameter	78
23	Comparison of Particle Size Distribution Between Inlet and Outlet of Packed Bed	79
24	Comparison of Particle Size Distribution Between Inlet and Outlet of Packed Bed	80
25	Comparison of Particle Size Distribution Between Inlet and Outlet of Packed Bed	81
26	Comparison of Particle Size Distribution Between Inlet and Outlet of Packed Bed	82
27	Particle Size Distribution from Outlet of Packed Bed and Outlet of EFB	83
28	Effect of Bed Voltage on EFB Capture Efficiency	89
29	Effect of Gas Velocity on EFB Capture Efficiency	90
30	Conductivity of Soda-Lime Pellets at Various Temperatures	91
31	Linear Regression of Packed Bed Efficiency Data	102
32	Schematic of Prototype Process	104

TABLES

Number		Page
1	Comparison of Particulate Control Devices	11
2	Operating Conditions for Capture Efficiency Tests	16
3	Capture Efficiency Data	17
4	Operating Conditions for Particle Size Distribution Tests	22
5	Particle Size Distribution by Sample Method WP-50	23
6	Particle Size Distribution by Sample Method 5	24
7	Equipment	28
8	Soda-Lime Pelletizing Batch	36
9	Pelletizing Conditions for Stable Operation of 1.37 m dia. x 0.355 m Deep Pan	43
10	Chemical Analyses of Pellets and Fines	46
11	Borosilicate Glass Batch	47
12	X-Ray Spectrometer Accuracy	58
13	Range of Experimental Variables	59
14	Experimental Conditions - Packed Bed	60
15	Experimental Conditions - EFB	61
16	Summary of Particulate Capture Efficiencies in the Packed Bed	63
17	Packed Bed "Blow-Off" and Capture Efficiency	64
18	Effect of Temperature on Efficiency (Packed Bed)	66
19	Packed Bed Efficiency Enhancement with Pre-charging of Particulates	67

TABLES (Continued)

Number		Page
20	Summary of Method 5 Catch and Impinger Catch	68
21	SO_2 and SO_3 Capture Efficiencies in Packed Bed	69
22	Aerodynamic and Physical Diameter Calculations	70
23	Inlet Particle Size Distribution - Impactor Data	71
24	Inlet Particle Size Distribution - Impactor Data	72
25	Outlet Particle Size Distribution - Impactor Data	73
26	Outlet Particle Size Distribution - Impactor Data	74
27	Particle Size Distribution Sampling Data	75
28	Chemical Analyses of Pellet Melts - Packed Bed	84
29	SO_3 and Seed Counts in Pellet Melts - Packed Bed	85
30	Qualitative Spectrographic Analyses of Particulates Packed Bed Inlet	85
31	Chrome and Color in Pellet Melts - Packed Bed	86
32	Summary of Particulate Collection Efficiencies in the EFB	87
33	Summary of Method 5 Catch and Impinger Catch	92
34	SO_2 and SO_3 Capture Efficiencies in EFB	94
35	Chemical Analyses, Color and Seed Counts in Pellet Melts - EFB	95
36	NO_x Measurements - Packed Bed and EFB	96
37	Stack Emissions Tests	96
38	Literature on Filtration	97

LIST OF ABBREVIATIONS AND SYMBOLS

ABBREVIATIONS

D_A	aerodynamic diameter
L	bed depth
Btu	British thermal unit
η	capture efficiency
cm	centimeter
CGW	Corning Glass Works
m^3/min	cubic meter per minute
m^3/hr	cubic meter per hour
°C	degree Celsius
°C/hr	degree Celsius per hour
°F	degree Farenheit
DOE	Department of Energy
d	diameter
dsm^3	dry standard cubic meters
dsm	dry standard meter
EFB	electrified filter bed
EPA	Environmental Protection Agency
ft/sec	feet per second
FMC	FMC Corporation
ft	foot
Tg	gas temp
Ug	gas velocity
gm	gram
g/cc	gram per cubic centimeter
g/min	grams per minute
J	joules
J/hr	joules per hour
J/kg	joules per kilogram

kg	kilogram
kg/m^3	kilogram per cubic meter
kg/day	kilogram per day
kg/hr	kilogram per hour
kg/min	kilogram per minute
kg/sec	kilogram per second
kg/yr	kilogram per year
kPa	kilopascal
KV	kilovolts
μm	micrometers
m	meter
mA	milliamperes
mg	milligrams
m/sec	meter per second
N	newton
PSD	particle size distribution
PPM	parts per million
Pa	pascals
P	pellet diameter
PGS	Pittsburgh Glass Sand
PRC	Process Research Center
rpm	revolution per minute
m^2	square meter

SYMBOLS

Al	aluminum
Al_2O_3	aluminum oxide
A	bed cross-sectional area
L	bed depth
B_2O_3	boron oxide
Ca	calcium
CaO	calcium oxide
CO_2	carbon dioxide
Cr	chromium

Cr_2O_3	chromium oxide
RHO	density of particulates
Fe_2O_3	ferric oxide
ρ	gas density
C_{pg}	gas specific heat
TC	gas temperature
H_2O_2	hydrogen peroxide
Fe	iron
Mg	magnesium
MgO	magnesium oxide
w	mass % finer than
mg	milligrams
mg/sm^3	milligrams per standard cubic meter
Ln	natural logarithm
NO_2	nitrogen oxide
NO_x	nitrous oxides
Nu	Nusselt number
O_2	oxygen
D	pellet diameter
%	percent
D_p	physical diameter
lbs	pounds
Pr	Prandtl number
Re	Reynolds number
Si	silicon
S_iO_2	silicon dioxide
Na_2O	sodium oxide
Na_2SO_4	sodium sulfate
sm^3	standard cubic meters
SO_4	sulfate
SO_2	sulfur dioxide
SO_3	sulfur trioxide
Sn	tin

SI CONVERSION FACTORS

To Convert From	To	Multiply By
Atmosphere (Atm)	Pascals (Pa)	1.013×10^{5}
Btu	Joule (J)	1.055×10^{3}
Erg	Joule (J)	10^{-7}
Foot (ft)	Meter (m)	3.048×10^{-1}
Foot^3 (ft^3)	Meter^3 (m^3)	2.832×10^{-2}
Inch (in)	Centimeter (cm)	2.540
Inch^2 (in^2)	Centimeter^2 (cm^2)	6.452
Kilogram force (kg)	Newtons (N)	9.807
Pound force (lb)	Newtons (N)	4.448
Pound mass (lb)	Kilogram mass (kg)	4.536×10^{-1}
Pounds per sq. in.	Pascals (Pa)	6.895×10^{3}
Standard Cubic Feet per hour	Cubic meters per hour	2.832×10^{-2}
Ton mass (short)	Kilograms mass (kg)	9.072×10^{2}

ACKNOWLEDGMENTS

This research study included efforts from many individuals at Corning Glass Works. Major contributors were Messrs. George G. Boettner, John H. Bruns, Kenneth R. Jones, Curtis V. Josey, Verne E. Kreger, James J. Long, Lee C. Nelson, Ashok Nayak, Paul A. Mortzheim, David L. Smith, William L. Schwab, Lloyd G. Young, and Benjamin W. Wilson.

The EFB Corporation was subcontracted to supply an electrified filter bed. The major contributor was Dr. Jeffrey C. Alexander.

The Midland-Ross Corporation was subcontracted to supply the drying system for pelletizing. Messrs. Morris J. Hakim, Thomas L. Moran, Frank G. Rinker, and Thomas J. Schultz were major contributors.

The Thatcher Glass Manufacturing Company was subcontracted to install equipment in the Elmira, New York plant, to supply flint glass container furnace flue gases for pollution capture tests and to evaluate crucible melts of pellets used in the packed beds for effects of pollutant capture on melting. Messrs. Del Harding, Charles Roberts and Wayne A. Wallding were major contributors.

SECTION 1

INTRODUCTION

The Environmental Protection Agency contracted with Corning Glass Works for the development of a glass batch pretreatment process which would reduce pollution emissions and energy usage in the melting furnace. The project was funded by the Environmental Protection Agency, the Department of Energy, and the Corning Glass Works.

The program consisted of two phases of work. Phase I was completed in 1981 and documented in report number EPA-600/57-81-038, May 1981.[1] That manual supplied information to design a pilot plant system, and based on this design, estimated the energy, pollution, and economic benefits of the system. The project team believed that the simulated particulates used in Phase I were not indicative of normal glass furnace emissions. Thus it was recommended in Phase I to further study the particulate capture efficiency of soda-lime glass batch pellets in a packed bed using actual regenerative furnace flue gas emissions. The preheating and melting demonstration was to follow that study.

Phase II was divided into Phase IIA and Phase IIB. Phase IIA consisted of forming dry soda-lime glass batch pellets and using these pellets in a packed bed to determine the capture efficiency of the bed for furnace flue gas particulates, SO_x, and NO_x. New source performance standards proposed in 1979 by the EPA[2] placed added emphasis on improving the efficiency of a pellet bed preheater for particulate capture. Consequently, tests with an electrified filter bed (EFB) using soda-lime glass batch pellets as filter media were also conducted in Phase IIA. Phase IIA work has been completed with the results reported in this document. Phase IIB will consist of a pilot plant preheating and melting demonstration to show the melting, energy, and pollution capture benefits with moving beds and the continuous melting system for preheating soda-lime glass batch pellets.

Phase I laboratory testing demonstrated;

- Soda-lime glass batch pellets could be formed and preheated to 600°C with strengths necessary for handling and feeding.
- Fifty percent of the possible prereaction had occurred at 800°C.
- Soda-lime glass batch pellets in a static laboratory packed bed captured 75%-85% of the SO_2 in a gas stream flowing at 0.43 m/sec through the bed[2].
- Thirty-two percent of 10 micron average diameter sodium sulfate particulate was captured in a static packed bed of pellets.

- Crucible melting of preheated pellets compared to normal loose batch materials showed that melting time could be reduced approximately by one half, or melting temperatures could be reduced approximately by 50°C.

- The combined effect of a 50°C temperature reduction and an associated 15% decrease in fuel should result in an overall 65% reduction in NO_x emissions.

It was believed by the project team that the simulated particulates used in Phase I were not indicative of normal glass furnace emissions. Thus, it was recommended in Phase I to further study the particulate capture efficiency of soda-lime glass batch pellets in a packed bed using actual regenerative furnace flue gas emissions. The preheating and melting demonstration was to follow that study.

SECTION 2

CONCLUSIONS

PELLETIZING

The following conclusions are based on work with the 1.37 m diameter pan pelletizer:

- Pan angle has a significant effect in determining pellet size.
- The optimum pelletizing rate in a 1.37 m dia. pan is 635 kg per hour with a depth to dia. ratio of 0.26. This rate is 80% of the maximum.
- The pelletizer can be operated without operator attention provided proper control of batch and water feed rates.
- Pelletizer wear, adding approximately 40 ppm iron into the batch does not cause color problems when the pellets are melted.
- A formula for scale-up of pelletizer rate is suggested.

DRYING

- 70%-80% of the water in pellets should be removed from pellets in the belt dryer before they enter a shaft dryer or preheater.
- Wet soda-lime pellets will stick together when subjected to heat in excess of 225°C in a belt dryer.
- Fines are generated by abrasion of pellets in a moving bed and are carried out in the exhaust gas.
- Fines generated in the shaft dryer, which were not carried out in the exhaust gas, amounted to 3%-5% of the weight of the pellets.

PELLET HANDLING

- Approximately 1.3 cm is the optimum diameter pellet for durability in handling.

- Crushing strength of pellets decreases as the size of pellet increases.

- In a production system wet pellets should be screened to remove occasional batch chunks generated in the pelletizer.

- Wet pellet strength exceeded what was necessary for handling between the pelletizer and belt dryer.

- The surface of dried pellets had 30%-42% higher SO_4 than the inner core.

- There was no carbonate surface enrichment on the pellets.

- Fines resulting from storage, trucking 15 miles, and emptying bins of pellets amounted to approximately 1%.

POLLUTION CAPTURE

- Inertial capture is the dominant mechanism for soda-lime furnace particulates in the packed bed.

- An increase in the packed bed depth increases particulate capture. An increase in gas velocity increases particulate capture. A decrease in gas temperature has little effect on packed bed capture.

- The soda-lime particulates are mostly submicron in size.

- The semi-empirical model developed from this testing may be used to predict capture efficiencies in the production units.

- There is a significant improvement in collection efficiency of the packed bed if the particulates are precharged.

- SO_2 collection can be greater than 95% in the packed bed. There is almost no pickup of NO_x in the packed bed.

- The static bed of soda-lime pellets in the pilot size EFB collected greater than 98% of furnace particulates.

- An increase in bed voltage in EFB increases particulate capture.

- SO_2 capture in the pellet bed (EFB) was about 75%.

ELECTRIFIED FILTER BED

- The concept of pollution capture from soda-lime furnace emissions using electrified filter bed technology was shown to be feasible.
- With the use of the gravel or soda-lime pellets as collection media, the particulate collection is greater than 95%.
- Due to the pellets' electrical properties, higher power consumption is required for obtaining the same collection efficiency as in the gravel bed.

SECTION 3

RECOMMENDATIONS

Work completed to date has resulted in the identification of additional background requirements to the basic program. However, the results do indicate that the pellet preheating concept using furnace waste gases is both feasible and important and that the final demonstration should be undertaken. Therefore, the following program actions are recommended:

1. The pilot plant Phase IIB preheating and melting demonstration should be pursued to confirm the pollution, energy, and cost savings benefits projected in Phases I and IIA and to identify the operating characteristics of a production system. Furthermore, this demonstration will decrease costs and risks in developing a full-scale production application.

2. An electrified filter bed should be used in conjunction with a pellet bed shaft preheater for the pilot plant demonstration to remove particulates not captured in the pellet bed, and to remove fines generated by the moving bed of pellets.

SECTION 4

ELECTRIFIED FILTER BED DEVELOPMENT

The electrified filter bed (EFB) is a pollution capture device whose design is based on the principle of charging particulates in the gas stream and capturing the charged particulates in a static or moving granular bed carrying electrostatic forces of attraction.

The objective of this test program was to evaluate the potential of the EFB concept in meeting the pollution standards for soda-lime glass furnace emissions. Initial testing utilized an EFB bench scale unit with the exhaust gases from a CORNING regenerative soda-lime glass melting furnace, located at Wellsboro, Pennsylvania. The bed was a static bed with gravel and soda-lime glass batch pellets used as collection media.

This section summarizes the results and conclusions of the EFB bench scale testing on the exhaust gases from the soda-lime glass furnace.

HISTORICAL BACKGROUND

In 1978, results of Phase I (Process Design Manual[1]) were presented to representatives of the glass industry. It was agreed that pollution studies undertaken during Phase I used simulated particulates which were larger than the typical size distribution of actual container furnace flue gas particulates. Thus, capture of particulates in a packed bed had not been clearly evaluated.

The recommendation, therefore, was to install a larger size packed bed near a container glass melting furnace, and pass a portion of the actual furnace flue gases through the bed to obtain more reliable pollutant capture data.

Studies were subsequently made to develop a system which would compliment the preheating of pelletized batch so as to fully allow the energy and melting benefits to be obtained while also allowing the industry to meet the new pollution standards[2]. These studies led to the investigation of an electrified filter bed manufactured by EFB Incorporated. The electrified filter bed,

in conjunction with drying and preheating, could be used to scrub furnace flue gases upstream of a drying and preheating system if the pollutants were considered contaminants, or downstream if pollutants were not a problem (Refer to Section 7). The use of glass batch agglomerates as the filter media had the added advantage of returning furnace flue gas pollutants back to the melting furnace with the agglomerates.

EFB CONCEPT AND EQUIPMENT

Figure 1 schematically represents the EFB concept. The polluted gas enters through the gas inlet and passes through an efficient corona ionizer operated at low power. In this region the particulates are given an electrical charge, usually negative. The charged particulate is then passed through an electric field imposed on the filter bed where the particulate is deposited on the filter media by electrostatic forces (Fig.2). Once collected, particulates are held to the collection surface until removed from the system. EFB's normally use beds of granular material such as coarse gravel as the collecting surface.

The filter media are retained between grounded louvered and perforated plate electrodes with a high voltage electrode suspended between them. The high voltage electrode is electrically insulated from the grounded enclosure and is maintained at high voltage by external power supplies. The electric field formed permeates the bed and polarizes the filter media granules. In this way, caps of positive and negative charges are induced on each bed granule. These charged caps then act as collection sites for the pre-charged particulates. During the operation of the system, the granules become coated with the collected particulates as they flow continuously through the system. For collection of dry particulates, the granular bed is moved downward slowly and continuously. In uncharged granule bed filters, the resulting agitation can result in significant reentrainment of collected particulate into the gas stream. In the EFB, the electric fields tend to "freeze" the dielectric bed granules, a phenomenon similar to a field forming strings of iron filings. Then the bed moves downward and reentrainment is drastically reduced. Typically, the weight of the granules may increase approximately 10 percent as they become loaded with particulates. The filter media moves down into a feeder which removes the dust laden media from EFB. This media is then cleaned before recycling into the EFB.

Glass batch agglomerates (such as pellets) were considered to be a more desirable filter media because the particulates and the filter media could be reintroduced back into the glass melting furnace resulting in no waste products requiring disposal.

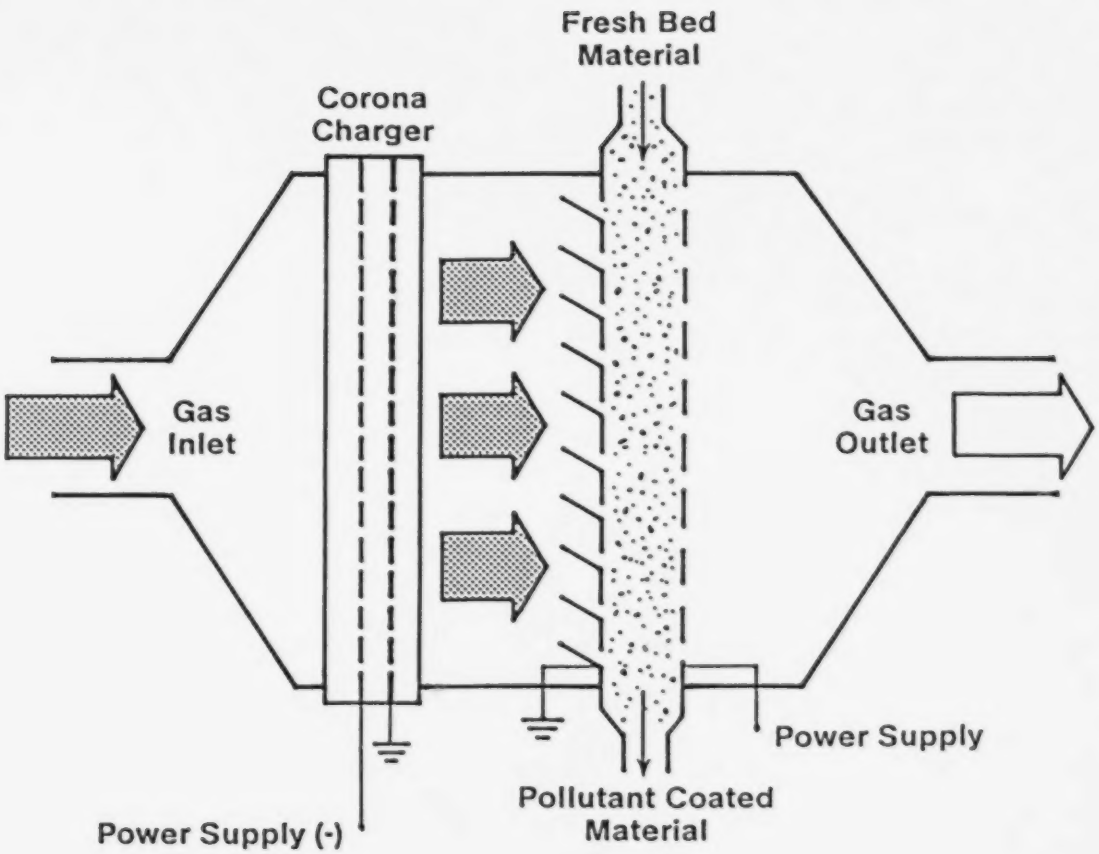

FIGURE 1. ELECTRIFIED FILTER BED SCHEMATIC

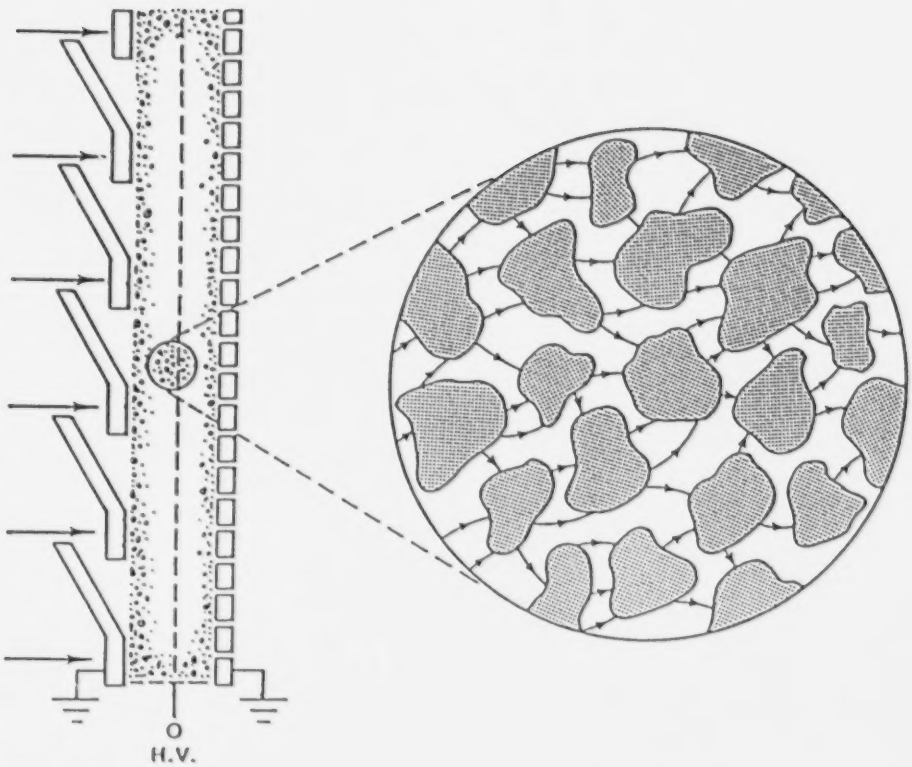

FIGURE 2. POLARIZATION OF BED GRANULES

The use of the EFB units potentially offers very high collection efficiencies for glass furnace particulates as low as 0.1um in diameter. Refer to Table 1 for a comparison of collection efficiencies for various industrial devices.

A laboratory model was supplied by EFB, Inc. of Woburn, Massachusetts. The EFB system components used during the pilot scale test are described below:

Collection Bed

The bed was constructed of two louvered retaining members spaced approximately 0.1m apart. A perforated high voltage electrode was located in the center of the bed. A dump gate below and a cover plate above the bed allowed removal and replacement of bed filter media.

Charger

The charger consisted of thin wires held at high voltage and located between grounded metal plates. Coarse metal mesh screens were located in front of the charger and behind the bed to protect components from foreign objects.

TABLE 1. COMPARISON OF PARTICULATE CONTROL DEVICES

	% Efficiency vs. Particle Size					
Device	.1 μm	1 μm	10 μm	100 μm	Temp. (max) °C	Pressure Drop - Pa
EFB	99	99.9	~100	~100	~800	1000-1500
Fabric Filters	96	99.1	~100	~100	~300	1000-4000
High Voltage ESP	96	98	99	99.99	500	300- 600
Scrubbers	28	97	99.99	~100	100	500-30,000
Cyclones	Negligible	1	88	99.99	800	1000-1500

Source: Sales Data from EFB report submitted to Corning Glass Works (July, 1979).

High Voltage Power Supplies

Continuously adjustable high voltage DC power supplies were provided at capacities of 15KV - 10mA for the bed and 15KV - 5mA for the charger. Upon testing with pellets it was found that more current capability was required for the bed power. As a result, a power pack capable of 10KV - 65mA was used for the pellet bed.

TEST SETUP AND TEST PROCEDURES

Figure 3 shows the schematic of the EFB test setup. A furnace exhaust slipstream was passed through a 0.6m x 0.6m cross-section packed bed that was 0.1m thick. The gas duct was 0.23m in diameter, approximately 3.6m long on the inlet side, and 3.5m long on the outlet side. Sampling ports were located on the duct at minimum distances of eight straight duct diameters upstream and two straight duct diameters downstream of the sampling point.

A 4KW blower with rated capacity of 30 m^3/sec @ 2500 Pa static pressure at Standard Temperature and Pressure (STP), equipped with heat slinger and all-weather enclosure was used for moving the gases through the system.

Most of the particulate concentration measurements were made using the WP-50 method described below. In addition, a modified EPA Method 5 sampling train was employed for some duplicate experimental conditions. Refer to Figure 4 for a comparison of filter location for the two sampling methods. The following paragraphs describe the two sampling methods.

WP-50 Method

The sampling train employed during the tests is depicted schematically in Figure 4. A filter holder probe tip assembly was mounted in the center of the duct pointing directly upstream into the gas flow. A 19x90mm glass fiber extraction thimble was mounted in the holder to collect the sampled particulate. A vacuum pump and valve assembly were used for drawing controllable gas flow rates. Gas flow was measured by an orifice, which was calibrated at 24°C. The gas sample was maintained at this temperature by means of a cooling bath.

Gas flow velocities in the duct were measured by a pitot tube manometer device. Gas temperature was measured by thermocouples at three locations: in the inlet sampling point, in the gas plenum just after the bed, and in the outlet sampling point. Pressure drop across the EFB was measured with a U-tube water manometer.

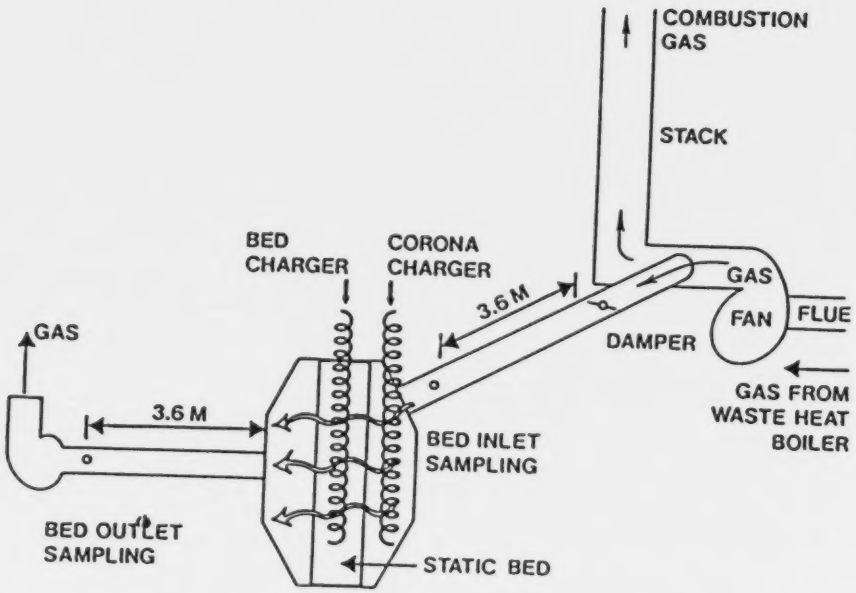

FIGURE 3. SCHEMATIC TEST SET-UP

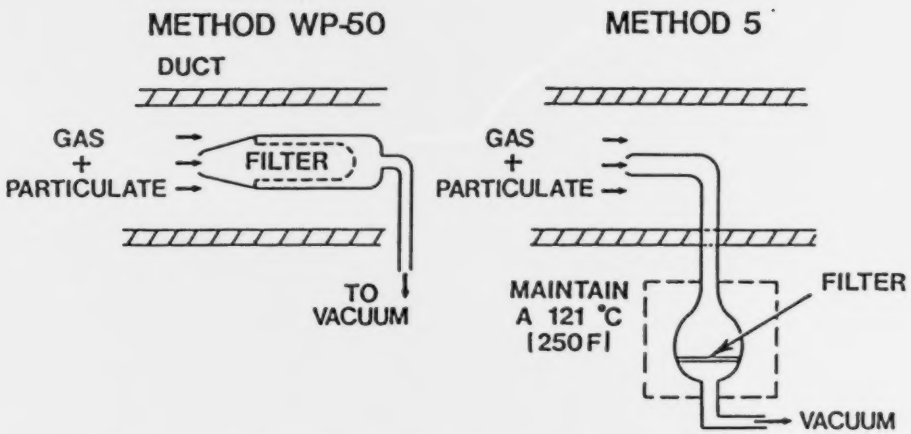

FIGURE 4. COMPARISON OF SAMPLING METHODS PARTICLE CONCENTRATION

The procedure for determining total mass efficiency was as follows: Filter thimbles for inlet and outlet sampling were dried in an oven for at least one hour prior to use. They were preweighed on a Mettler microbalance (accuracy ±.0001 grams) before being loaded into the holders. The holders were then mounted inside the ducting at the inlet and outlet sampling locations and connected to the sampling train. Desired flow and EFB electrical power conditions were established and the system was allowed to equilibrate thermally. Flow velocity was measured in the ducts at the sampling locations and isokinetic sampling rates were calucated. Simultaneously the inlet and outlet sampling trains were turned on and set at the isokinetic rates. During the sampling run, gas temperatures and EFB electrical power levels were periodically monitored and recorded. The sampling flow rates were held at the calculated isokinetic rates. Sampling durations were one to three hours. After the desired sampling time, the sampling trains were simultaneously turned off. Filter thimbles were removed and weighed. The change in weight represented the deposited particulates, and was used to calculate mass loadings in the gas.

Modifed EPA - Method 5

A sampling train was used for Method 5 in accordance with EPA approved standards. The deviations from the standard method were 1) single point sampling at the center of the 0.23m diameter duct and 2) less than 0.3m duct diameter. Western Precipitator model EPA-11 stack sampling trains were used. The control consoles were modified by replacing the factory supplied temperature-compensated gas meters with thermocouples in the inlet and outlet pipe connections. The magnehelic gauges normally used on the consoles for the velocity head readings were replaced by Dwyer Model 421-10 reclined-vertical manometers or Model 171 vertical manometers. All other sampling procedures were in conformity with Federal Register Standards of performance for new stationary sources, Title 40, part 60, including revisions through September 19, 1977.

EFB COLLECTION EFFICIENCY RESULTS

As discussed previously, the EFB bench scale unit was tested in two modes of operation. The first mode was with gravel as the bed material. The second mode was with pellets in order to test its adaptability to a pellet preheater system. This bench scale testing using pellets in the bed was successful in verifying the fundamental theory of EFB collection, and was useful for design scale-up.

Collection efficiency tests were run under various operating conditions, as summarized in Table 2. The measured capture efficiencies are listed in Table 3, and are classified with regard to the sampling methods used. The bed conditions are also listed.

TABLE 2. OPERATING CONDITIONS FOR CAPTURE EFFICIENCY TESTS

Date	Run No	Sampling Method	Inlet Gas Temp °C	Material **	Bed Conditions Avg. Gas Flow m^3/sec.	Bed Conditions Exit Gas Temp °C	Voltage (KV)	Final Outlet Gas Temp °C
6/12/79	1	WP-50	177	Gravel	0.22	--	10	143
6/12/79	3	WP-50	177	Gravel	0.23	160	10	141
6/13/79	4	WP-50	171	Gravel	0.23	165	10	143
6/13/79	5	WP-50	182	Gravel	0.23	168	2	143
6/13/79	6	WP-50	182	Gravel	0.23	174	0	149
6/12/79	2	Method 5 (Mod.)	185	Gravel	0.23	--	10	141
6/14/79	7	WP-50	193	Pellets	0.18	168	3	151
6/19/79	9	WP-50	193	Pellets	0.17	171	10	146
6/20/79	10	WP-50	171	Pellets	0.09	161	10	141
6/20/79	12	WP-50	166	Pellets	0.05	--	0	105
6/21/79	13	WP-50	154	Pellets	0.05	--	10	104
6/21/79	14	WP-50	154	Pellets	0.05	--	10	104
6/22/79	17	Method 5 (Mod.)	186	Pellets	0.11	150	8@	135

** Gravel in diameter (avg.) = 3mm.
Pellets diameter (avg.) = 10mm.

@ Bed shorted out resulting in 0 volt condition for nearly 1/3 of test duration.

TABLE 3. CAPTURE EFFICIENCY DATA

Filter Media	Sampling Method	Run No.	Bed Conditions (Depth = 0.1m) Field Strength KV/m	Face Velocity m/sec	Grain Loading G/DNCM Inlet	Capture Efficiency (%) (Based on mass total)
Gravel	Modified Method 5	2	100	0.63	0.062	89
	WP-50	4	100	0.61	0.0251	99+
	WP-50	5	20	0.61	0.032	94.3
	WP-50	6	0	0.63	0.0366	27.3
Pellet	Modified Method 5	17	80	0.30	0.073	79@
	WP-50	9	100	0.45	0.0343	82.6
	WP-50	10	100	0.24	0.0434	93.1
	WP-50	12	0	0.13	0.0297	34.5
	WP-50	13&14	100	0.13	0.0343	98.15*

@ Bed frequently shorted out due to heavy rains.

* Average value of two runs (98.1 and 98.2)

NOTE: Field strength = $\frac{\text{Applied Voltage}}{\text{Bed Depth}}$

Conclusions

The grainloading measurements from WP-50 method were consistent and repeatable (runs 13 and 14). The following conclusions may be drawn from these results of the WP-50 method.

The capture efficiency is strongly dependent on the applied bed voltage for fixed bed depth and gas velocity. As the bed voltage is increased, the capture efficiency also increases. For example, the gravel bed efficiency increased from 94.3% to 99+% when the bed voltage was changed from 2 to 10 KV (i.e. field strength from 20 to 100 KV per m).

When the bed voltage is zero, the EFB is a mechanical collector, and the collection efficiency was found to be less than 35% for both the gravel and pellet beds.

Decreasing the gas velocity increases collection efficiency. For example, in pellet mode at a velocity of 0.45 m per sec. The efficiency was 82.6%, whereas a 93.1% efficiency was obtained at about 0.24 m/sec (Run nos. 9 and 10).

EFB Collection Efficiency Correlation

The theoretical capture mechanisms of an EFB have been developed by EFB Inc. A dimensionless group called Electrostatic Collection parameter has been successfully used, by EFB Inc., in characterizing and predicting the capture efficiencies in EFB devices.

A plot of the EFB test data (Table 3) and the corresponding theoretically predicted collection efficiencies is shown in Figure 5. Also shown are the experimental data obtained during this testing.

It is demonstrated that there is a reasonably good agreement between the theory and the experimental data especially at the higher efficiency range. This means that EFB designs can be adequately scaled up from these test data for high efficiencies as needed. It is also viewed that for desired values of collection efficiencies one needs to manipulate the electrostatic collection parameter by proper design and operation.

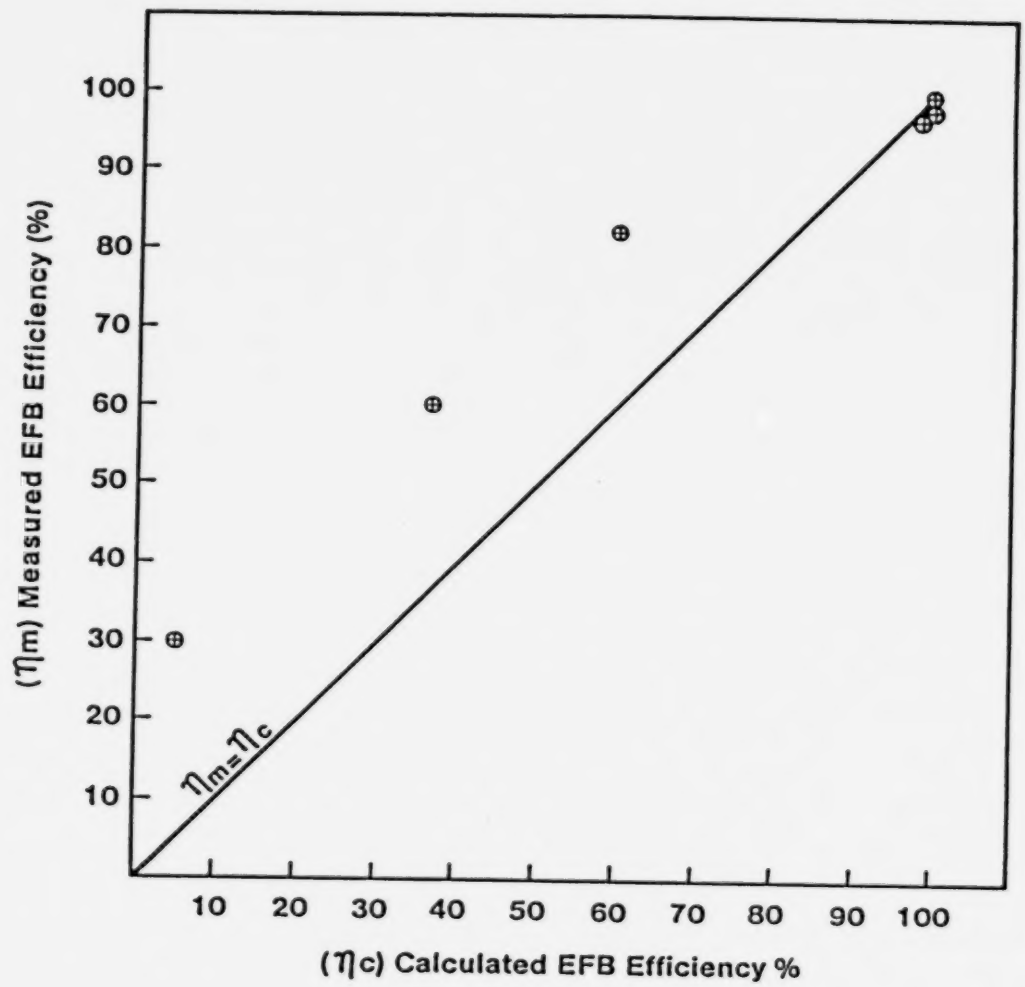

FIGURE 5. CAMPARISON OF THEORETICAL AND ACTUAL CAPTURE EFFICIENCY FOR EFB

PARTICLE SIZE DISTRIBUTION SAMPLING AND RESULTS

One of the objectives of this test program was to characterize particulate size distribution in the stack gases as a function of particle size distribution. Therefore, the slipstream of gases entering the EFB bench scale unit was sampled for analysis of particle size distribution.

Equipment and Sampling Procedures

Particle size distributions were measured using a cascade impactor made by Anderson 2000 Inc. As done for the particulate concentration measurements, two separate techniques were used for measurement. First, with cascade impactor outside of the gas duct and second, with the cascade impactor inside the gas duct. Refer to Figure 6 for a schematic representation of the two sampling methods. The sampling procedures were the same as described earlier in the section on total mass concentration measurements.

Under Method 5, the cascade impactor outside the duct was maintained as nearly isothermal as possible by surrounding it with insulation materials. The gases were drawn isokinetically with a probe extended into the center of the duct. Glass fiber substrates were used for the cascade impactor. Individual weighings were made of the substrates before and after sampling.

In Method 5, shown in Figure 6, the cascade impactor unit was a Mark III high temperature type. The gooseneck nozzle upstream of the impactor was washed after sampling and the weighing was added to the downstream stage weighing for data reduction.

The operating conditions for the test setups during the particle size distribution measurements are shown in Table 4.

Conclusions from Particle Size Distribution Data

Approximately 70% to 95% by weight of the particulates have physical diameters of less than 1 micron. These data (Aerodynamic diameter and physical diameter) are shown in Tables 5 and 6. For details of particle size calculations, please refer to Section 6.

There are differences between the particle size data measured by the two methods - especially in the super micron range. It should be noted that the Method 5 (Runs A&B) includes particulates washed from the nozzle of the impactor (probe wash). The fractional weights are shifted towards the larger size range because the washings were added to the first stage, which contain the larger particulates. A close review of Figure 6 shows that some amounts of the particulates could be trapped in the gooseneck section, under Method 5; however, the particulates are mostly sub-micron in size.

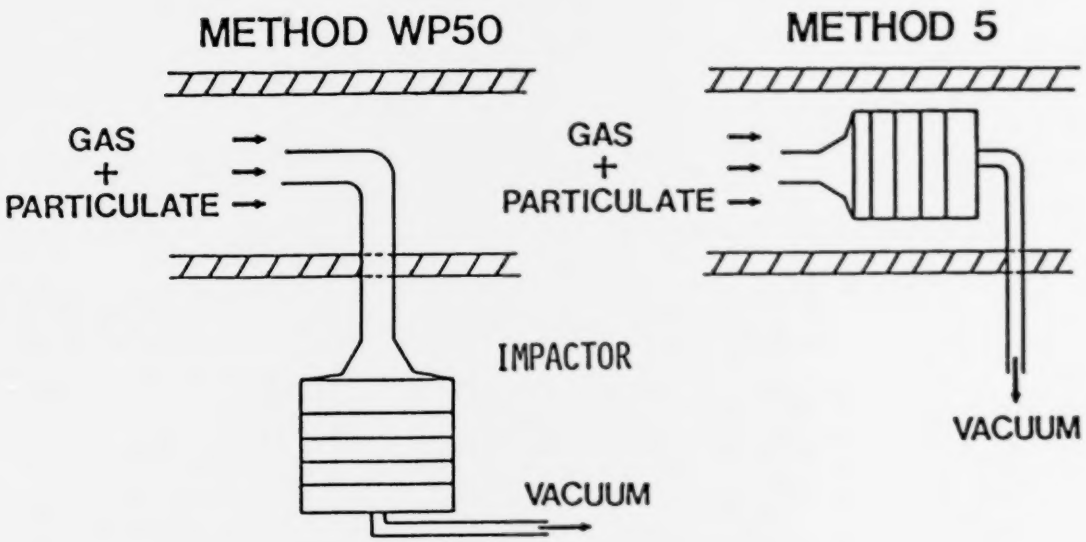

FIGURE 6. COMPARISON OF SAMPLING METHODS
PARTICLE SIZE DISTRIBUTION

TABLE 4. OPERATING CONDITIONS FOR PARTICLE SIZE DISTRIBUTION TESTS

Date	Run No.	Measurement Method (Fig. 6)	Inlet Gas Temp °C	Bed Material	Avg. Gas Flow m^3/sec	Bed Voltage (KV)
6/20/79	11	WP-50	177	Pellets	0.06	8.3
6/21/79	15	WP-50	167	Pellets	0.04	10.0
6/28/79	A	5	171	Pellets	0.12	0.0
6/28/79	B	5	169	Pellets	0.12	0.0

TABLE 5. PARTICLE SIZE DISTRIBUTION BY SAMPLING METHOD WP-50

Stage No.	Anderson 50% Cut Dia. μm	Aerodynamic Diameter μm	Physical Diameter μm	Deposited Weight (mg)	% Mass ≤ Diameter Shown
		Run 11			
0	11.0	14.9	9.1	0	100
1	7.0	9.5	5.8	0.1	99.8
2	4.7	6.4	3.9	0.0	99.8
3	3.3	4.5	2.7	0.1	99.7
4	2.1	2.8	1.7	0.6	98.6
5	1.1	1.5	0.92	2.7	94.0
6	0.65	0.88	0.54	4.9	85.7
7	0.43	0.58	0.35	9.7	69.2
F	--	--	--	40.6	--
		Run 15			
0	11.0	20.0	12.0	0.3	98.6
1	7.0	13.0	7.9	0.1	98.2
2	4.7	8.6	5.2	0.0	98.2
3	3.3	6.0	3.7	-0.2	99.1
4	2.1	3.8	2.3	0.1	98.6
5	1.1	2.0	1.2	1.0	94.0
6	0.65	1.2	0.73	1.9	85.3
7	0.43	0.78	0.48	3.0	71.1
F	--	--	--	15.5	--

NOTE: (1) Deposited weights do not include nozzle wash.
(2) Density of particulates 2.68 gm/cc.

TABLE 6. PARTICLE SIZE DISTRIBUTION BY SAMPLING METHOD 5

Stage No.	Anderson 50% Cut Dia. µm	Aerodynamic Diameter µm	Physical Diameter µm	Deposited Weight (mg)	% Mass ≤ Diameter Shown
			Run A		
Wash				10.9	
0	16.0	14.15	8.52	0.6	76.9
1	11.0	8.86	5.29	0.0	76.9
2	7.1	6.03	3.56	0.51	75.9
3	4.8	4.14	2.41	0.69	74.5
4	3.2	2.69	1.52	0.67	73.2
5	1.51	1.34	0.70	1.01	71.1
6	0.96	0.88	0.43	2.59	65.9
7	0.66	0.68	0.31	5.66	54.6
F	--	--	--	27.17	--
			Run B		
Wash				8.8	
0	16.0	12.65	7.60	0.0	80.7
1	11.0	7.93	4.72	0.0	80.7
2	7.1	5.4	3.17	0.41	79.8
3	4.8	3.7	2.14	0.00	79.8
4	3.2	2.4	1.34	0.34	79.0
5	1.51	1.24	0.64	0.86	77.1
6	0.96	0.63	0.28	2.79	71.0
7	0.66	0.37	0.13	5.18	59.6
F	--	--	--	27.15	--

SECTION 5

PELLET DEVELOPMENT AND EVALUATION

Prior to construction of the pelletizing and drying part of the Preheating and Melting Demonstration in the Pilot Plant, most of the pelletizing work done for this project was done on laboratory scale (0.355m and 0.61m dia.) pelletizers. A trial was also done on a 0.91m diameter pelletizer. The objectives of pelletizing on a larger scale were to make the pellets for the packed bed pollution capture testing and to develop the relationship between pellet variables and operating parameters.

To this end the pelletizing and drying phase of the pilot plant was constructed at the Corning Glass Works Process Research Center (PRC) in Corning, New York. The completed equipment essentially followed the description and specifications given in section 6 of the Phase I Process Design Manual[1]. The schematic flow sheet is shown in Figure 7.

Pelletizing work was done entirely with the soda-lime batch formulation developed during Phase I. The effect on pellet size, strength, and pelletizing rate of operating parameters, such as pan angle, rotational speed, and depth were studied. In addition, valuable experience with batch, pellet conveying, and storage was gained.

PELLETIZING AND DRYING SYSTEM

The pelletizing/drying system performed three operations:

(1) Brings mixed batch and water separately to the pelletizer;

(2) Adds batch and water in a carefully controlled fashion in the pelletizer;

(3) Drys the pellets and delivers them to containers;

Control of the system was effected through separate control of the three parts of the process.

Batch System

Operating batches of 1043 kg were mixed at the batch house and moved in tote bins to the batch system. The tote bin of batch was manually raised to a tote tilt which emptied the

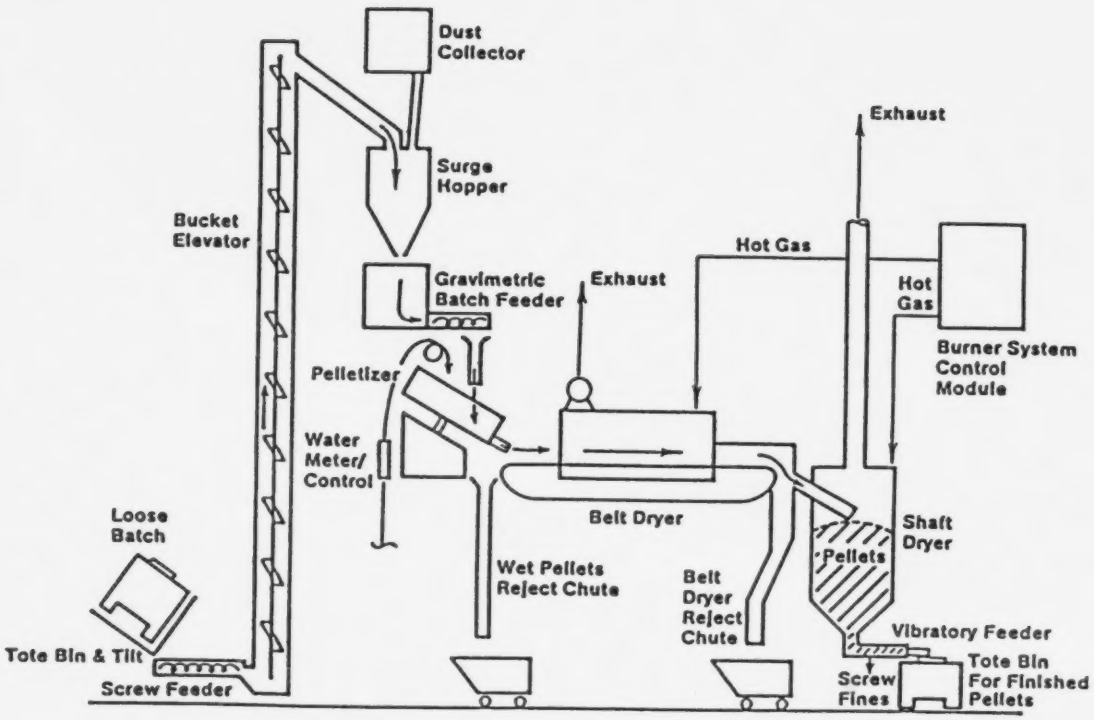

FIGURE 7. PELLETIZING SYSTEM SCHEMATIC

tote bin into a screw feeder. The screw feeder fed a bucket elevator which filled a surge hopper. The surge hopper capacity was equal to an operating batch and could be filled in about 10 minutes. In addition, a dust collector recycled dust continuously from the feeder and pelletizer back to the surge hopper.

The heart of the batch system was the gravimetric feeder. The feeder, capable of gravimetric or volumetric feed, included its own hopper with a capacity of 1/2 an operating batch. The batch feed rate to the pelletizer could be accurately controlled in a gravimetric mode to within plus or minus 2% of set point. The maximum feed rate was about 1815 kg per hour. The feeder was equipped with its own microprocessor which allowed a number of control options.

Batch System Control

The batch system was designed to operate in either a manual or automatic mode. Since batches were manually brought to the batch system, automatic control depended on always having a fresh tote bin of batch on the tote tilt when batch was called for. Thus, the system was actuated by the operator acknowledging when the tote bin had been emptied (actually when the surge hopper had been filled). When this was done, filling of the surge hopper when it became empty was done automatically when a low level indicator in the hopper actuated the screw feeder and bucket elevator.

The gravimetric feeder continuously monitored its own hopper. When the hopper level reached a preset low level, the control system opened a keystone valve between surge hopper and feeder hopper, filling the feeder hopper until closed by a high level signal. If filling the feeder hopper caused the level in the surge hopper to go below low level, the screw feeder and bucket elevator would be started to refill the surge hopper (provided that the previous fill had been acknowledged).

Sequencing of the screw feeder, bucket elevator, dust collector and surge hopper was done with a microprocessor control unit. The gravimetric feeder had its own microprocessor.

Gravimetric Feeder Control

The gravimetric feeder was supplied by Acrison, Inc. and was capable of operation from either an internally or externally generated set point. In addition, the feeder could be operated in the volumetric mode.

The original control concept was based on using a signal generated by the water flow meter to control the batch feed rate. In this fashion it was possible to set the water to batch ratio

using the feeder's microprocessor. Control was also accomplished by setting the water and batch feed rates separately using an internal set point for the gravimetric feeder.

TABLE 7. EQUIPMENT

Equipment	Manufacturer	Model No. (Size)
Belt Dryer	Midland-Ross Corp.	(2' x 1.6')
Bucket Elevator	Dover Conveyor & Equipment Co.	(6" x 4" x 58' 8")
Dryer Control Module	Midland-Ross Corp.	
Dust Collector	W.W. Sly Co.	PC104
Gravimetric Feeder	Acrison, Inc.	403
Keystone Valve	R. M. Headlee Co.	D160
Pelletizer	Feeco International, Inc	072
Shaft Dryer	Midland-Ross Corp.	(5' x 21')
Screw Feeder	Dover Conveyor	(6" x 5')
Vibratory Feeder	Eriez Manufacturing Co.	62B
Water Flow Controller	W.A. Kates Co.	MFA 1-1
Water Flow Meter	Fischer-Porter	51-1101 KB-650 3NS

Pelletizer

The pelletizer was a pan type (Table 7), nominal 1.37 m diameter by 0.355 m deep. An extension of the pan depth to 0.457 m was possible with a split ring rim extension. When full of batch, the pan held a nominal 340 kg of material (430 kg with the pan extension).

The pan angle measured between the axis of rotation and the horizontal could be varied between 35° and 50°. The pan rotational speed was variable between 5 and 20 RPM. Total water flow to the pan was controlled with a flow controller and a flow meter. Water flow in the individual sprays was controlled by needle valves on the pelletizer.

The pelletizer utilized three plows to channel flow in the pelletizer into three streams. The plows were adjustable to allow for more or less flow in each stream.

Feed location in the pan was an important parameter for both the batch and the water spray. Batch was fed from the gravimetric feeder through a fixed horizontal pipe. A funnel was hung under the feeder pipe to which was attached a flexible pipe which could be adjusted to direct feed to any part of the pan. The three

water sprays were individually adjustable to spray on to any part of the pan. They were made of coiled copper tubing which holds its shape once bent to the proper shape.

Pelletizer Operation--

It is convenient to describe operation of the pelletizer by referring to what one would see as one faces the open pan. Thus, the pelletizer rotates clockwise with pellets forming essentially in the lower left quadrant. The face of the pan appears generally as shown in Figure 8.

During operation the batch and pellets in the pan appeared essentially as shown in the schematic view in Figure 9. Most of the material in the pan was swept into the left side of the pan with finished pellets rolling over the pan rim in the lower left quadrant. Unfinished pellets circulated in the upper left quadrant with some carried over the left plow into the center stream along with recirculating batch. A smaller amount of batch passed over the center plow into the right stream. The finished pellets rolled on top of the circulating batch and unfinished pellets causing the finished pellets to become smooth. Then the finished pellets rolled over the pan rim and down a chute which distributed them uniformly on to the belt dryer.

Dryer System

The finished wet pellets were dried to give them strength and allow them to be stored without sticking together. The dryer system, supplied to specifications in Section 6 of the Phase I report by Midland Ross Corporation (Table 7), consisted of three components: a belt dryer, a shaft dryer and a dryer control module containing the burner systems for the two dryers. Each dryer was gas fired and capable of sustained operation of 350°C.

Belt Dryer--

The belt dryer consisted of a 0.61 m wide by 5.1 m long wire mesh belt which moved through a heated kiln. The capacity of the belt was 300-1200 kg per hour of pellets based on a maximum belt speed of 0.4 m per second and a minimum speed of 0.1 m per second. A Surface Combustion EA2000 Excess Air Burner was used to supply hot gases. Fans were used to recirculate the gases. The heated kiln was baffled into three compartments for recirculating the gases. The gases moved counter-currently with the pellets; and the burner was at the pellet discharge end of the box.

The design of the belt dryer included a pellet leveling roller. This was designed to distribute pellets evenly over the width of the belt to allow for uniform drying. It was found during start-up that an adjustable deflector in the pelletizer discharge chute could do a better job of spreading the pellets without deforming or crushing any pellets.

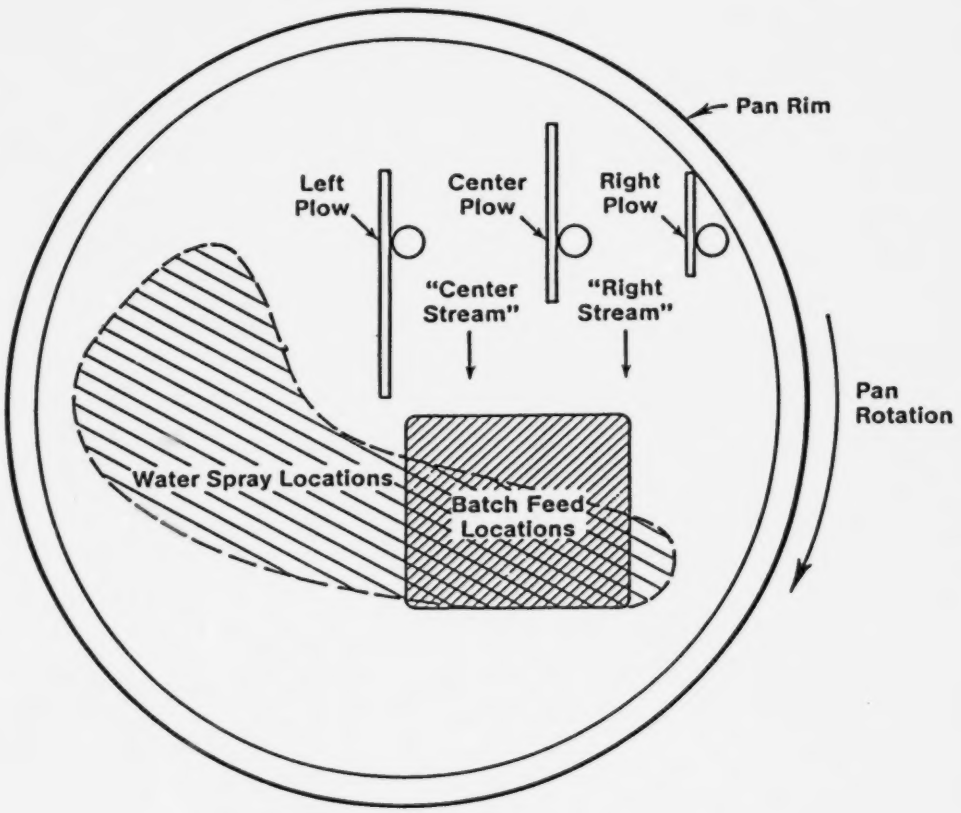

FIGURE 8. PELLETIZER PAN — PLAN VIEW

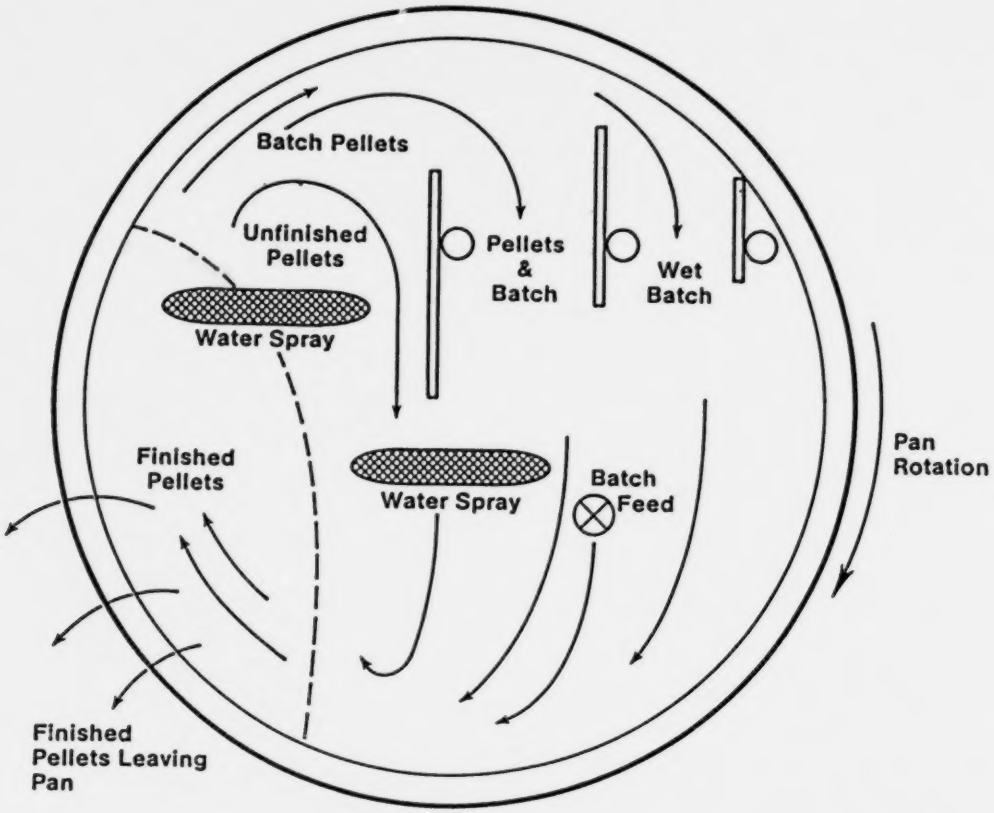

FIGURE 9. SCHEMATIC VIEW OF BATCH AND PELLETS IN THE PELLETIZER PAN

In the event that pellets leaving the pelletizer did not meet specifications, the adjustable pelletizer chute was interchangeable with a discharge chute which sent the wet pellets directly to a hopper in the cave. The chutes were changed by manually replacing one with the other.

A chute at the discharge end of the dryer conveyed the partly dried pellets from the belt to the shaft dryer. This chute was equipped with a manually operated trap door which allowed the operator to reject pellets to a hopper in the cave when it was necessary. Otherwise the pellets rolled into the top of the shaft dryer.

Shaft Dryer--

The shaft dryer was a vertical cylindrical shell 0.91 m diameter and 3.5 m long. To the bottom of this shell was attached a cone 1.37 m long which tapered to a diameter of 0.2 m. A nominal 0.15 m diameter pipe 1.59 m long connected the bottom of the cone with a vibratory feeder.

Heat was supplied by a Surface Combustion EA2000 Excess Air Burner and introduced to the dryer through four pipes connected to the burner manifold. The pipes entered the shaft 1.95 m above the top of the cone extending down the inside of the shaft to within .58 m of the top of the cone. The hot gases entered through these pipes, rose through the bed of pellets, and exited through the stack at the top of the shaft.

Cooling air designed to cool the pellets before they were discharged from the shaft was introduced into the lower cone. It was heated as it cooled the pellets and exited as it blended with the burner gases.

Pellets were fed to the shaft from the belt dryer chute. The height of the pellet bed was approximately 2.75 m above the cone. Including the pellets in the cone and the discharge pipe, the pellet bed obtained approximately 2,750 kg of pellets.

The level of pellets in the shaft was controlled by varying the speed of the vibratory feeder to keep the level between two level indicators spaced 0.23 m apart. The vibratory feeder was set for a high speed and a low speed by two adjustable rheostats. When the low level signal was on or when the level was between the low and the high, the feeder operated on slow speed. This was set to allow the shaft to fill slowly. When the high level signal was actuated, the feeder was shifted to fast speed to reduce the level. Control of the vibratory feeder was handled by the batch system microprocessor.

Dryer Control Module--

Controls for both dryers were contained separately from the dryers in a control module where the pilot system had dedicated burners, as opposed to using waste heat for control. Only the burners themselves were actually located at the dryers.

Combustion air was supplied by a blower common to both systems and capable of 5100 m^3/hr at 140 cm of water pressure. Air flow was regulated with butterfly valves and measured by a calibrated orifice. Cooling air for the shaft was also supplied by this fan. A recirculating fan and an exhaust fan for the combustion products were located on the belt dryer itself and operated from the control panel.

Temperatures in the dryers were controlled by individual temperature controllers, thermocouples, and high limit devices. Each dryer also had its own temperature indicator. There were three additional thermocouples on the belt dryer and five on the shaft dryer which were monitored by a multipoint temperature recorder.

The burner system was equipped with alarms so that if the burner shut down for any reason, audible and visual alarms would be activated. The safety devices included flame sensors, high and low pressure switches, manual reset shut-off valves and hydramotor valves.

Start-Up of the Pelletizing System

The start-up and debugging phase uncovered a number of unanticipated pellet handling problems. The major ones were:

- Pellet distribution on the belt
- Filling the empty shaft dryer with pellets
- Pellets sticking to each other and the belt
- Clogging in waste chutes

Distribution of the wet pellets leaving the pelletizer onto the belt was complicated because the pellets rolled down the left side of the pelletizer discharge chute. If left undisturbed, they would roll off the left side of the chute and angle toward the right side of the belt. The problem was to design a distribution chute which would fit between the pelletizer chute and the dryer belt and would disperse the pellets evenly across the width of the belt. The simple design shown in Figure 10 accomplished this by dividing the pellets into two streams which distributed themselves evenly by bouncing and rolling within the chute. The deflector was adjustable to any position. The wet pellets were strong enough to withstand the bouncing in the chute.

The problem with filling the empty shaft dryer was the fall of almost 6 m that the initial pellets had to survive. It was decided to fill the dryer directly with pellets dried as much as possible in the belt dryer. Many of the first pellets did not survive the fall. The first material fed from the bottom of the shaft was

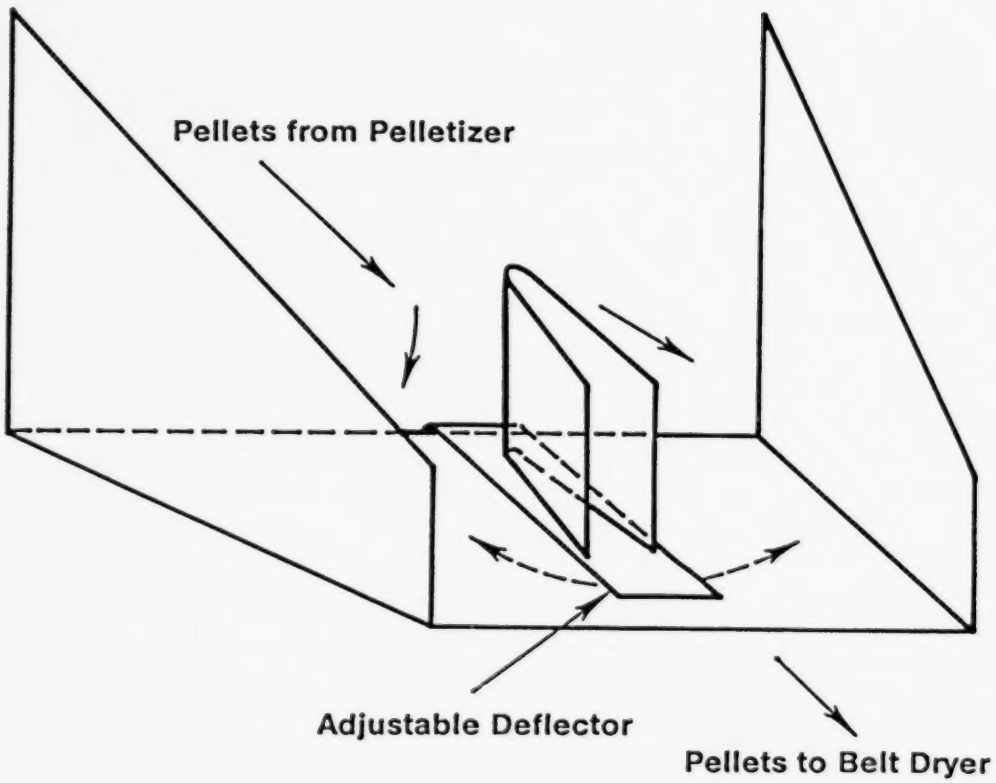

FIGURE 10. PELLET DISTRIBUTION CHUTE FROM PELLETIZER TO BELT DRYER

mostly broken pellets. However, after filling the dryer, the breakage ceased to be a problem. An alternative approach to filling the shaft dryer would have been to fill it with a media such as gravel so that the first pellets would not experience a long fall. This was not done, primarily to avoid contamination of the pellets and shaft.

Drying on the belt at temperatures above 225-250°C caused the pellets to stick to each other and to the belt. Small pellets with a wet surface exhibited this more than large pellets with a dry surface. Pellets with a wet surface almost always exhibited sticking and, if not broken apart in their fall to the shaft dryer, could harden into agglomerations of many pellets, posing a potential clogging problem at the shaft dryer discharge pipe. In normal operation, pellets would often leave the belt in sheets which would break into individual pellets when they hit the belt dryer discharge chute. However, when small wet pellets were subjected to temperatures over 250°C, they stuck tenaciously to the belt and would not break off at the end of the belt. These pellets might return for a second pass through the dryer or drop on the floor under the dryer. Trouble-free drying was achieved when the control temperature was set at 215°C, which confirms results reported in Phase I.[1]

Clogging of the reject chutes was not limited just to wet batch from the pelletizer. Wet and dry pellets also caused reject chutes to become clogged, usually at elbows. Dry pellets have an angle of repose of 34° from horizontal, so they would build up even in sloped ducts or chutes. Wet pellets are more of a problem because they stick together and then dry to form a blockage which is difficult to remove. The intersection between the shaft dryer cone and discharge pipe had to be modified because the original design called for a cup-shaped transition which allowed the dry pellets to bridge the opening to the discharge pipe. When the discharge pipe was changed from nominal 10 cm to nominal 15 cm diameter, blockages ceased to be a problem.

OPERATION OF THE PELLETIZING SYSTEM

To start a typical day of pelletizing, batch was mixed in the mixhouse and brought in tote bins to the batch area. Ordinarily, four to six tote bins each containing 1,043 kg of batch were required per day. The soda-lime batch used for most of the pellet development studies was developed during Phase I and is shown in Table 8.

A tote bin of batch was raised by forklift to the tote tilt. Once tilted the bin was emptied by a screw feeder at a nominal rate of 4,500 kg per hour into a bucket elevator. The bucket elevator filled the surge hopper above the gravimetric feeder in less than 15 minutes. The surge hopper capacity was 11,000 kg of batch. The feeder hopper capacity was approximately 550 kg. It

was filled automatically from the surge hopper when its low level indicator signaled the batch system microprocessor to open the Keystone Valve. The refill cycle would start when the level of batch in the surge hopper level dropped below its low level indicator.

TABLE 8. SODA-LIME PELLETIZING BATCH

Raw Material	Weight Percent
PGS Berkeley No. 1 Dry Sand	38.7
200 Mesh Supersil, PGS	20.8
Limestone, National Gypsum #4	11.7
Burned Dolomite, National Lime and Stone 40 Grade	3.3
Nephaline Syenite, Indusmin 7-340	7.2
Soda Ash, Dense Western, Stauffer Chemical Co.	17.7
Salt Cake, FMC Corp.	0.5
Carbocite, Shamokin Filler Co. #2	0.1
	100.0

Operation of the pelletizer has already been outlined in a previous section. The pelletizer was set at the desired rotational speed and pan angle. The gravimetric feeder was set to operate at the desired feed rate in gravimetric mode. After the pan was started, batch and water were turned on simultaneously. The water flow was adjusted manually to meet the desired percentage in the pellets. It was important to start simultaneously because the difference in water between pellets which were too dry and too wet was small.

Ordinarily, the first pellets to be discharged from the pan once it was filled were large and non-uniform sizes. If the pan was set to start at the pan angle that produced the steady uniform size pellets required, the pellets following the initial ones were usually smaller than expected and would grow slowly to the equilibrium size. To increase the speed at which pellets grew to the equilibrium size, the pan angle was often set higher than the anticipated operating value to start with and as the pellets approached the desired size the angle was reduced to the desired angle. After steady operation was achieved, no further adjustment of the angle was required.

Once the pelletizer was started the belt and shaft dryer burners were lit. It took about 15 to 20 minutes to reach steady temperature, about the same time required for the first pellets to roll off the pan. Initial pellets were usually unacceptable due to size or irregular shape and were diverted directly to the

cave without going through the dryer. Once the size stabilized in the acceptable range, pellets were sent through the drying system. Production of acceptable pellets was usually achieved within one-half hour after filling the pelletizer. The pelletizer could then run unattended for the rest of the operating day (6-8 hours). The estimated loss of pellets due to unacceptable size or quality at start up is about 15 to 30 minutes production for a pellet size distribution of 1.27 cm ± 0.32 cm.

PELLETS FOR THE PACKED BED TESTING PROGRAM

Uniform size pellets were required for the shaft preheating and pollution capture testing program. Phase I laboratory work[1] showed that the best size for these pellets should be 1.27 cm diameter plus or minus 0.32 cm for durability and ease of pelletizing. This size in this pilot plant study was found to be achievable and approximately the mid-point of the pan's stable pellet size range. It also reflects the optimum size found by Morelissen, Rikken and van Tinen.[4]

PELLETIZING DEVELOPMENT

The pelletizing system was designed to produce 955 km per hour of dried finished pellets in a pelletizer 1.37 m diameter and 0.457 m deep. In order to test the effect of pan depth, the pelletizer was built with an adjustable rim. The rim ring could be removed to give a 0.355 m deep pan.

However, steady production of 1.27 cm diameter pellets was not achieved in the deep pan. Although production rates of up to 1,050 km per hour were recorded for short periods, no stable operating condition where production of stable size pellets could be sustained for several hours was achieved in the deep pan. Many of the pellets used in the pollution capture test were made in the deep pan but usually during short periods of up to an hour during which pellet size was growing through the desired size range. The pan had a strong tendency to produce pellets in the 2-3 cm diameter range.

Pellets in the desired size range, but not at the desired production rate, were produced in the shallow (0.355 m deep) pan. Stable size and production were achieved at 635 km per hour with the pelletizer running unattended. The shallow pan responded more quickly to changes in pan angle or feed location than the deep pan.

Pelletizing Problems

An unanticipated problem with the pelletizer was the formation of chunks of compacted wet batch. These were produced when batch would build up on the plows or sides of the pan and then break off into the pan and roll onto the belt with the pellets.

These irregularly shaped pieces were often about the same size and composition as the pellets; however, there were pieces as large as 25 cm diameter which broke away from the plows behind the support posts. Large pieces such as these will certainly occur in any production system. There was no screening device for the wet pellets; consequently some of these pieces went through the dryer system causing crushed pellets on the belt dryer and plugs in the shaft dryer discharge pipe. A production system should include screening for wet pellets to remove the occasional large pieces.

The only point of noticeable wear in the pelletizer was the wall plow. Despite the use of overlay hardening, the plow edge wore quickly, allowing a layer of batch to build up on the sides of the pan. This layer could build up during a day's operation to a thickness as much as 1-2 cm although there is no indication that this was harmful to the stability of the pelletizing process. The rate of wear was approximately 4×10^{-5} kg/kg of batch. This was considered to be less than that which would cause color problems. Future work should examine the use of ceramic plows to prolong the life of the plows and to decrease maintenance required for replacing the plows.

Maximum Pelletizing Rate

A goal of this development was to establish the maximum pelletizing rate for the pan. Beyond this rate so many seed pellets are produced that they cannot grow to the desired size. This effect was seen when the pan discharged most of the pellets, with loose wet batch or seed pellets taking their place. The maximum rate was somewhat difficult to determine because the takeover by batch did not occur immediately. The pan could run about two hours before it became apparent that the pellets were being displaced by batch. In addition, inability to operate the deep pan at stable conditions affected the maximum output rate. It was estimated that 1,000 kg per hour was the maximum out put rate for the deep pan and 770 kg per hour was the estimated maximum output rate for the shallow pan.

Pellets made at or near the maximum rate tended to be more grainy and less spherical than pellets made at a rate lower than the maximum. The optimum pelletizing rate at which pellets have a smooth spherical surface appeared to be approximately 80% of the maximum. This was shown by the fact that the best pellets were made in the shallow pan (a depth to diameter ratio of 0.26) at a production rate of 635 km per hour, or about 82% of the maximum.

The Phase I Report[1] recommended a relatively deep ($0.4 < H/D > 0.6$) pan for pelletizing the soda-lima batch presented in Table 8. However, the results of this work show that it is preferable to pelletize this batch on a large scale in a shallow ($H/D=0.26$) pan. It is reasonable to expect from these observations that pelletizers larger than 1.37 m diameter will operate best at lower depth to diameter ratio.

Pelletizing rate data from the 61 cm. diameter Mars drum pelletizer and the 92 cm. diameter Feeco pan taken during Phase I were correlated with data taken during this work with the following equation:

$$R = CD^{*3}HN \sin\theta$$

Where
- R = Pelletizing rate (kg/hr.)
- C = 1.7 kg/m^4 (constant for 1.3 cm dia. soda-lime pellets)
- D* = Pelletizer diameter (m)
- H = Pelletizer depth (m)
- N = Pelletizer rotational speed (rev/hr)
- θ = Pelletizer pan angle (degrees)

The pelletizing data are shown in Figure 11. The constant, C, appears to be a function of batch parameters such as density, particle size distribution and pellet diameter. It seems reasonable to calculate C for a particular batch and pellet size based on laboratory scale pelletizing and then to scale up to larger pelletizers and rates.

Pellet Size Control

Pan angle (See Figure 12) is an important pelletizing control variable effecting the size of the pellets. Pellet size is sensitive to pan angle. Figure 13 is an approximation of the effect of pan angle on pellet size. No statistical analysis was performed on this small amount of data. Even a 1° change can have a large effect on pellet size. Generally, pellets decrease in size as the pan angle is decreased. This is expected since the residence time in the pan is decreased. Pan angle was used to "adjust" the pelletizer to the correct size range of pellets. In a production application where the pelletizer may have a fixed angle to reduce cost, the angle should be carefully determined ahead of time.

Fine tuning for pellet size was done by controlling the batch feed location. For this batch, feeding was done in the fairly narrow area shown in Figure 9. Feeding to the left (towards the center of the pan) caused pellets to be larger. Feeding to the right caused them to be smaller. The overall difference in pellet dia. at the extremes in feed location was about 0.3 cm.

For the pilot plant system the pelletizing conditions which best produced the pollution capture pellets are shown in Table 9.

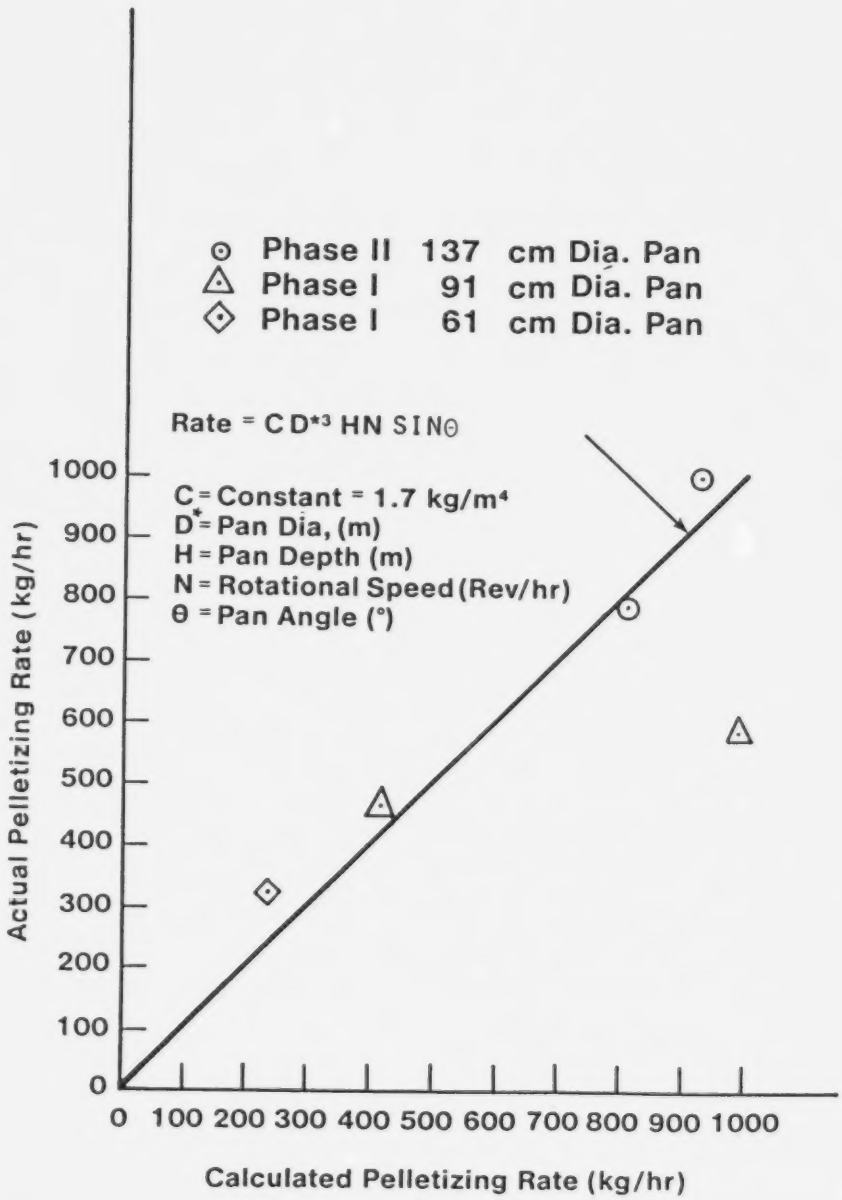

FIGURE 11. PELLETIZING RATE CORRELATION

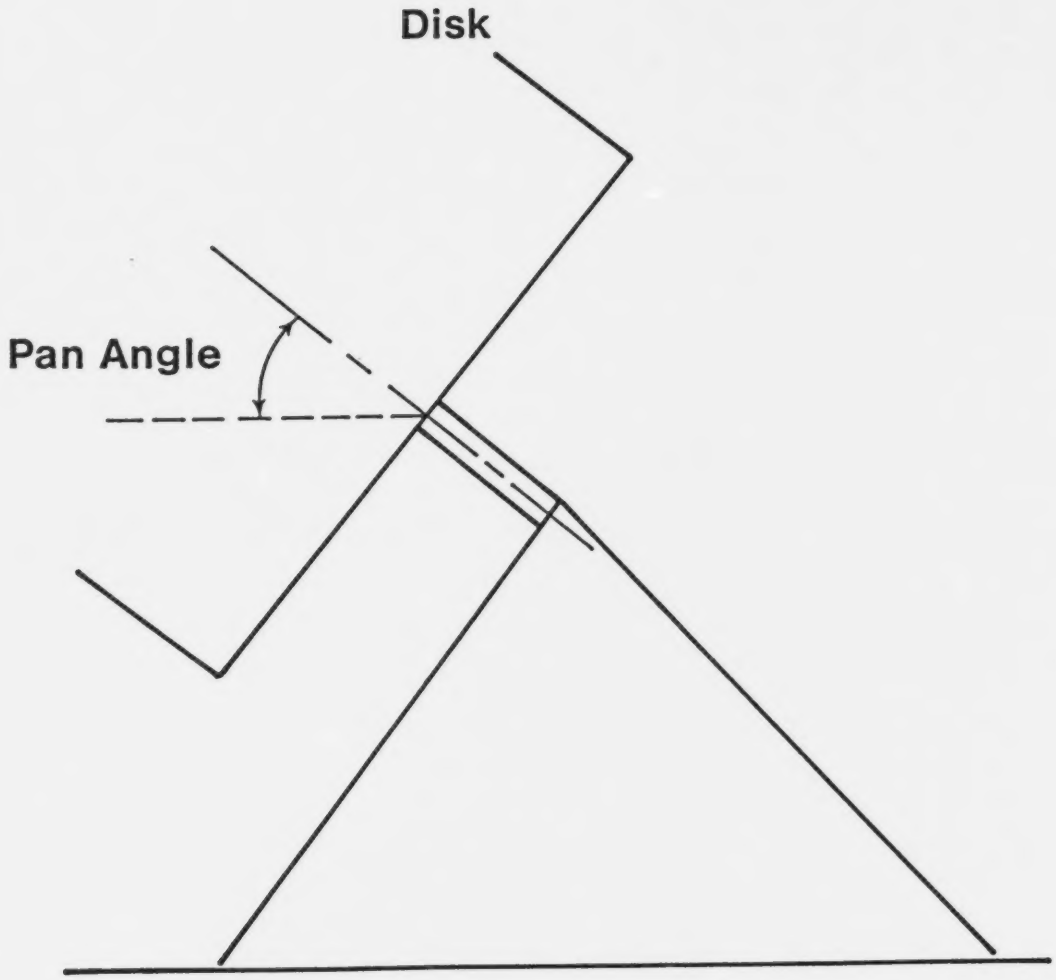

FIGURE 12. PAN ANGLE

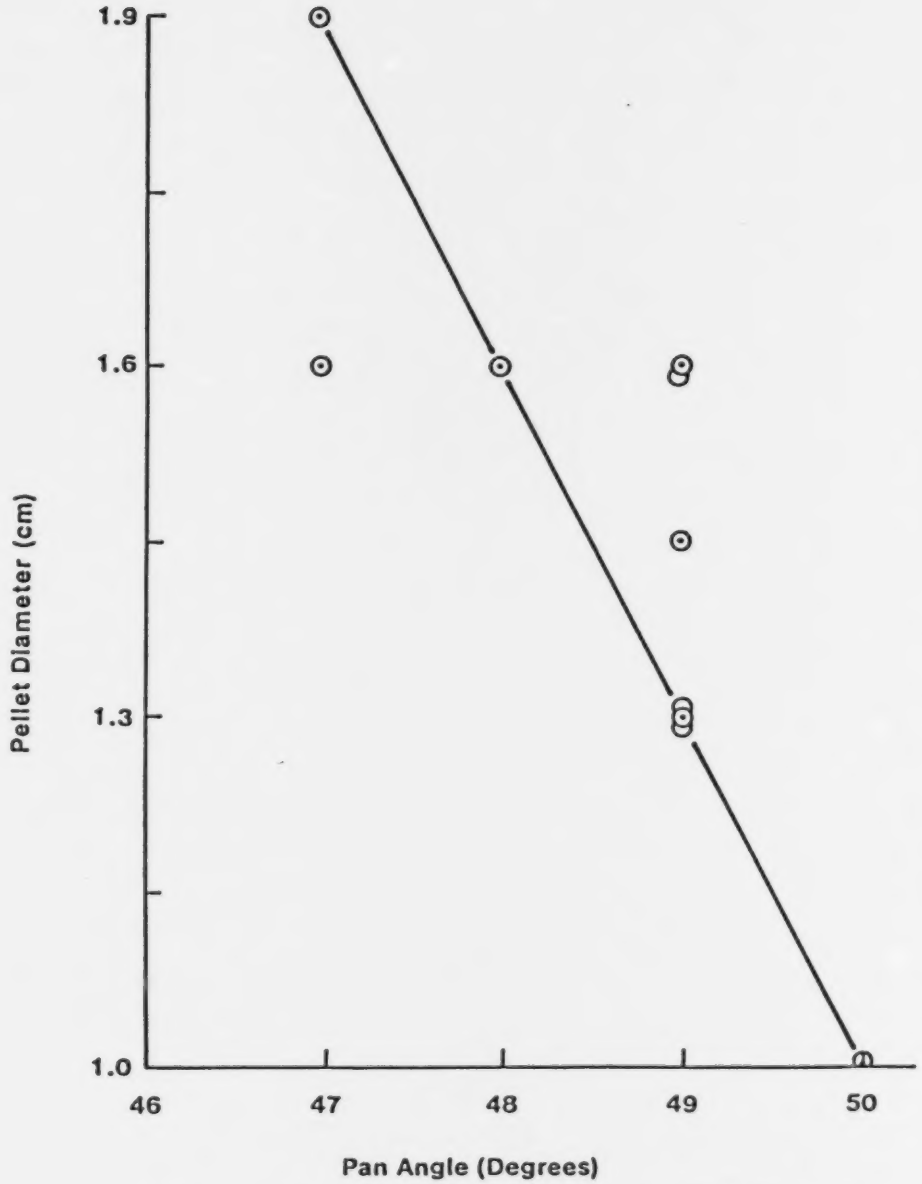

FIGURE 13. PELLET SIZE AS A FUNCTION OF PAN ANGLE (0.355M DEEP PAN)

TABLE 9. PELLETIZING CONDITIONS FOR STABLE OPERATION OF 1.37 m DIA. x 0.335 m DEEP PAN

Batch Feed Rate	635 kg/hr
Water Feed Rate	84 kg/hr
Water Added to Pellets	11.7%
Pan Angle	41°
Pan Rotational Speed	13 RPM
Pan Linear Speed at Rim	56 m/min
Batch Feed Location	
0.4 m Below Center Plow (See Figure 9)	
Water Spray Location	
One on center stream adjacent to batch feed One on recirculating pellets (See Figure 9).	

Pellet Size and Strength

Pellet size and strength were used as the quality control properties for the pelletizing process. Size was measured by screening samples of wet pellets in Tyler sieves. Ordinarily, the pan produced a very narrow pellet size range during stable operation. Throughout a day of stable operation the pan consistently produced 90-95% of the pellets of 1.27 cm diameter with the remainder plus or minus 0.3 cm.

Pellet strength was measured by a Chatillon model DPP-50 compression gauge. It measured the compressive force on the dry pellet at the time of pellet failure. Data in Figure 14 show that crushing strength (force divided by cross-sectional area) decreases as the size of the pellet increases. Also compared in the same figure are strength data for pellets made in the deep and shallow pans. Data for H/D = .26 were obtained for pellets from two different runs.

The results of the strength test were expected because the smaller pellets seemed to be stronger in casual handling. It is difficult to speculate on why the pellets from the deep pan had less than half the strength of the pellets from the shallow pan. This may be confirmation of unstable pelletizing experienced in the deep pan.

Dust and Fines

The pelletizing process produced dust and fines as a natural by-product. Once the finished pellets were packed in containers, dust from handling was much reduced from what was produced by handling loose batch.

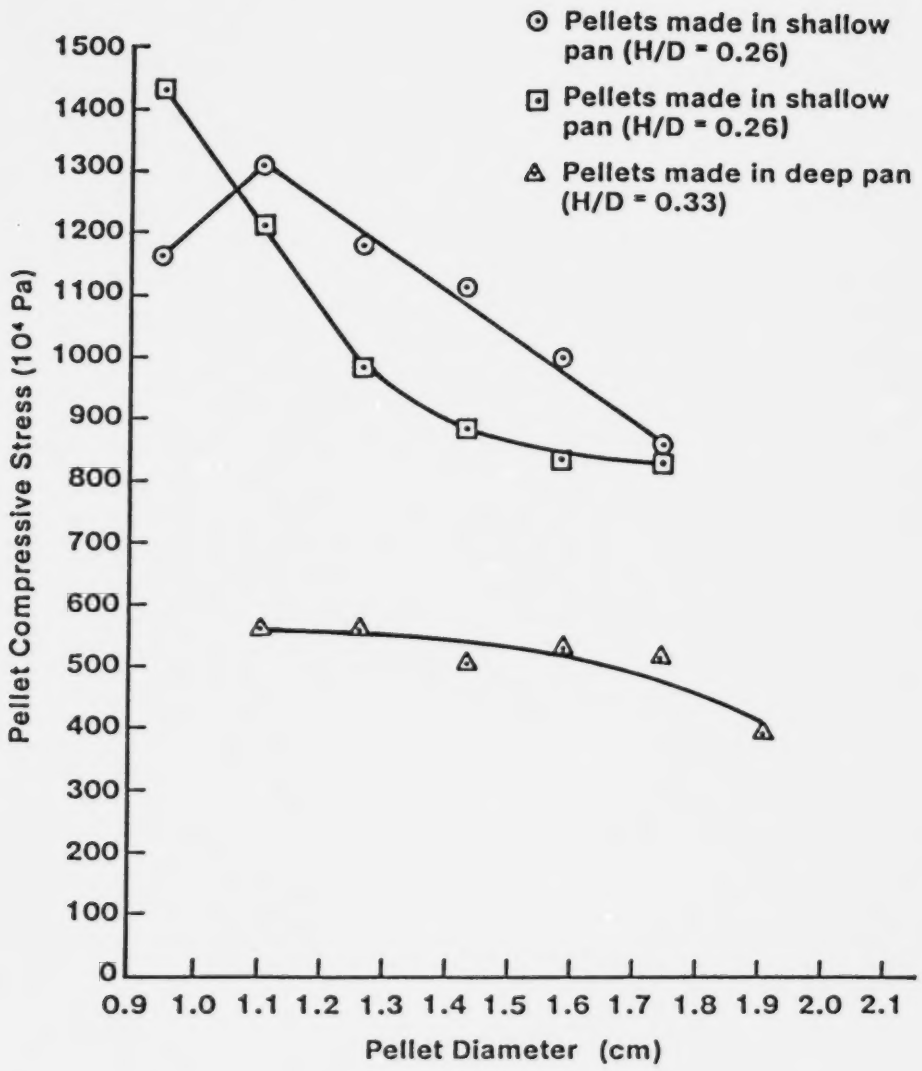

FIGURE 14. PELLET STRENGTH AS FUNCTION OF SIZE

In the PRC installation dust collection was effected at the pelletizer by the dust collector. A 20 cm diameter pipe was mounted on the chute cover just behind the batch feed and a 10 cm diameter pipe hung on the pelletizer superstructure just above the feed location. This combination controlled dust quite well. Location of the water sprays was also important. Water sprayed directly on the batch stream actually increased the dust by blowing the stream. It was desirable to spray water beside the location where the batch hit the pan so that it was immediately wet without being blown about.

It is believed that prewetting of the batch before it reaches the pelletizer will eliminate dust. Addition of 2%-3% water in the batch system may also increase the pelletizing rate.

Dust was produced in the drying system and was much more difficult to control. The major source of dust was the shaft dryer. Fines were produced in the shaft dryer by abrasion of the pellets as they moved through the dryer. Some fines were blown off by the hot gases, exiting in the exhaust duct, and some came out through the vibratory feeder with the pellets. The latter fines were collected when the pellets rolled over a screen and amounted to losses of about 2%-4% of the batch. Overall it is impossible to state how much batch was lost as fines. However, samples of dust from the shaft dryer showed essentially the same assay as the batch. It is believed that a cyclone would be sufficient to recycle the exhaust fines back to the batch system.

Surface Enrichment

Surface enrichment of sulfate in dried pellets has been reported in the literature and confirmed during Phase I.[1] Results of this work also confirmed that some enrichment does take place. Total sulfur was determined by a Leco IR-32 Infrared Sulfur Determinator and reported as SO_3. Alkalinity was determined by titration of the water soluble materials and reported as CO_3. Table 10 shows SO_3 and CO_3 assay results for dried pellets and shaft dryer fines. In the case of the pellets, each pellet was weighed and the surface was scraped until half the weight was scraped off. The SO_3 percentage in the outer shell was 30%-42% higher than in the inner core. Analysis of the fines however, was somewhat contradictory because it showed the sulfate in the fines matched the sufate in the inner cores, although it is believed the fines come from the surface of the pellets.

The carbonate assay was reasonably uniform for all of the samples including the fines.

TABLE 10. CHEMICAL ANALYSIS OF PELLETS AND FINES

SAMPLE	%SO_3	PPM CO_3
Fines from Vibratory Feeder	0.27	9.99×10^4
Inner Core #1	0.26	9.66×10^4
Outer Shell #1	0.34	1.09×10^5
Inner Core #2	0.25	1.00×10^5
Outer Shell #2	0.34	1.07×10^5
Inner Core #3	0.26	9.15×10^4
Outer Shell #3	0.37	8.79×10^4

Handling Wet Pellets

An experiment was conducted in which wet pellets were put directly into a shaft dryer. The intent was to determine whether preliminary drying was necessary before pellets could be put in a shaft dryer.

The temperature in the shaft was increased to 300°C during the experiment. The pellets were delivered from the pelletizer to the shaft dryer on the belt with the belt dryer burner turned off. The effect of the hot gases and wet pellets in the shaft was to produce masses of agglomerated pellets which eventually plugged the shaft dryer.

The results of the experiment indicate that a temperature of 300°C will fuse wet pellets. If the temperature had been below 200°C, it is possible that pellet sticking would not have been as severe, but also likely that the pellets would not have been completely dried.

Operation of the system confirmed results of abrasion tests with partially dried pellets were sometimes weaker than wet pellets. Possibly this is because the dry shell formed with partial drying is less flexible than the exterior of a wet pellet. Partial drying with attendant pellet weakness is more of a problem with large pellets (diameter greater than 1.3 cm.) than with small ones. Some partially dried pellets were less able to survive the drop from the belt dryer to the shaft dryer than undried pellets. From this experience it seems desirable to dry pellets before they enter a shaft and that at least 70%-80% of the water should be driven off in the belt dryer. Larger pellets should be drier than smaller pellets.

BOROSILICATE GLASS BATCH

Borosilicate glass batch was successfully pelletized in the 1.37 m (4.5 ft) pelletizer. The batch used is shown in Table 11. The pelletizer was run with a depth of 0.355m, the angle set at 49° and a speed of 10 RPM. Pellets were made in a continuous operation at 363 kg per hour. The maximum and minimum throughput rates were not investigated. Pellets were formed with 10.6% water added. This batch was relatively easy to pelletize and made uniform, strong pellets.

TABLE 11. BOROSILICATE GLASS BATCH

Glass Composition

Oxide	Weight %
SiO_2	8.60
B_2O_3	12.90
Na_2O	4.25
Al_2O_3	2.25

Batch Material

Raw Material	Weight %
Oklahoma Dry Sand, PGS Corp	54.6
200 Mesh Supersil Sand, PGS Corp	23.4
Boric Acid, U.S. Borax	7.0
Anhydrous Borax, U.S. Borax	12.6
A-1 Alumina, Alcoa	2.2
Sodium Chloride, Watkins Salt Co.	0.2

Drying the borosilicate batch proved to be difficult with the pilot plant equipment. In the first attempt to dry the pellets, they slumped into a sticky mass on the belt. It was found that if wet pellets were heated to 150°C, they would slump and deform. This was attributed to the release of the water of hydration from boric acid. Through trial and error a way to dry the pellets without significant sticking or deformation was found. The successful procedure was to air dry the pellets in the shaft overnight and then heat the pellets to 300°C at 50°C per hour. The air drying reduced the pellet moisture to approximately 2%. More work is needed to determine an optimum drying schedule for this batch. It seems certain that the proper equipment for drying borosilicate glass batch with boric acid will be different from that for soda lime.

SECTION 6

PACKED BED TESTING

This section deals with the particulate capture studies on soda-lime furnace gases passing through a static bed of pellets (packed bed) and through an electrified filter bed device (EFB) in static mode.

Objectives of the test program are discussed first. They are followed by descriptions of the test setup, equipment dimensions test procedures and sampling techniques. Finally, the test results and conclusions are presented. The results are grouped into three catagories: the data on particulate capture, the data on gaseous components capture (or wet catch) and melt studies on pellets.

BACKGROUND AND OBJECTIVES

During Phase I of this project[1], particulate capture tests were conducted on a miniature packed bed of pellets using burner exhaust gases laden with commercial grade sodium sulfate particulates to simulate particulate emissions from a glass furnace. The results were not considered conclusive, because this rather small sized bed introduced wall effects on the particulate capture characteristics, and because the sodium sulfate particulates used were not representative of the usual submicron size condensation products in an actual production furnace environment. Thus, it was recommended that further work be carried out to conduct a more representative test program using a larger size bed and actual soda-lime furnace exhaust gases. The additional work was performed as part of this Phase IIA work plan.

Tests were made on a 0.76 m dia. x 1.52 m deep bed using a slipstream of gases from a soda-lime container furnace operated by Thatcher Glass Manufacturing Company in their Elmira, N.Y. Plant. The soda-lime pellets used in the tests were approximately 1.3 to 1.6 cm in diameter. The testing period lasted six weeks and 19 test runs were completed.

The objectives of these tests were to:

1. Determine particulate capture efficiencies in the packed bed and electrified filter bed using EPA approved pollution testing procedures.

2. Determine particulate size distribution of the emissions at the inlet and outlet of the packed bed.

3. Evaluate the effect of particulates entrained by the pelletized batch with regard to their melting characteristics.

Role of Electrified Filter Bed

During the planning stages of the packed bed test program, preliminary predictions of the collection efficiencies were made using an existing math model[5]. The predicted efficiencies of the packed bed were significantly lower than would have been desirable. Therefore, alternative ways to improve the collection efficiencies of the pellet bed were reviewed. Thus, an electrified filter bed was included in this test program for further evaluation. For details of the EFB concepts and lab-scale EFB test results at Corning Glass Works' Wellsboro Plant, please refer to Section 4. The test of a larger size EFB at the Thatcher Plant provided an opportunity to evaluate the EFB designed specifically for use with glass batch pellets.

TEST SETUP AND EQUIPMENT

A schematic of the packed bed testing equipment is shown in Figure 15. About 5% of the volume of the furnace flue gases was passed through a duct to the packed bed. The duct was designed to include a damper for controlling gas flow through the packed bed system. The gases coming out of the packed bed were drawn into the EFB pilot unit. A cold air inlet was provided for the EFB in order to cool gases if it became necessary. The gases coming out of the EFB were drawn through an induced draft fan and released to the atmosphere. The entire ductwork was insulated with 7.5 cm thick fiberglass insulation in order to minimize heat losses and moisture condensation on the colder parts of the duct. The sampling locations in the system were 1) upstream of the packed bed, 2) between the packed bed and the EFB, and 3) after the EFB. All sampling ports were located at least eight diameters of straight ducting upstream, and two diameters of straight ducting downstream, of the sampling ports. The duct material from the flue to the EFB was made of stainless steel in order to provide for high temperature operation and minimize corrosion inside the duct.

The pellets in the packed bed (Figure 16) were supported by a stainless steel wire mesh screen welded to the bottom of the cylindrical portion of the packed bed. Four access doors (approximately 15 cm by 30 cm) were provided on the side of the packed bed. The access doors were designed for sampling, loading and unloading of the pellets into the packed bed.

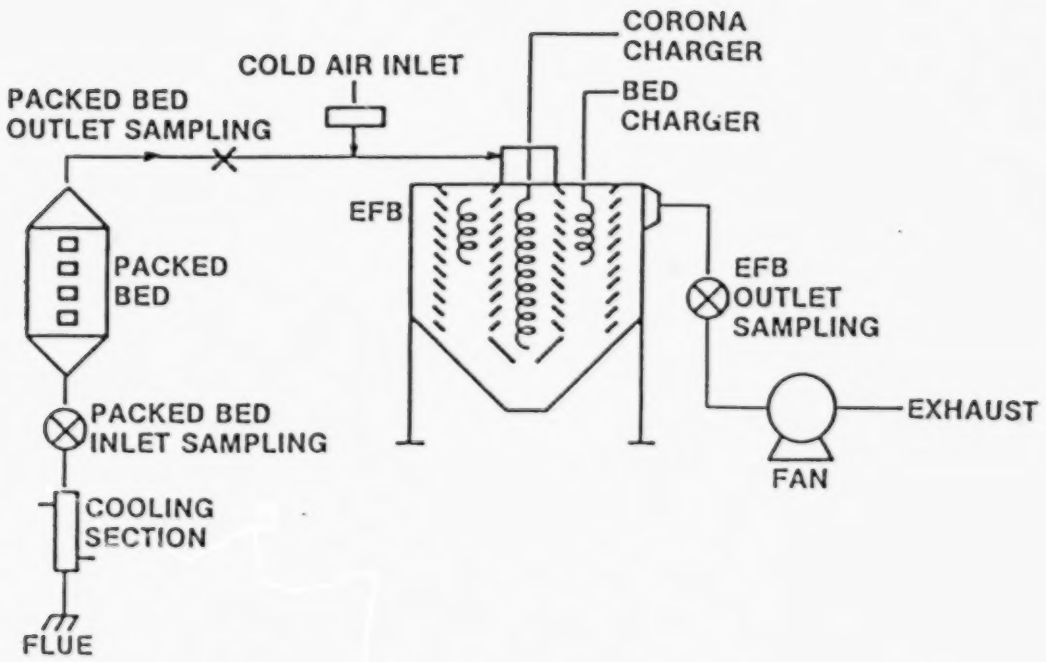

FIGURE 15. SCHEMATIC TEST SET-UP

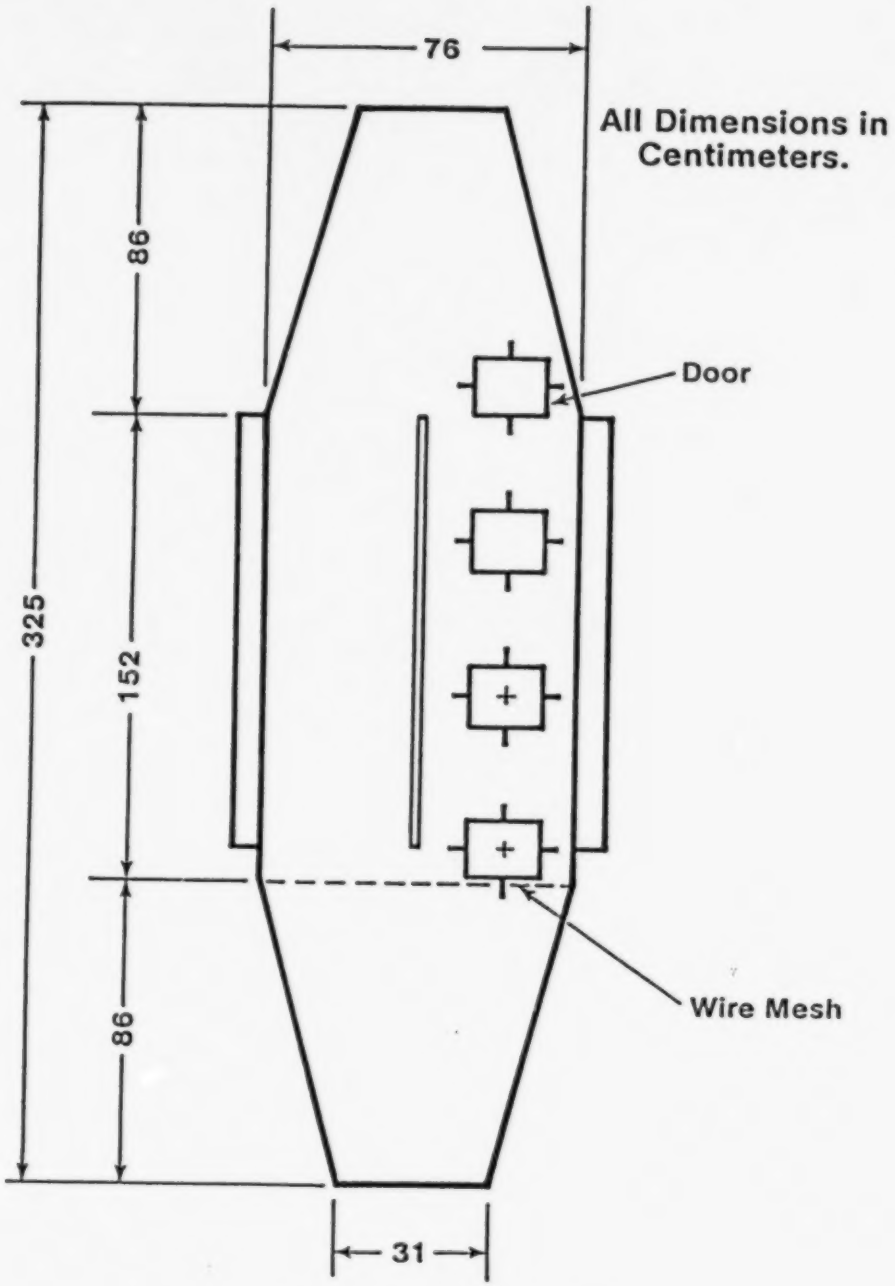

FIGURE 16. PACKED BED DIMENSIONS

The EFB unit used in this program was model no. FDC4K purchased from EFB Inc. This EFB unit was approximately 2 m in diameter, 3 m tall, and was supported on four legs (Figure 17). The bed depth of the pellets inside the EFB was approximately 38 cm in the radial direction. The pellets were fed from the top of the EFB through 15 cm diameter holes located vertically above the annular space of the bed material. The EFB was tested as a static bed. After several tests, the pellets were discharged in the bottom of the annular space through a conical section. This section had a swing lock mechanism to prevent pellet run-off during the batch mode operation. There were two power supply units connected to the EFB. These units were used (1) to charge the particulates before entering the EFB, and (2) to polarize the bed for the capture of the charged particulates. The power units had built-in transformers and rectifiers so that 440 volt or 220 volt A.C. supply lines from the plant could be used.

TEST PROCEDURES

The first step in the procedure was to fill the packed bed and EFB with the necessary quantities of pellets.

Prior to the start of each experiment, fresh pellets were loaded into the packed bed to the desired depth. Because of the very high capacity of EFB ($\cong$ 4,000 kg of pellets) it was not practical for loading EFB on a daily basis. Also, the amounts of particulates collected in the EFB during each day's testing were not sufficiently large enough to require a fresh load of pellets in the EFB every day. Therefore the EFB was refilled only periodically (approximately once a week).

The system was started up by first turning on the exhaust blower to pull a portion of flue gases from the furnace main flue. The dampers in the ducting, were adjusted to maintain the desired gas flow conditions at the packed bed. For the experiments with cooler bed inlet temperatures, the water cooling on the duct was turned on. For some tests, the water cooling was augmented with some dilution air cooling. After a period of warmup in the EFB, the power to the EFB Corona Charger and Bed Charger were turned on and adjusted to predetermined set points. The gas temperatures, static pressures, EFB voltages and EFB currents were recorded frequently during the test.

At least three hours were allowed for the system to reach thermal equilibrium. After this period, the inlet particle size distribution was measured with an 8-stage cascade impactor. This was followed by particulate concentration measurements using EPA Method 5 procedures. Concentration measurements (particulate loading) were made simultaneously both at the inlet and the outlet of the packed bed and the EFB.

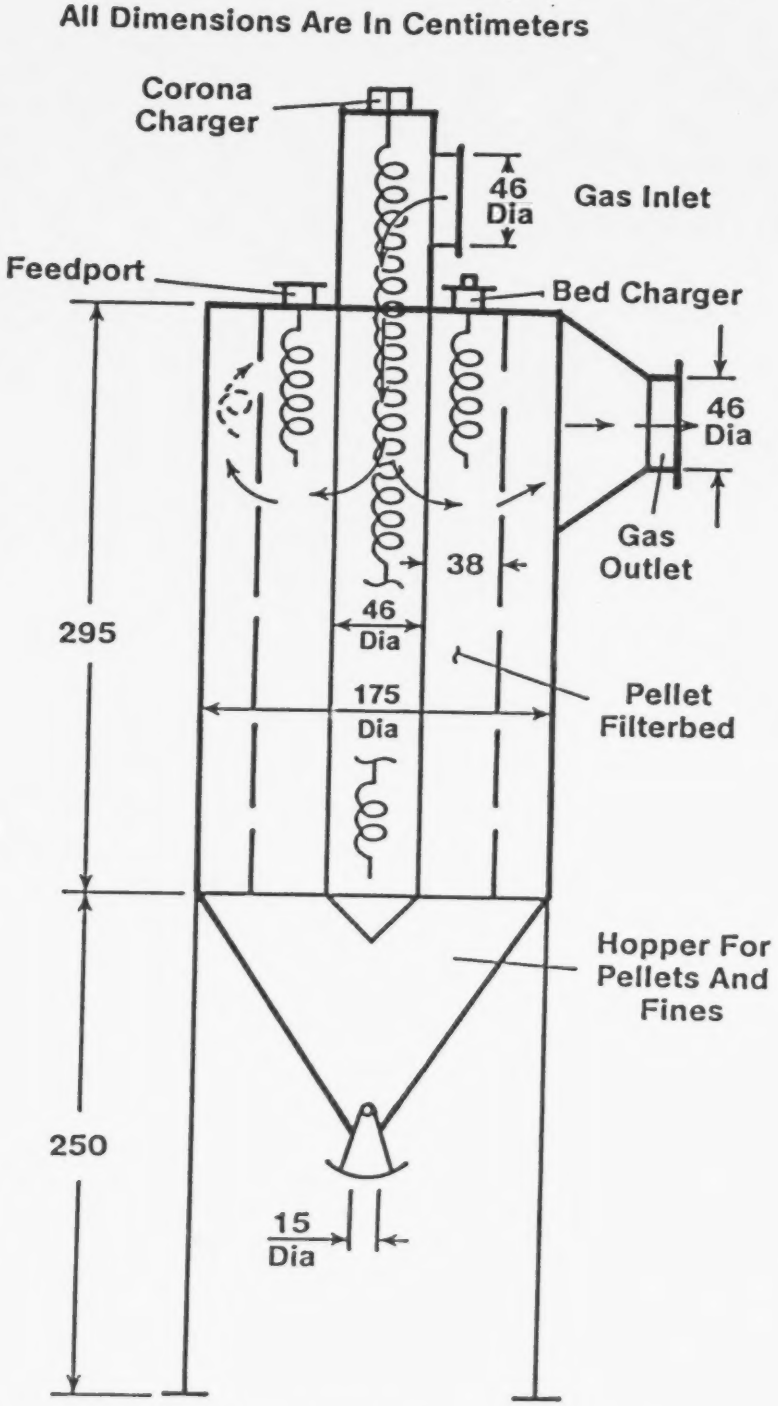

FIGURE 17. ELECTRIFIED FILTER BED DIMENSIONS

Usually, after the particulate concentrations were measured, the particle size distribution at the outlet of the packed bed was measured using an 8-stage cascade impactor. At the end of these measurements the blower was turned off.

In the initial stages of testing, two sets of particulate concentrations were measured for each experiment in the day in order to determine if the bed capture efficiencies reached a steady state or not. The results and conclusions of these tests are discussed later in this section.

In addition to the Method 5 and particle size distribution sampling, periodic measurements for NO_x and SO_x were made at the inlet and outlet of the beds.

The particulate concentrations in the main flue stack were also measured periodically during the test program using EPA Method 5 procedures.

SAMPLING AND ANALYTICAL PROCEDURES

Particulates (Front Half)

Western Precipitator model EPA-11 stack sampling trains were used for particulate sampling (Figure 18). The control consoles were modified by replacing the factory supplied temperature-compensated gas meters with thermocouples in the inlet and outlet pipe connections. The magnehelic gauges normally used on the consoles for the velocity head readings were replaced by Dwyer Model 421-10 inclined-vertical manometers or Model 171 vertical manometers. The choice of manometers was determined by the velocity head in the gas duct. The gas sampling probes were EPA approved stainless steel or glass-lined, with various effective lengths as determined by the location of the sampling point inside the gas duct. The type of nozzles used for the testing were made of stainless steel as approved by EPA. The nozzle diameter was individually selected for each experimental condition in order to facilitate acceptable gas sampling volume at iso-kinetic conditions. The dry test meters and sampling rate orifices of the control consoles were calibrated with a Precision Scientific wet test meter traceable to N.B.S. meter prover bottle. The nozzle diameters were measured with an inside micrometer.

Each test consisted of 16 sampling points (Figure 19) sampled for a total of 80 minutes at the rate of 5 minutes per sampling point. Before and after each sample run, a leak check was performed by sealing off the tip of the nozzle and adjusting it to a vacuum of about 38 cm of Hg.

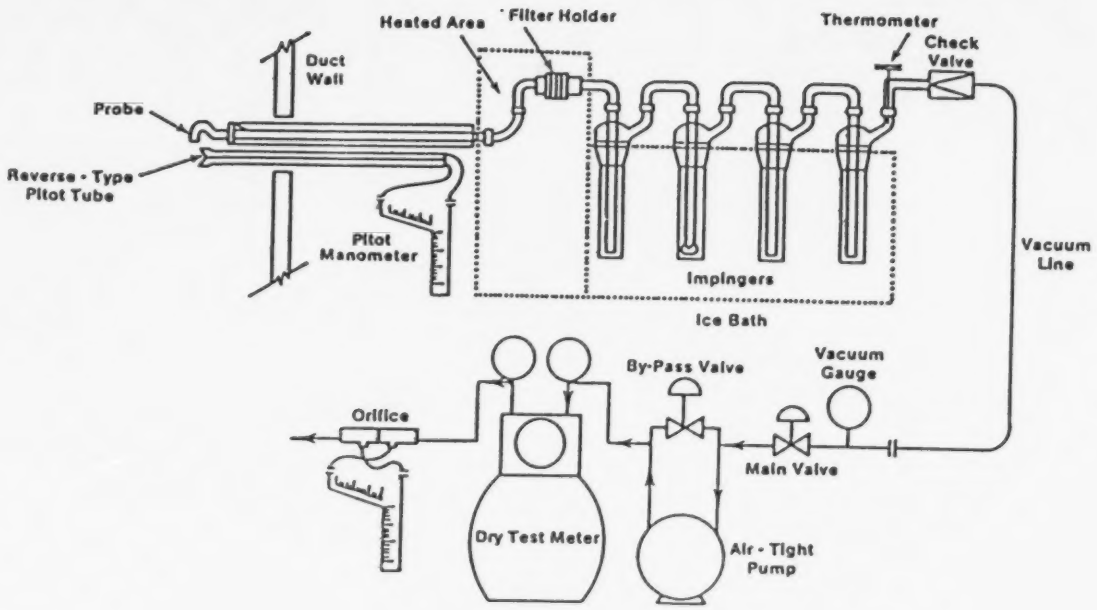

FIGURE 18. PARTICULATE SAMPLING TRAIN

DISTANCE FROM WALL TO SAMPLE LOCATION IN CM

1)	2.2	5)	20.6
2)	3.2	6)	24.6
3)	5.8	7)	27.3
4)	9.9	8)	28.0

I.D. of Duct = 30.5 cm

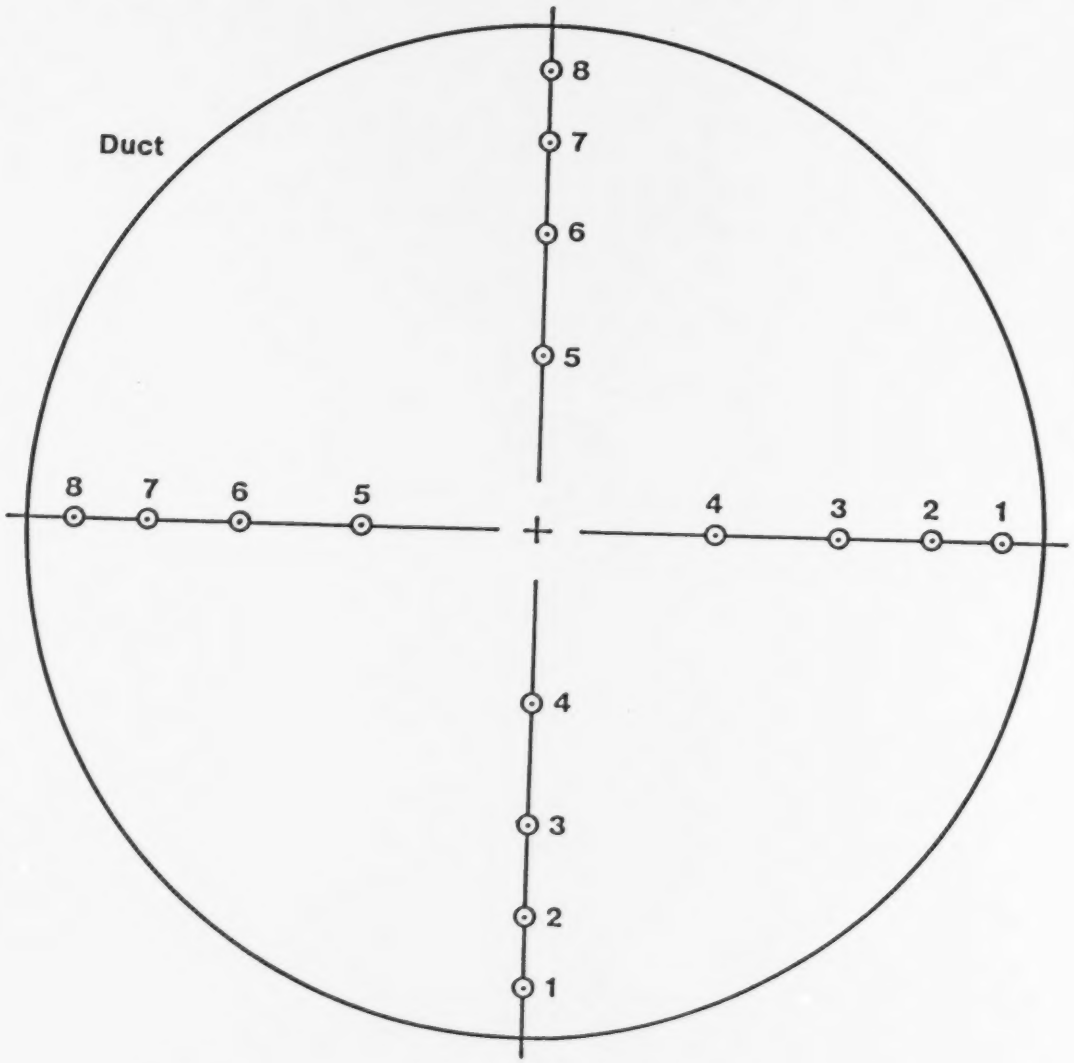

FIGURE 19. METHOD 5 SAMPLING LOCATIONS

After each test, the probes were removed from the sample cases and allowed to cool to ambient temperature. The probe liners were then rinsed with Reagent Grade Acetone. These probe washes were collected in a wide mouth polyethylene bottle. A nylon brush with a teflon handle was used with subsequent rinses to assure collection of particulate matter from the inside surface of the probe. The sample cases were removed to a clean area after each test. Filters were then removed from the case and immediately placed in a desiccator. All inner glass surfaces, upstream of the filter, were rinsed with Reagent Grade Acetone. A rubber policeman and a nylon brush were used with subsequent rinses to assure collection of all particulate matter. These rinses were added to the respective probe wash bottle for each sample.

The glass fiber filters were removed from the desiccator and weighed to the nearest 0.1 mg. The filters were redesiccated and reweighed until the net weight gains were constant within 1% of the weight of the filter catch. The contents of each probe wash bottle were placed in tared evaporating dishes. The acetone was then allowed to evaporate at ambient temperature and pressure. The dishes were weighed to the nearest 0.1 mg and weight gain was added to filter catch and reported as particulate (front half).

Solubles and Condensibles (Back Half)

The liquid from the impinger section of the sampling train was emptied into a graduated cylinder and the net volume gain was recorded as condensate. The silica gel impinger was removed and weighed to the nearest 0.5 gm. The net weight gain in the gel was added to the condensate volume and reported as moisture content. In some tests a 80% Isopropanol and 3% H_2O_2 solution in water was used in order to analyze for the SO_2 and SO_3 content in the gases. After sampling, the isopropanol and hydrogen peroxide solutions were treated in the lab with excess quantity of barium chloride. The resulting barium sulfate was quantatively determined using precipitation or turbidiametric techniques. These sulfate data were converted to SO_3 concentration for the isopropanol catch, and to SO_2 concentration for the hydrogen peroxide catch.

In addition to SO_x measurements, the gas stream was also sampled for NO_x. The NO_x sampling was done using Monitor Laboratory's Model 8430 NO_x analyzer.

Particle Size Distribution Sampling

An Anderson 2000 Inc. 8-stage hi-temperature cascade impactor was used for this sampling. Reeve Angel fiberglass substrates were used on all stages. The sampling was done at the midpoint

of the duct with the probe facing the gases and particulates. The sampling duration was approximately 15 minutes. Before each iso-kinetic sampling was begun, the impactor was placed inside the gas duct with the probe closed off to the gas stream and allowed to reach thermal equilibrium for about 45 minutes. The substrates were stored carefully in clean aluminum foils before and after sampling. The handling of the substrates during the assembly and disassembly of the 8-stage impactor was done in a clean environment. The weighings were done before and after sampling to the nearest 0.01 mg.

Pellet Melts

About 2 kg of pellets were collected from the packed bed before the start of two of the experiments. After each experiment was completed, about 2 kg of pellets were collected from the top of the packed bed, and from the bottom of the packed bed. (The bottom of the bed faced the inlet gas stream.) The samples collected after the experiment were cooled and stored in polyethylene bags. In the case of the EFB, sample pellets were collected occasionally as the EFB was being drained and refilled. The melt study data and conclusions are reported later in this section.

For melt studies, about .45 kg samples of pellets were melted in platinum crucibles for three hours at 1400°C using an electric furnace. The melts were poured into 0.6 cm thick discs and annealed. A portion of each melt disc was cut out, then ground and polished. The ground and polished samples were then analyzed by a Siemens SRS-1 X-ray spectrometer using a chromium x-ray tube operating at 2000 watts as the source of x-rays. Accuracy of the SRS-1, based on XRF statistics of counts and x-ray standards, is shown in Table 12.

TABLE 12. X-RAY SPECTROMETER ACCURACY

Al_2O_3	±	.05%
Fe_2O_3	±	.005%
CaO	±	.05%
MgO	±	.05%
BaO	±	.03%
Na_2O	±	.10%
K_2O	±	.03%
SO_3	±	.02%
Cr_2O_3	±	.003%

For seed counts, a 10 sq. cm portion from the melt disc was submerged into a monochlorobenzene filled petri dish. The sample was placed in a "seedscope" (a black shadow box with a magnifying lens overtop and lit from the side). The seeds were counted and reported as number of seeds per gram of glass weight.

TESTING STRATEGY AND EXPERIMENTAL CONDITIONS

The overall strategy of the bed testing was to move toward maximizing the bed capture efficiency by setting the operating conditions for each experiment. Additional experiments were also conducted in order to establish reproducibility of testing and scale-up parameters. The bed study variables were bed depth, gas velocity and gas temperature. A summary of the range of variables studied is shown in Table 13.

A limitation in the packed bed testing was that a wide range of gas temperatures could not be studied due to lower than anticipated flue gas temperatures. The size distribution of the particulates in flue gases was dictated by the furnace operating conditions during testing. However, it was found that the particle size distributions at the inlet of the packed bed remained relatively constant (as will be seen later). The specific operating conditions for the packed bed testing are shown shown in Table 14.

TABLE 13. RANGE OF EXPERIMENTAL VARIABLES

	Units	Range
Packed Bed:		
Bed Depth	m	0.6-1.5
Gas Velocity	m/sec	0.6-2.9
Gas Temperature	°C	260-370
EFB:		
Gas Volume	m^3/min	25-200
Gas Temperature	°C	150-265
Bed Voltage	kv	0-9.5
Corona Current	mA	1.5-3.5

TABLE 14. EXPERIMENTAL CONDITIONS - PACKED BED

Test No.	Date (1980)	Flue Gas Temp. °C	Gas Temp. In °C	Gas Temp. Out °C	Bed Depth m	Pressure Drop Pa	Gas Velocity (Avg.) m/sec
1	4/12	449	371	339	1.52	2490	1.60
2	4/13	420	347	303	1.52	2950	1.52
3	4/14	393	269	225	1.52	750	0.75
5	4/21	458	307	264	1.52	3750	1.74
6	4/22	449	392	347	0.61	1244	1.84
7	4/23	400	318	274	0.61	374	0.85
8	4/26	450	320	291	0.61	2000	1.60
9	4/29	436	302	252	1.52	4000	1.55
10	4/30	455	302	244	1.52	750	0.58
11	5/1	469	310	259	1.52	7719	1.95
12[2]	5/2	471	268	246	1.07	6972	2.84
18[2]	5/14	445	307	270	1.52	2500	2.65
19[2]	5/15	450	366	319	1.52	7110	2.90

1. The gas velocity was computed based on the average of inlet and outlet gas volumes in the packed bed. The leakage into the packed bed was assumed to be 10%.

2. These two experiments were conducted by pre-charging the particulates upstream of the packed bed.

The EFB was tested at different gas volumes, gas temperatures, bed voltages and corona currents. Since the collection mechanism in the EFB is conceptually different than in the packed bed, the strategy of EFB experimentation was to:

1. Test EFB initially at gas volumes and temperatures as dictated by the packed bed experiments. During this period, the bed voltage was primarily at 5 kv and the corona current at 3 mA.

2. Test EFB at design gas velocities using bed voltage and corona current as experimental variables. (Tests 13 to 17).

The specific operating conditions for the EFB are shown in Table 15.

TABLE 15. EXPERIMENTAL CONDITIONS - EFB

Test No.	Date (1980)	Flue Gas Temp. °C	Gas* Temp. °C	Pressure Drop Pa	Velocity+ (Avg.) m/sec	Bed Voltage kv	Bed Current mA	Corona Voltage kv	Corona Current mA
4A	4/17	426	213	<200	0.1	9.5	685	39	3.1
4B	4/17	426	213	<200	0.1	5.0	300	39	3.3
5	4/21	458	193	<200	0.18	5.0	53	34	3.3
6	4/22	449	252	<200	0.16	5.0	284	33	3.2
7	4/23	400	166	<200	0.08	9.8	115	36	3.0
8	4/26	450	210	<100	0.15	5.0	68	33	3.1
9	4/29	436	186	<100	0.14	5.3	43	32	3.6
10	4/30	455	160	<200	0.05	2.1	8	36	3.1
11	5/1	469	191	700	0.2	2	8	29	2.9
12	5/2	471	193	250	0.27	5	34	30	3.0
13A	5/5		260	1600	0.65	5	667	27	3.0
13B	5/5		265	1600	0.64	0	0	27	3.0
14A	5/7	467	227	<200	0.49	5	408	28	3.0
14B	5/7	472	232	<200	0.51	2	174	28	3.1
15A	5/8	469	227	1000	0.48	5	535	22	1.5
15B	5/8	467	231	1000	0.48	0	0	27	3.0
16	5/9	470	206	750	0.48	9	442	28	3.0
17A	5/12	467	204	<200	0.63	9	467	29	3.0
17B	5/12	438	204	<200	0.17	0	0	33	3.0

* Average of EFB inlet and outlet gas temperature.

+ The gas velocity was computed based on the average of the inlet and outlet gas volumes in the EFB.

In summary, a total of 19 experiments were conducted on the packed bed and/or EFB. Data collected, using EPA approved procedures, showed excellent consistency in sampling and led to generally conclusive results as will be seen in the next subsection.

Since the main objective of the test program was to test the effectiveness of a packed bed and EFB in controlling pollution, a data base was necessary for comparison purposes. Therefore, the emissions from the main stack were measured periodically during this test period. The stack gas flow rates during the test period ranged between 850 m^3/min and 1000 m^3/min while the glass production was approximately 2.5 x 10^5 kg/day.

RESULTS AND CONCLUSIONS

Because of the considerable extent of the experimental work done in this test program, the results and conclusions are categorized and discussed in the following order:

- °PACKED BED
  - -Capture Efficiency Studies
  - -Particle Size Distribution Studies
  - -Pellet Melt Studies
- °ELECTRIFIED FILTER BED
  - -Collection Efficiency Studies
  - -Pellet Melt Studies
- °NO_x DATA FROM PACKED BED AND EFB
- °STACK EMISSIONS DATA
- °PACKED BED EFFICIENCY CORRELATION AND SCALE-UP

Capture Efficiency Studies in Packed Bed

Particulate Collection

Table 16 summarizes the particulate collection efficiencies of the packed bed for different bed depths and gas velocities. At a first glance, these data show that capture efficiency can be increased by increasing bed depth and/or gas velocity. A more detailed discussion of capture efficiencies will follow, after the phenomenon of "blow-off" in the packed bed is discussed.

TABLE 16. SUMMARY OF PARTICULATE CAPTURE EFFICIENCIES IN THE PACKED BED

Bed Diameter (D) = 0.76m
Pellet Diameter (d) = 1.38 cm
(weighted avg.)

Run No.	Avg.** Gas Temp. (Tg) °C	Bed Depth (L) m	Avg. Gas Velocity (Ug) m/Sec	Capture*** Efficiency %
7	296	0.61	0.85	20
8	306	0.61	1.60	30
6	370*	0.61	1.84	31
12	257	1.07	2.84	54
10	273	1.52	0.58	43
3	247	1.52	0.75	48
2	325*	1.52	1.52	60
9	277	1.52	1.55	66
1	355*	1.52	1.60	59
5	286	1.52	1.74	72
11	285	1.52	1.95	71

NOTES:

1. Collection efficiences are listed in the increasing order of bed depth (L) and gas velocity (Ug).
2. * Higher temperature experiments.
3. ** Average of inlet and outlet process gas temperatures (not Method 5 Probe).
4. *** Ratio of difference between inlet and outlet concentrations and the inlet concentration.

Table 17 shows two sets of collection efficiency data for some of the 1.52m bed experiments. These were the early experiments in the test program. During these early tests, in each day, particulate concentrations were measured twice to verify that the capture efficiency in the bed reached a steady state. However, it was observed that the second sampling usually showed higher capture efficiency than the first sampling. Interestingly, there was little difference in the capture efficiency data for the two samplings in the test run 3 (low gas velocity). Prior to these tests, during pelletizing operations the finished pellets were found to contain some amounts of surface fines. Therefore, it was theorized that these surface fines in the pellets were being continually blown away (especially at higher gas velocities)

for a period of time until the dusting decreased and until the particulates formed a more rigid surface on the pellets. This "blow off" phenomenon is time dependent as one would expect. Thus, an experiment was devised wherein the initial sampling was done after allowing time for this "blow-off" effect. The time allowed was about 6 hours and the gas velocity was 1.55 m/sec. (Run No. 9). Results of this experiment showed very good agreement between initial and final sampling data as shown in Table 17. Based on this conclusion, all further tests were conducted after about 4-6 hours from the start of the gas flow. Thus the conclusions that are presented below are based on a consistent frame of reference, namely static bed conditions.

TABLE 17. PACKED BED "BLOW OFF" AND CAPTURE EFFICIENCY

Bed depth (L) = 1.52m

Run No.	Gas Velocity m/Sec.	Capture Efficiency Initial Sampling %	Capture Efficiency Final Sampling %
1	1.6	43	59
2	1.52	46	60
3	0.75	48	48
5	1.74	61	72
9	1.55	65 (after 6 hrs.)	66

Effect of Gas Velocity on Efficiency:

Packed bed results (Table 16) consistently show that the capture efficiency can be increased significantly by increasing gas velocity. For example, capture efficiency increased up to one half when the gas velocities were approximately doubled. This was observed for both 1.53m and 0.61m bed depths. (Run No. 5 and 8 respectively). Refer to Figure 20 for a graphical representation of the effect of velocity on particulate collection efficiency.

Effect of Bed Depth on Efficiency:

In the range of bed depths studied, a proportionate increase in capture efficiency is observed when the bed depth is increased. This is also shown in Figure 20.

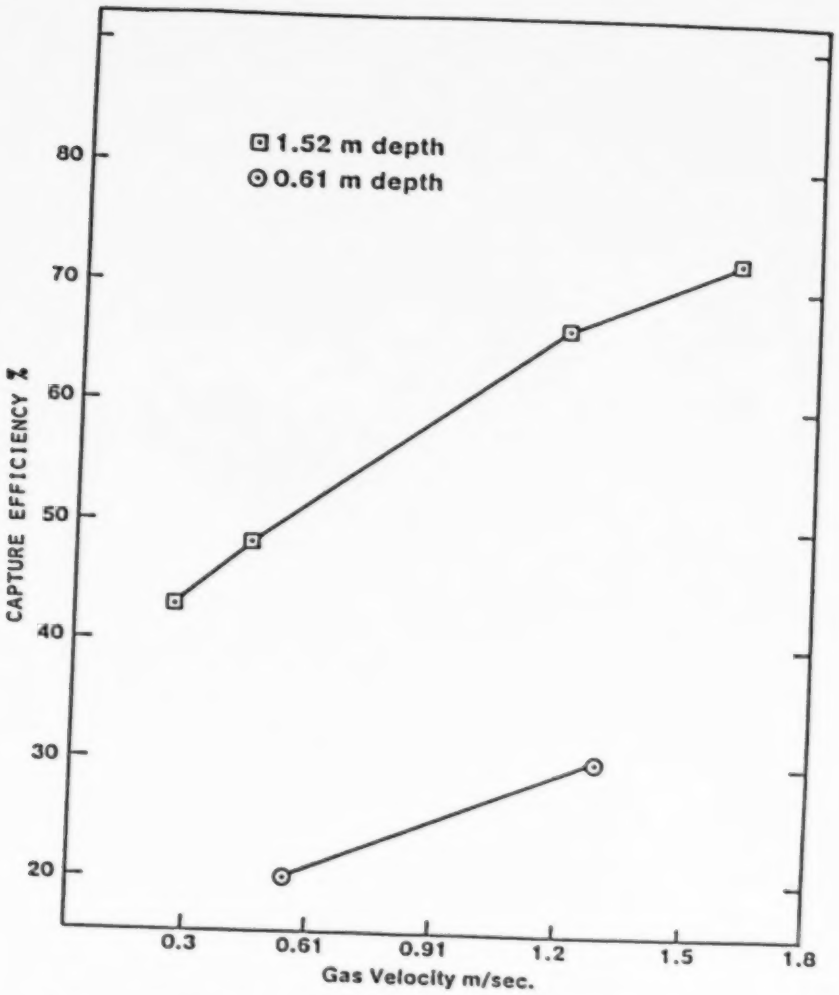

FIGURE 20. PACKED BED CAPTURE EFFICIENCY: EFFECT OF GAS VELOCITY AND BED DEPTHS

Effect of Gas Temperature on Efficiency:

In the range of gas temperatures studied, the capture efficiency decreased when the gas temperature was increased. Table 18 lists the results showing the temperature effect on the packed bed capture efficiency.

TABLE 18. EFFECT OF TEMPERATURE ON EFFICIENCY (PACKED BED)

Run No.	Avg. Gas Temp. °C	Bed Depth (L) m	Avg. Gas Velocity m/sec	Collection Efficiency %
8	306	0.61	1.6	30
6	370	0.61	1.84	31*
9	277	1.52	1.55	66
2	325	1.52	1.52	60
1	355	1.52	1.60	59

* Temperature effect may be offset by the gas velocity effect.

Effect of Pre-Charged Particulates on Efficiency:

The electrified filter bed principle of capturing particulates by imposing an electric charge on them was extended to the packed bed under the guidance from EFB Inc. A corona charger was placed just ahead of the packed bed and the packed bed itself was not electrified. This principle is described as "image-charging" whereby charged particulates would naturally deposit on the bed of pellets, without any electrostatic augmentation in the bed. Two experiments were conducted both aimed at the maximum achievable collection efficiency for the packed bed. Thus, the deepest (1.52m) bed was chosen for both experiments. The first experiment was conducted in order to establish a base point for gas velocity (1.5 m/sec) for comparison of collection efficiency for particulates with no pre-charging. These experimental results are shown in Table 19. The second experiment was conducted by significantly increasing the gas velocity to increase collection efficiency, as seen in earlier experiments.

These two tests show that there is a significant improvement in collection efficiency of the packed bed, if the particulates are pre-charged. Further experimental work should be included in the planned pilot plant preheating and melting demonstration.

TABLE 19. PACKED BED EFFICIENCY ENHANCEMENT WITH PRE-CHARGING OF PARTICULATES

Run No.	Corona Volt KV	Corona Current mA	Avg. Gas Temp °C	Bed Depth (L) m	Avg. Gas Velocity m/sec	Collection Efficiency %
			No Pre-charging			
2	0	0	325	1.52	1.52	60
			Pre-charging			
18	26	2.3	300	1.52	1.5	83
19	22	2.5	360	1.52	2.8	88

Summary Data for Method 5--Filter Catch and Impinger Catch (Packed Bed Experiments)

The weighings from the filters, probe washes and impinger "dry down" were used for computing the particulate concentrations in the gases. From the concentration data and measurements of total gas volume at the sampling locations, the total mass flow rates for the particulates were calculated. The results of these computations are listed in Table 20. The mass flow rate data were used for calculating the capture efficiencies.

SO_x Collection Efficiency of the Packed Bed

The impinger in the sampling train contained H_2O_2 in order to allow SO_2 and SO_3 to be oxidized to SO_4. Thus, the wet catch in the impingers containing H_2O_2 solutions at the inlet and outlet of the packed bed were analyzed for SO_4 content. These SO_4 data were converted to SO_2 equivalents. It was assumed that the presence of SO_3 is insignificant in the total gas make-up. From these equivalents data, the mass loading expressed as SO_2 and packed bed capture efficiencies were calculated. These results are shown in Table 21. It is seen that the SO_2 capture in a 1.52m deep bed is significantly higher than a 1.07m bed. However, it is not clear whether or not the upstream charging of the gases and particulates improves the capture efficiency of the packed bed.

TABLE 20. SUMMARY OF METHOD 5 CATCH (FRONT-HALF) AND IMPINGER CATCH (BACK-HALF) - PACKED BED

Run No.	Packed Bed Inlet					Packed Bed Outlet				
	Gas Temp °C	Front Half (Particulates)		Back Half (Condensibles)		Gas Temp °C	Front Half (Particulates)		Back Half (Condensibles)	
		$\frac{mg}{dsm^3}$	g/min	$\frac{mg}{dsm^3}$	g/min		$\frac{mg}{dsm^3}$	g/min	$\frac{mg}{dsm^3}$	g/min
1	391	107	1.70	28	0.5	218	39	.70	~0	~0
2	353	95	1.60	21	0.3	259	36	.64	6	0.1
3	270	103	0.95	25	0.2	169	42	.50	1	~0
5	293	122	2.32	20	0.4	222	32	.66	7	0.2
6	396	104	2.01	26	0.5	315	66	1.40	11	0.2
7	323	111	1.07	20	0.2	199	71	0.85	9	0.1
8	323	150	2.67	18	0.3	226	83	1.86	13	0.3
9	310	106	1.70	23	0.4	196	29	.57	8	0.2
10	302	173	1.19	15	0.1	196	80	.68	~0	~0
11	310	118	2.56	--	--	173	25	.74	--	--
12	268	98	3.27	--	--	173	35	1.49	--	--
18	305	88	1.62	--	--	265	15	0.27	--	--
19	363	115	3.34	--	--	316	15	0.39	--	--

NOTES:

All values were as measured at each sampling port and rounded to first decimal.

Gas temperatures shown are averages for sampling period measured by Method 5 sample probe, and are not the same as process temperatures reported in Table 16.

For run Nos. 11-18, H_2O_2 solutions were used in the impingers. These H_2O_2 solutions were analyzed for SO_2 (Table 9). In all previous runs, water was used as per Method 5 procedures.

TABLE 21. SO_2 AND SO_3 CAPTURE EFFICIENCES IN PACKED BED

Bed Diameter (D) = 0.76m
Pellet Diameter (d) = 1.38 cm
(weighted avg.)

Run No.	Avg. Gas Temp °C	Bed Depth m	Avg. Gas Velocity m/Sec	SO_2* Inlet Mass Loading g/min	SO_2* Capture Efficiency	SO_3** Inlet Mass Loading g/min	SO_3** Capture Efficiency
			No Precharging of Particulates				
7	296	0.61	0.85	2.1	98	0.21	24
12	257	1.07	2.84	4.6	30	0.97	30
10	273	1.52	0.58	0.2	96	0.12	13
9	277	1.52	1.55	2.4	98		
11	285	1.52	1.95	3.7	96	0.37	58
			Precharging of Particulates				
18	300	1.52	1.5	3.9	96	0.09	56
19	360	1.52	2.8	6.7	91	0.06	51

*From H_2O_2 impingers

**From Isopropanol impingers

Particle Size Distribution Studies:

The type of capture mechanism in a given collection device depends, to a large extent, on the size of the particulates being captured. Therefore, it is important to characterize the particulate size distribution.

It was mentioned earlier that size distribution data were gathered with the use of an 8-stage cascade impactor. This was done according to the state-of-the-art sampling techniques available. The aerodynamic and physical diameter calculations were made from equations shown in Table 22 (from NTIS publication PB-290710, Nov. 1978, "Cascade Impactor Data Reduction with SR52 and TI59 programmable calculators). The data are reported, for various runs, in Tables 23-27. Both aerodynamic and physical diameters were calculated for each sampling and for the outlet and inlet of the packed bed.

TABLE 22. AERODYNAMIC AND PHYSICAL DIAMETER CALCULATIONS

$$DA50I = \left[\frac{(CI)(MU)}{(Q \times 10^{-8})}\right]^{1/2}$$

$$DPHY = \frac{DA50I}{(RHO \times C)^{1/2}}$$

Where $C = 1 + (2)(A)\left[\frac{LAMDA}{DPHY}\right]$

DA50I = Aerodynamic cut diameter (μm)
DPHY = Physical diameter (μm)
TC = Gas temp (°C)
MU = Gas viscosity(poise)$(1.68 \times 10^{-4}) + (2.292 \times 10^{-7} \times (1.8\ TC+32))$
C = Cunningham's correction factor
A = Constant 1.246 to determine Cunningham's correction factor
RHO = Density of particulates (2.68 gm/cm^3)
LAMDA = mean freepath $(.0653)\ \frac{(76)\ (T°K)}{(P)\ \ (296.2)}$
Q = Sample gas flow rate (l/min)
$CI = (0.137)(\pi)(D_i^3)(N_i)K_{50i})$

Where: $K_{50i} = .2$ (constant)

$D_0 = 0.1613$ cm	$N_0 = 264$
$D_1 = 0.1181$ cm	$N_1 = 264$
$D_2 = 0.0914$ cm	$N_2 = 264$
$D_3 = 0.0711$ cm	$N_3 = 264$
$D_4 = 0.0533$ cm	$N_4 = 264$
$D_5 = 0.0343$ cm	$N_5 = 264$
$D_6 = 0.0254$ cm	$N_6 = 264$
$D_7 = 0.0254$ cm	$N_7 = 156$

TABLE 23. INLET PARTICLE SIZE DISTRIBUTION - IMPACTOR DATA

D_A = Aerodynamic diameter (μm)

Run No.		Stage No. 0	1	2	3	4	5	6	7
2	W	88.7	87.2	82.9	81.6	79.3	72.0	51.3	21.1
	D_A	7.31	4.58	3.12	2.14	1.39	.72	.46	.35
3	W	90.6	89.9	88.1	87.5	87.0	75.2	50.6	18.5
	D_A	6.73	4.21	2.87	1.97	1.28	.66	.42	.32
4-1	W	89.0	88.5	88.5	88.4	85.8	76.3	52.0	22.3
	D_A	7.07	4.43	3.02	2.07	1.34	.69	.44	.34
4-2	W	86.8	86.8	86.5	86.5	85.3	77.0	56.6	23.4
	D_A	8.71	5.46	3.72	2.55	1.65	.85	.54	.42
5	W	89.2	89.2	88.1	86.7	84.5	75.6	51.3	21.9
	D_A	7.46	4.68	3.18	2.18	1.48	.73	.47	.36
6	W	92.7	92.2	91.8	90.7	88.4	67.4	40.4	13.0
	D_A	7.19	4.5	3.06	2.10	1.36	.70	.45	.35
7	W	88.0	88.0	87.8	87.8	80.1	80.1	56.7	23.9
	D_A	8.02	5.93	3.42	2.35	1.52	.79	.50	.39
8	W	96.3	95.4	94.7	94.2	92.4	84.0	59.0	22.5
	D_A	7.96	4.99	3.4	2.33	1.51	.78	.50	.38
11	W	86.5	86.5	85.8	84.7	83.1	74.4	49.7	16.2
	D_A	7.35	4.6	3.14	2.15	1.4	.72	.46	.35

W = mass % finer than

TABLE 24. INLET PARTICLE SIZE DISTRIBUTION - IMPACTOR DATA

Dp = Physical diameter (μm)

Run No.		Stage No. 0	1	2	3	4	5	6	7
2	W	88.7	87.2	82.9	81.6	79.3	72.0	51.3	21.1
	Dp	4.29	2.63	1.74	1.14	.69	.29	.15	.10
3	W	90.6	89.9	88.1	87.5	87.0	75.2	50.6	18.5
	Dp	3.93	2.40	1.50	1.04	.62	.26	.13	.08
4-1	W	89.0	88.5	88.5	88.4	85.8	76.3	52.0	22.3
	Dp	4.14	2.53	1.67	1.09	.66	.28	.14	.09
4-2	W	86.8	86.8	86.5	86.5	85.3	77.0	56.6	23.4
	Dp	5.14	3.15	2.09	1.38	.84	.37	0.19	.13
5	W	89.2	89.2	88.1	86.7	84.5	75.6	51.3	21.9
	Dp	4.39	2.69	1.78	1.18	.71	.31	.16	.10
6	W	92.3	92.2	91.8	90.7	88.4	67.4	40.4	13.0
	Dp	4.21	2.57	1.7	1.12	.67	.28	.14	.09
7	W	88.0	88.0	87.8	87.8	80.1	80.1	56.7	23.9
	Dp	4.72	2.89	1.92	1.26	.77	0.33	.17	.11
8	W	96.3	95.4	94.7	94.2	92.4	84.0	59.0	22.5
	Dp	4.70	2.88	1.91	1.26	.77	.33	.18	.12
11	W	86.5	86.5	85.8	84.7	83.1	74.4	49.7	16.2
	Dp	4.33	2.65	1.76	1.16	.70	.30	.16	.10

W = mass % finer than

TABLE 25. OUTLET PARTICLE SIZE DISTRIBUTION - IMPACTOR DATA

D_A = Aerodynamic diameter (μm)

Run No.		Stage No. 0	1	2	3	4	5	6	7
2	W	75.1	74.3	69.4	68.8	68.1	61.3	44.7	18.8
	D_A	6.06	3.8	2.59	1.77	1.15	.59	.38	.29
3	W	91.2	90.0	88.2	87.9	85.9	80.1	62.4	31.8
	D_A	9.95	6.23	4.24	2.91	1.89	.98	.62	.48
5	W	84.1	84.1	84.1	82.6	82.1	74.5	46.0	13.2
	D_A	7.13	4.47	3.04	2.09	1.35	.70	.45	.34
6	W	91.8	90.9	90.9	90.3	89.1	79.7	52.9	18.9
	D_A	7.64	4.79	3.26	2.24	1.45	.75	.48	.37
7	W	85.9	85.9	85.9	85.9	83.9	77.5	55.0	24.3
	D_A	7.98	5.00	3.41	2.34	1.52	.78	.50	.38
9-1	W	84.2	84.2	84.2	84.2	84.2	79.5	53.8	18.2
	D_A	7.54	4.72	3.22	2.21	1.43	.74	.47	.36
9-2	W	84.4	84.4	84.4	84.4	84.4	79.3	48.2	13.3
	D_A	7.40	4.63	3.16	2.16	1.49	.77	.49	.38
10	W	96.6	95.8	95.8	94.2	91.3	83.2	59.8	26.8
	D_A	7.84	4.91	3.35	2.30	1.49	.77	.49	.38
11	W	75.5	75.5	75.5	75.5	75.5	69.7	39.8	10.0
	D_A	6.91	4.33	2.95	2.02	1.31	.68	.43	.33

W = mass % finer than

TABLE 26. OUTLET PARTICLE SIZE DISTRIBUTION - IMPACTOR DATA

D_p = Physical diameter (μm)

Run No.		Stage No. 0	1	2	3	4	5	6	7
2	W	75.1	74.3	69.4	68.8	68.1	61.3	44.7	18.8
	Dp	3.56	2.18	1.44	.95	.57	.24	0.13	0.08
3	W	91.2	90.0	88.2	87.9	85.9	80.1	62.4	31.8
	Dp	5.89	3.62	2.40	1.59	.97	.43	.23	.15
5	W	84.1	84.1	84.1	82.6	82.1	74.5	46.0	13.2
	Dp	4.22	2.59	1.72	1.14	.70	.31	.16	.11
6	W	91.8	90.9	90.9	90.3	89.1	79.7	52.9	18.9
	Dp	4.5	2.76	1.83	1.21	.73	.32	.17	.11
7	W	85.9	85.9	85.9	85.9	83.9	77.5	55.0	24.3
	Dp	4.73	2.91	1.93	1.28	0.79	.35	.19	.12
9-1	W	84.2	84.2	84.2	84.2	84.2	79.5	53.8	18.2
	Dp	4.47	2.75	1.83	1.22	.75	.33	.18	.12
9-2	W	84.4	84.4	84.4	84.4	84.4	79.3	48.2	13.3
	Dp	4.38	2.70	1.79	1.19	.73	.32	.17	.12
10	W	96.6	95.8	95.8	94.2	91.3	83.2	59.8	26.8
	Dp	4.64	2.86	1.90	1.26	0.77	.34	.18	.12
11	W	75.5	75.5	75.5	75.5	69.7	39.8	10.0	
	Dp	4.09	2.51	1.67	1.11	.68	.30	.16	.11

W = mass % finer than

TABLE 27. PARTICLE SIZE DISTRIBUTION SAMPLING DATA

Run No.	Sample Gas Temp. °C	Sample Gas Temp. dsm^3	Particulate Collected in the Probe mg	Total Particulates Collected mg
A. Inlet to Packed Bed				
2	353	0.18	1.05	13.85
3	354	0.27	1.44	21.29
4-1	377	0.20	2.22	20.13
4-2	388	0.13	2.13	17.37
5	324	0.176	2.56	24.28
6	366	0.19	1.53	23.38
7	363	0.15	1.82	15.23
8	321	0.15	0.84	22.57
11	313	0.18	2.64	19.59
B. Outlet of Packed Bed				
2	242	0.28	2.06	11.65
3	156	0.29	0.9	11.02
5	227	0.37	1.87	11.55
6	318	0.31	1.58	19.2
7	254	0.30	2.89	21.07
9-1	216	0.33	1.30	8.23
9-2	213	0.34	1.20	7.69
10	252	0.32	0.6	15.46
11	202	0.39	2.64	10.79

Conclusions Based on Particle Size Distribution Data

One should note that the calculated particle size data for the inlet and outlet of the packed bed cannot, in theory, be compared with full rigor. The reasons are twofold: The sampling gas flow rate effect and the sampling gas temperature effect. For example, in the sampling range of variables studied, a 50% increase in gas sampling rate could increase the calculated diameters by about 20%. Also a 50% increase in temperature could decrease the diameter calculations by about 10%. These two variables enter into the calculations for both aerodynamic and physical diameters. One could normalize these data to some pre-set base temperature. The following conclusions were based on the assumption that the above effects were not significant.

1. The particle size distribution is bimodal. Thus characterization of the particulate size by means of a single geometric mean diameter would be inappropriate. See Figures 21 and 22 for average inlet particle diameters (aerodynamic and physical).

2. The packed bed in most cases appears to preferentially capture the fines. The Figures 23-26 show that the outlet of the packed bed contained less fines than the inlet.

3. A comparison of the outlet size distributions for the packed bed and the EFB (Figure 27) showed that the EFB outlet contained a lesser percentage of fines. However, this is based on only one set of data and thus may not be generalizable.

Pellet Melt Studies - Packed Bed

The crucible melts of the pellets from the packed bed after the pollution tests were chemically analyzed for oxides. The SO_3 and Cr_2O_3 contents of the pellets increased significantly as compared to the untested pellets. These results are shown in Table 28. Also, pellets from the bottom of the packed bed appear to have preferentially captured a higher proportion of these pollutants than pellets in the top of the bed.

The effect of the capture of the particulates on the pellets is reflected in both the color and the seed counts of the pellet melts. It has been generally observed that the presence of Cr_2O_3 contributes the greenish color and the presence of SO_3 is related to the seediness of the glass. The effect of pollutants captured in the pellets appears to be beneficial from the standpoint of seeds in the glass. Table 29 shows the laboratory data on SO_3 and seed counts for the pellet melts. The data show that the seeds are reduced to a significantly lower count for the pollutant coated pellets. The fining action in the melting process may have been enhanced due to the presence of the sodium sulfate particulates.

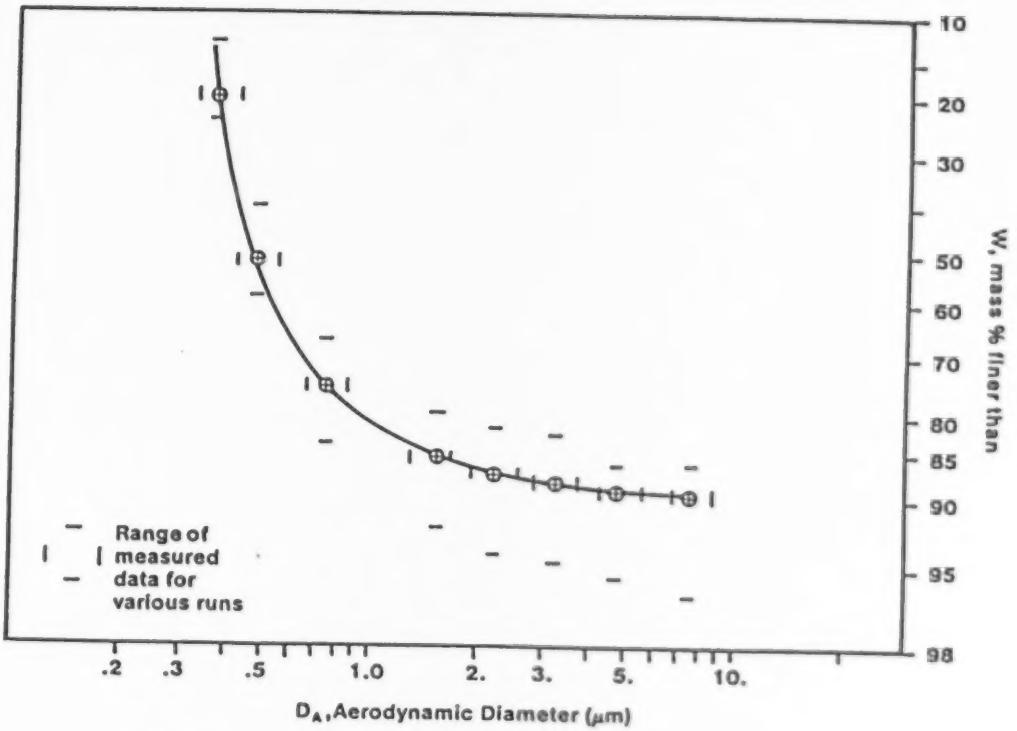

FIGURE 21. PACKED BED INLET PARTICLE SIZE DISTRIBUTION — AERODYNAMIC DIAMETER

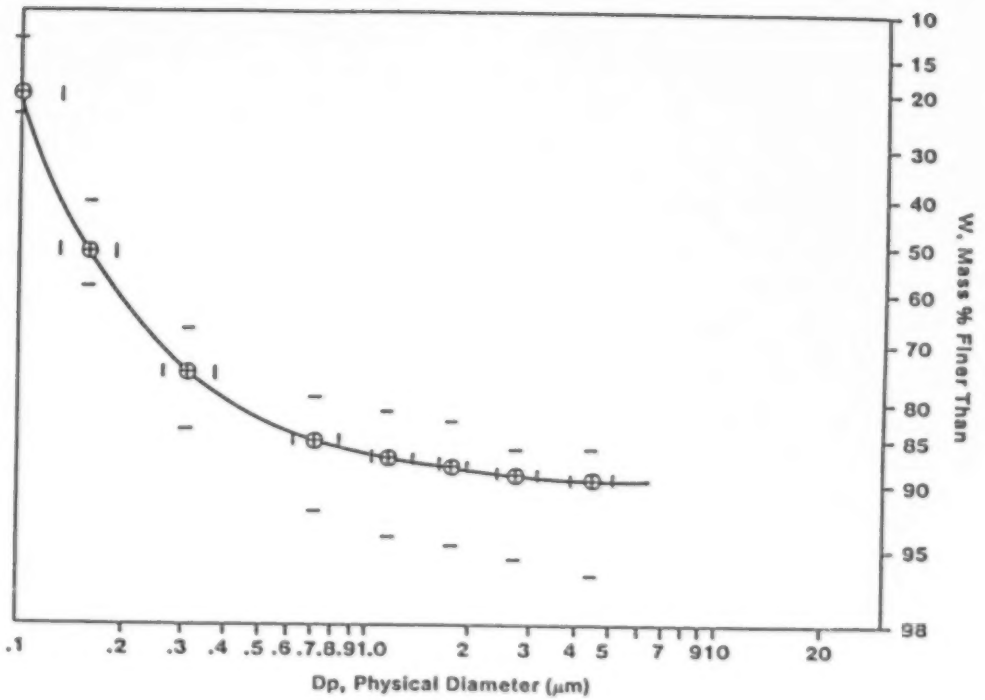

FIGURE 22. PACKED BED INLET PARTICLE SIZE DISTRIBUTION — PHYSICAL DIAMETER

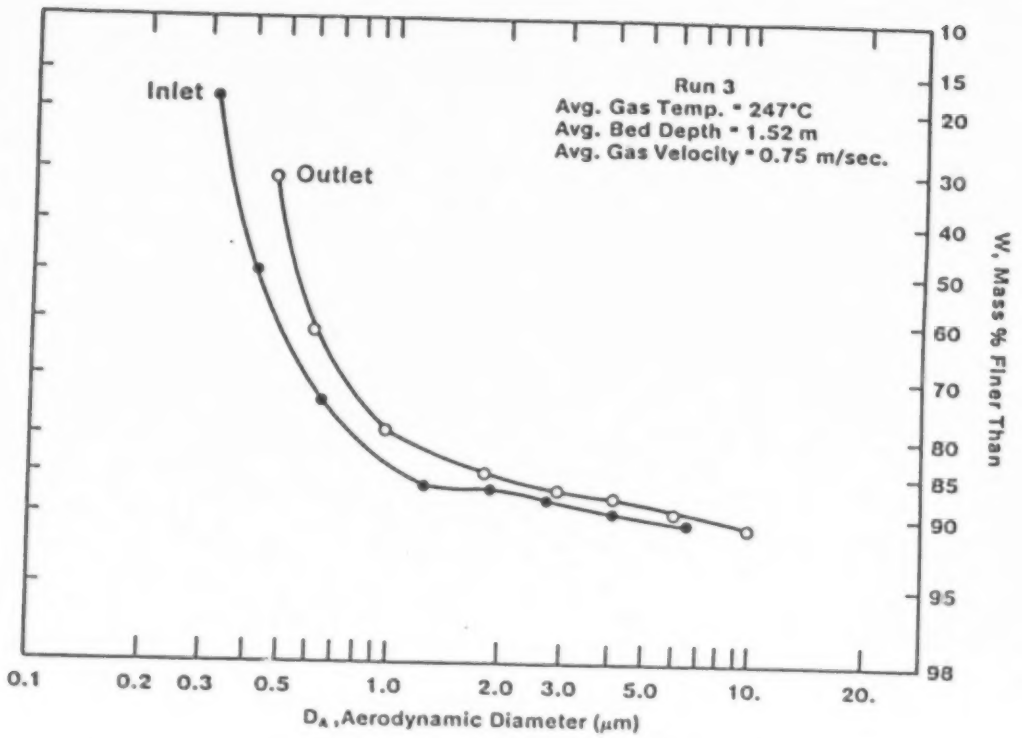

FIGURE 23. COMPARISON OF PARTICLE SIZE DISTRIBUTION BETWEEN INLET AND OUTLET OF PACKED BED

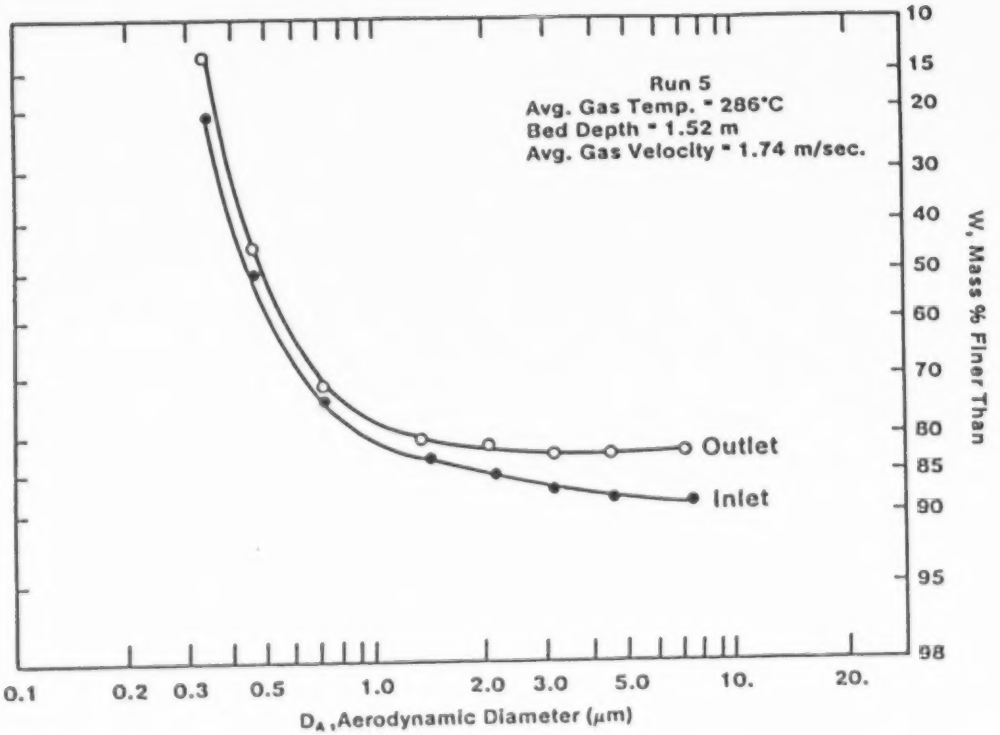

FIGURE 24. COMPARISON OF PARTICLE SIZE DISTRIBUTION BETWEEN INLET AND OUTLET OF PACKED BED

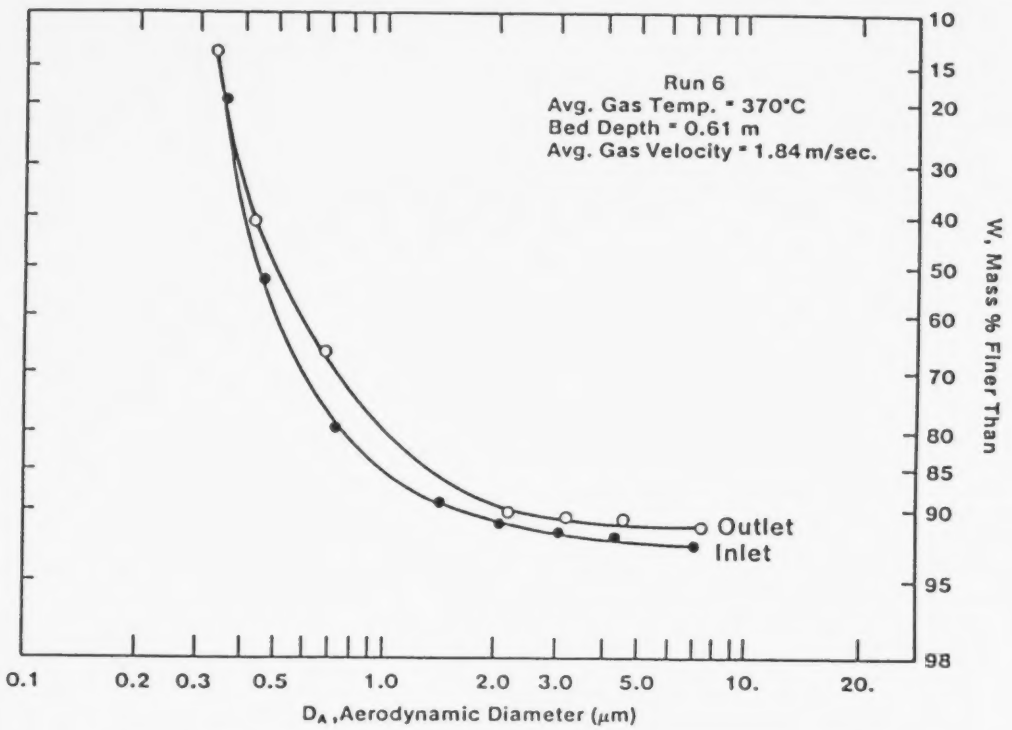

FIGURE 25. COMPARISON OF PARTICLE SIZE DISTRIBUTION BETWEEN INLET AND OUTLET OF PACKED BED

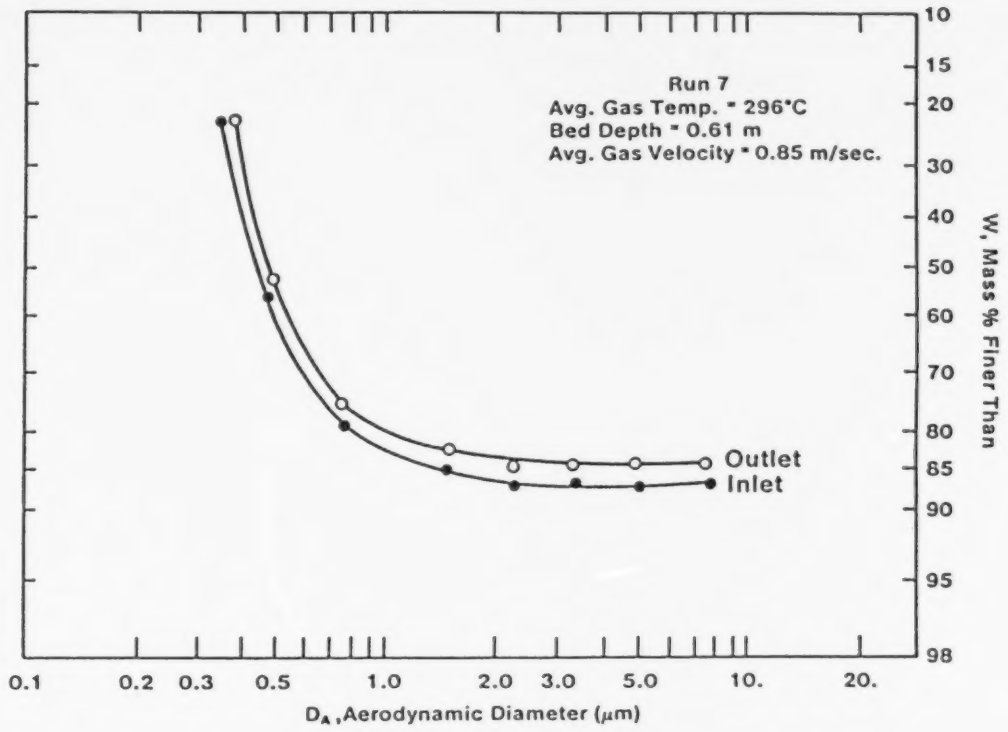

FIGURE 26. COMPARISON OF PARTICLE SIZE DISTRIBUTION BETWEEN INLET AND OUTLET OF PACKED BED

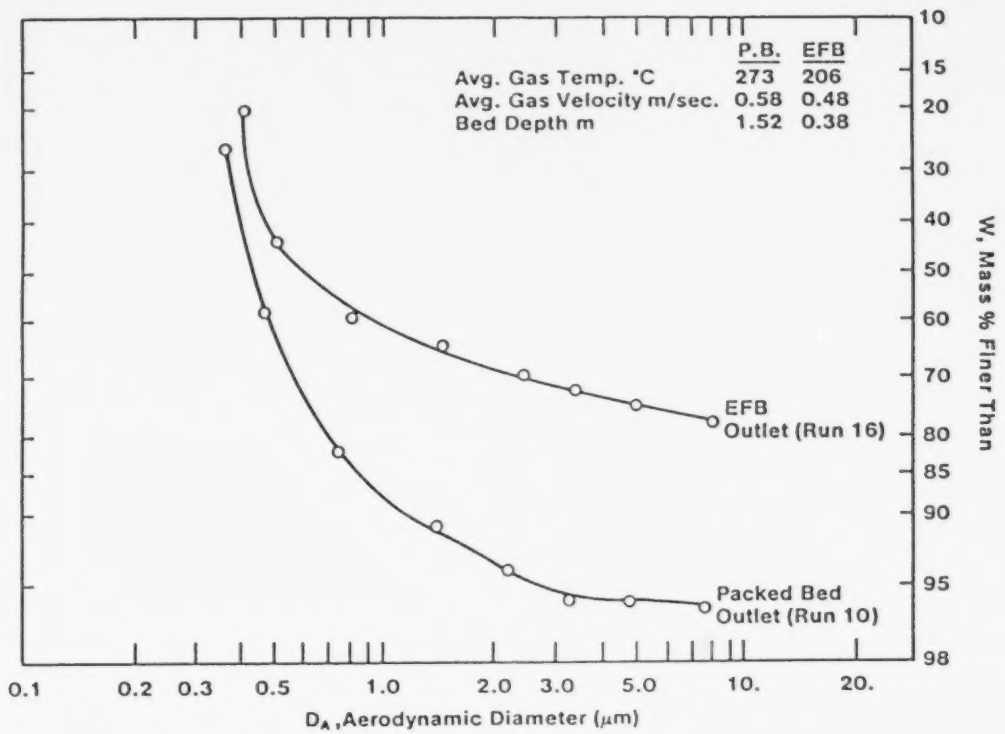

FIGURE 27. PARTICLE SIZE DISTRIBUTION FROM OUTLET OF PACKED BED AND OUTLET OF EFB

TABLE 28. CHEMICAL ANALYSES OF PELLET MELTS - PACKED BED

Sample Type	Avg. Wt. %							
	SiO_2	Al_2O_3	Fe_2O_3	CaO	MgO	Na_2O	SO_3	Cr_2O_3
Fresh Pellets	72.69	1.93	0.076	9.12	2.45	13.04	0.20	≦0.003
Top of Bed	73.35	1.69	0.074	9.05	2.46	12.64	.27	≦0.003
Bottom of Bed	72.95	1.70	0.074	9.10	2.48	12.65	.58	.005

TABLE 29. SO_3 AND SEED COUNTS IN PELLET MELTS - PACKED BED

Sample Type	Measured Range SO_3 %	Seed Counts No/28.3 gm
Fresh Pellets[1]	0.2	>100
Pellets from Top[2] of Bed	0.25-0.45	45-100
Pellets from Bottom[2] of Bed	0.50-0.69	25-45

1. From a total of two melts
2. From a total of 11 melts (11 tests).

The composition of the pollutants collected upstream of the packed bed was determined through qualitative spectrographic analysis. The increase of Cr_2O_3 in the pellets from the packed bed is evident from the Table 30 which shows the presence of chrome in the particulates.

TABLE 30 QUALITATIVE SPECTROGRAPHIC ANALYSIS OF PARTICULATES PACKED BED INLET

	Range in % (oxides)	
Elements	Sample 1 (Run No. 5)	Sample 2 (Run No. 18)
Na	>10	>10
Ca	.1-1	0.5-5
Si	0.05-0.5	0.5-5
Cr	0.05-0.5	0.05-0.5
Al	0.01-0.1	0.5-5
B	0.005-0.05	0.1-1
Mg	.01-0.1	0.05-.5
Fe	0.005-0.05	0.05-0.5
Sn	0.001-0.01	0.005-0.5

The effect of Cr_2O_3 on the color is shown in Table 31. The color obtained with pellets from the bottom of the bed was too intense to be acceptable. However, it is believed that with the addition of decolorizers the Cr_2O_3 diluted with the rest of the batch pellets could be tolerated.[3] The amount of Cr_2O_3 pickup in the full scale pelletizing and preheating process will depend on the following factors:

1. Physio-chemical conditions of the chrome refactories in the brick work. This in turn depends on the particular time period of the campaign for the refractory.

2. The tank operating parameters, particularly the gas temperatures.

3. The proportion of furnace exhaust gases that will be used for preheating the pellets.

4. The residence times and particulate capture efficiencies of the pellet bed.

TABLE 31. CHROME AND COLOR IN PELLET MELTS - PACKED BED

Sample Type	Measured Cr_2O_3 (max.) %	Color of Glass
Fresh Pellets[1]	≤0.003	Blue
Pellets from Top[2] of Bed	≤0.003	Blueish Green
Pellets from Bottom[2]	0.005	Green[3]

1. From a total of two melts.
2. From a total 11 melts (11 tests).
3. Unacceptable flint glass color.

It is therefore important to quantitatively evaluate these parameters before a conclusion can be sought regarding the impact of pellet preheating process on glass color for a given melting operation.

'Particulates' Collection Efficiency in EFB:

The EFB was also tested in the static bed mode. The collection efficiency of the EFB is generally in the 95% range at the design conditions. The collection efficiency of the EFB is influenced by two major factors: applied bed voltage and the gas velocity through EFB. The following conclusions apply to a static bed EFB. A moving pellet bed may alter the generality of these conclusions to some degree. A summary of the EFB capture efficiency data is presented in Table 32.

TABLE 32. SUMMARY OF PARTICULATE COLLECTION EFFICIENCIES IN THE EFB

Bed Depth = 0.38m
Average Bed
Cross-section = 4.97m^2

Run No.	Avg.* Gas Temp. °C	Corona Current mA	Bed Voltage KV	Avg. Gas Velocity m/Sec	Collection Efficiency %	Inlet Particulate Loading mg/dsm^3
17B	204	3.0	0.0	.17	78	70.9
15B	231	3.0	0.0	.48	58.0	10.9
13B	265	3.0	0.0	.64	57.8	86.9
10	160	3.1	2.1	.05	99.9	80.
11	191	2.9	2.0	.20	93.4	25.2
14B	232	3.1	2.0	.51	76.1	64.0
4B	213	3.3	5.0	.1	98.7	109.8
9	186	3.6	5.3	.14	99.5	29.7
8	210	3.1	5.0	.15	90.8	86.9
6	252	3.2	5.0	.16	95.8	66.3
5	193	3.3	5.0	.18	99.9	38.9
12	193	3.0	5.0	.27	96.4	34.3
14A	227	3.0	5.0	.49	86.4	66.3
13A	260	3.0	5.0	.65	78.3	102.9
15A	227	1.5	5.0	.48	80.6	68.6
7	166	3.0	9.8	.08	99.6	70.9
4A	213	3.1	9.5	.10	97.6	105.2
16	206	3.0	9.0	.48	95.0	52.6
17A	204	3.0	9.0	.62	86.6	

*Average of inlet and outlet process gas temperatures (not Method 5 probe temperatures).

Effect of Bed Voltage

Figure 28 shows the results of EFB capture efficiency at design velocity of about 0.5 m/sec and a corona current of 3mA. It can be seen that the efficiency of the EFB jumped from 58% to 95% (or an 8 fold decrease in penetration) when the bed voltage was raised from 0 to 9 KV. The main criterion of applied bed voltage is the power consumption in the bed. Compared to gravel, the electrical conductivity of soda-lime pellets is much higher and it increases further with increasing temperature. Therefore, it could require high power input especially at elevated temperatures.

Effect of Gas Velocity

The velocity shown was calculated based on a mid-plane cross-sectional area of the EFB annulus. Figure 29 shows the capture efficiency data for the EFB as a function of the gas velocity. The efficiency decreases as the gas velocity is increased.

Effect of Gas Temperature

Within the range of temperatures studied here, there appears to be no effect of temperature on the EFB particulate efficiency. However as mentioned previously, a change in temperature will change the electrical resistivity of the pellets thereby altering the power supplied to the bed.

The relationship between the pellet electrical characteristics and applied voltage at different temperatures is shown in Figure 30.

Summary Data for Method 5 - Filter Catch and Impinger Catch (EFB Experiments)

The weighings from the filters, probe washes and impinger "dry down" were used for computing the concentrations of the particulates in the gases. From concentration data and measurements of total gas volume at the sampling locations, the total mass flow rates for the particulates were calculated. The results of these computations are listed in Table 33. The mass flow rate data were used for calculating the capture efficiencies.

SO_x Capture in the EFB

In addition to the particulate capture studies, the wet catch data for the gaseous components were generated using H_2O_2 solutions in the impingers of the sampling train. The H_2O_2 was used to allow the lower oxides of sulfur (SO_2, SO_3) to be oxidized to SO_4 and captured in the impingers.

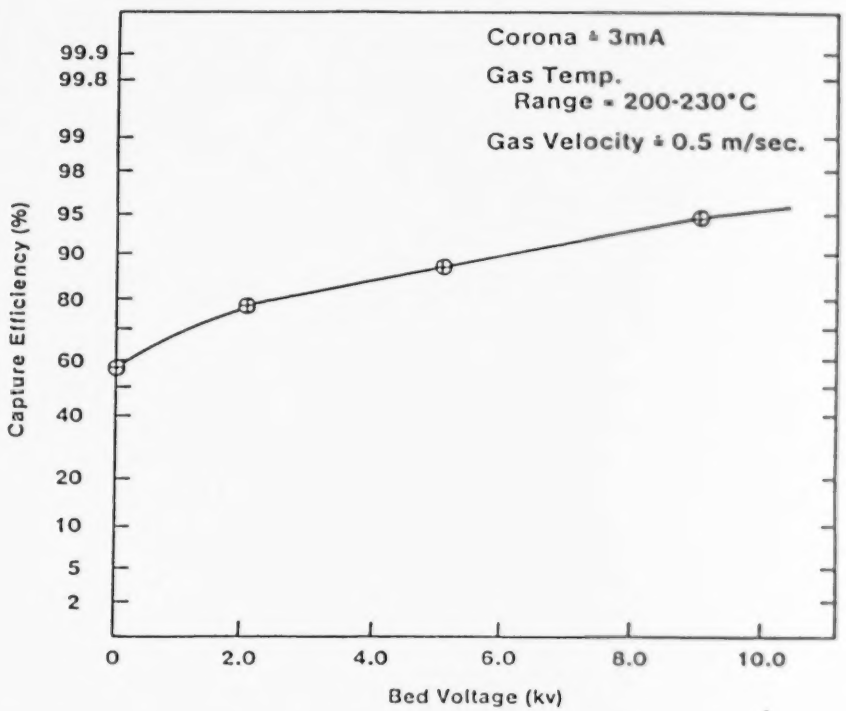

FIGURE 28. EFFECT OF BED VOLTAGE ON EFB CAPTURE EFFICIENCY

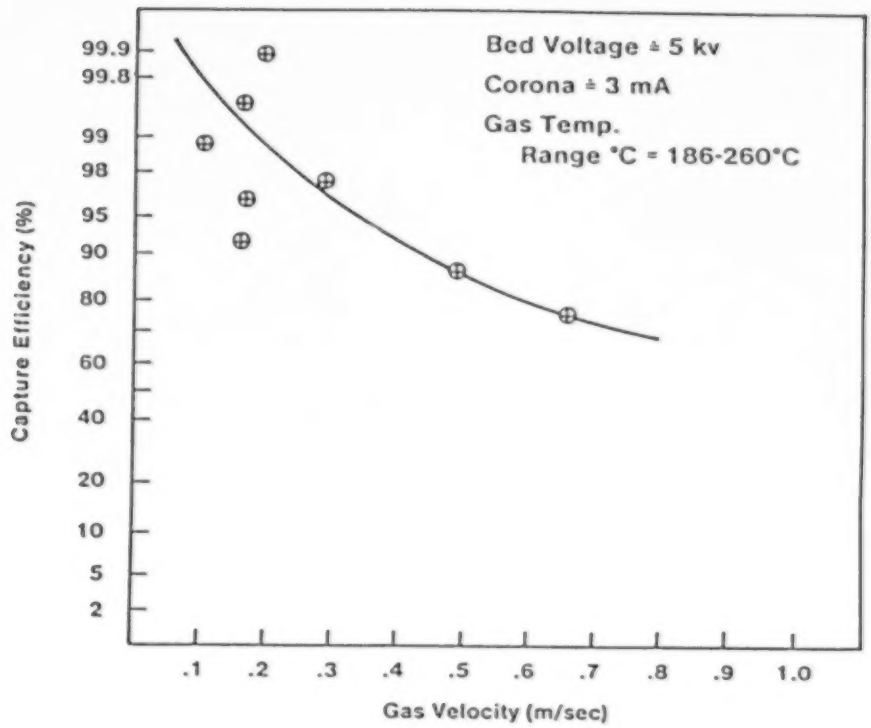

FIGURE 29. EFFECT OF GAS VELOCITY ON EFB CAPTURE EFFICIENCY

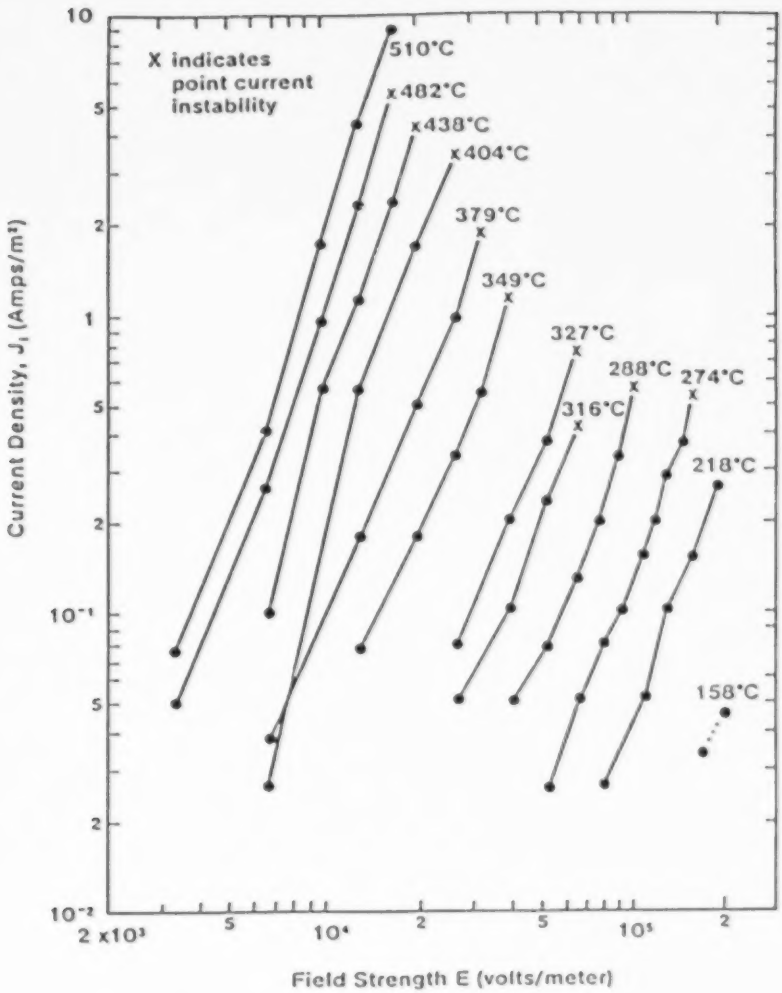

FIGURE 30. CONDUCTIVITY OF SODA-LIME PELLETS AT VARIOUS TEMPERATURES

TABLE 33. SUMMARY OF METHOD 5 CATCH (FRONT-HALF) AND IMPINGER CATCH (BACK-HALF) - EFB

Run No.	EFB Inlet Gas Temp °C	EFB Inlet Front Half (Particules) $\frac{mg}{dsm^3}$	EFB Inlet Front Half (Particules) g/min	EFB Inlet Back Half (Condensibles) $\frac{mg}{dsm^3}$	EFB Inlet Back Half (Condensibles) g/min	EFB Outlet Gas Temp °C	EFB Outlet Front Half (Particules) $\frac{mg}{dsm^3}$	EFB Outlet Front Half (Particules) g/min	EFB Outlet Back Half (Condensibles) $\frac{mg}{dsm^3}$	EFB Outlet Back Half (Condensibles) g/min
4A	272	104	1.6	27	0.4	177	2.2	.04	0.9	0.02
4B	274	110	1.6	31	0.5	176	1.3	.02	≅0	≅0
5	222	32	0.8	7	0.2	163	≅0	≅0	≅0	≅0
6	315	66	1.4	11	0.2	185	2.3	.06	≅0	≅0
7	199	71	0.9	9	0.1	132	0.2	≅0	≅0	≅0
8	226	83	1.9	13	0.3	169	6.9	.17	≅0	≅0
9	196	29	0.7	8	0.2	154	≅0	≅0	≅0	≅0
10	196	80	0.7	≅0	≅0	126	≅0	≅0	≅0	≅0
11	173	25	0.7	--	--	167	1.4	0.05	--	--
12	173	35	1.5	--	--	176	1.1	0.05	--	--
13A	276	102	9.2	--	--	246	21.0	2.0	--	--
13B	293	87	7.4	--	--	249	33.0	3.2	--	--
14A	224	67	4.9	--	--	209	8.9	0.7	--	--
14B	227	65	5.1	--	--	214	10.0	1.2	--	--
15A	227	70	5.1	--	--	212	13.7	1.0	--	--
15B	259	65	4.4	--	--	213	24.7	1.8	--	--
16	238	53	3.6	--	--	189	2.3	.18	--	--
17A	235	51	5.0	--	--	195	6.4	.66	--	--
17B	251	72	1.5	--	--	180	10.7	.34	--	--

NOTES: [1]Gas temperatures shown are averages for each sampling period measured by Method 5 sample probe, and are not the same as process temperatures reported in Table 32.

[2]For runs 11-17B the H_2O_2 was used in the impingers for generating of SO_x data (Table 32). In all previous runs, water was used as per Method 5 procedures.

All impinger catch solutions in H_2O_2 were analyzed for SO_4 capture. Then SO_4 mass flow rates and EFB capture efficiencies for SO_2 and SO_3 were then computed. These data are shown in Table 34. For the ranges of variables studied the SO_2 capture efficiency appears to show no trend for dependency. The average capture efficiency in the EFB is 79% and this is significantly higher than the SO_2 capture efficiency in packed bed of depth 1.07m. The bed depth in the EFB is 0.38m. The higher capture efficiency in the EFB may be attributed to the greater gas residence time and lower gas temperatures. Thus the electrostatic forces of collection do not appear to contribute to gaseous capture mechanisms.

Pellet Melt Studies - EFB

Table 35 lists the chemical analyses color and seed counts on the pellet melts from EFB. As can be expected, more SO_3 and Cr_2O_3 are picked up by pellets that have been exposed to larger volumes of gases containing the particulates. These pellet melts do not show significant amount of green color since the Cr_2O_3 pickup is not sufficiently high. This may be due to two factors:

1. Because of the arrangement of the two beds in series, the gases passed through the packed bed first before entering the EFB. Thus, a lower amount of Cr_2O_3 is available to EFB for pickup by pellets.

2. The particulates to pellets ratio in the EFB is significantly lower since EFB contained about four times the amount of pellets in even the deepest (1.52m) packed bed.

NO_x Data from Packed Bed and EFB

The NO_x concentrations at the inlet and outlet of the packed bed and EFB are listed in Table 36. As was expected, there was minimal capture of the NO_x in the packed bed. The small decrease in the concentration of NO_x at the packed bed outlet was mainly due to some air infiltration in the packed bed.

TABLE 34. SO_2 AND SO_3 CAPTURE EFFICIENCIES IN EFB

Run No.	Avg. Gas Temp. °C	Avg. Gas Velocity m/Sec	Bed Voltage KV	Corona Current mA	SO_2* Inlet Mass Loading g/min	SO_2* Capture Efficiency %	SO_3** Inlet Mass Loading g/min	SO_3** Capture Efficiency %
7	166	0.08	10	3.0	0.05	43	0.19	31
9	186	0.14	5	3.6	0.05	77	0.72	89
12	193	0.27	5	3.0	1.5	86	0.79	70
13A	260	0.65	5	3.0	22.4	92		
13B	265	0.64	0	3.0	17.4	86		
14A	227	0.49	5	3.0	14.0	88		
14B	232	0.51	2	3.1	13.5	79		
15A	227	0.48	5	1.5	15.7	83		
15B	231	0.48	0	3.0	23.6	72		
16	206	0.48	9	3.0	11.5	69		
17A	204	0.63	9	3.0	16.7	61		
17B	204	0.17	0	3.0	4.3	85		

NOTES:

1. Large changes in mass loading resulted from large changes in gas flow rates between runs.

2. Gas samples, for runs 7, 9 and 12, were taken through pressure taps (non Method 5) but using both isopropanol and H_2O_2 solution in the impinger.

*From H_2O_2 impinger solutions

**From isopropanol impinger solutions (when used)

TABLE 35. CHEMICAL ANALYSES, COLOR AND SEED COUNTS IN PELLET MELTS - EFB

Sample Type	Chemical Analysis Avg. Wt. % SiO_2	Al_2O_3	Fe_2O	CaO	MgO	Na_2O	SO_3	Cr_2O_3	Color	No./28g
EFB Pellets hrs. exposed to gas 35	73.12	1.82	0.06	9.06	2.33	12.82	0.28	±0.03	Blueish* Green	35-100+
EFB Pellets hrs. exposed to gas 100	72.93	1.79	0.06	9.01	2.28	12.97	0.48	±0.003	Blueish* Green	86-100+

*Acceptable color

TABLE 36. NO_x MEASUREMENTS - PACKED BED AND EFB

	Packed Bed				EFB		
Run No.	Avg. Gas Temp. °C	Bed Depth (L) M	Inlet NOx PPM	Outlet NOx PPM	Avg. Gas Temp. °C	Inlet NOx PPM	Outlet NOx PPM
2	325	1.52	630	550	-		
6	370	0.61	370	350	252	280	280
9	277	1.52	440	360	186	350	340
11	285	1.52	360	330	191	250	250

Stack Emissions Data

Table 37 shows the stack data taken periodically during the test program. The glass pull stayed relatively constant within 5% variation. Based on the efficiency studies in the packed bed and EFB these stack data can be used for calculating the final emissions to the atmosphere when a packed bed or an EFB or both are installed in the process.

TABLE 37. STACK EMISSION TESTS

			Gas Analysis Volumetric			Particulate Loading Emissions	
Date (1980)	Gas Flow m^3/min	Gas Temp °C	$\%O_2$	$\%CO_2$	$\%H_2O$	mg/m^3	Kg/hr
4/12	866	376	14	7	12	121	5.7
4/18	969	377	12	7	9	117	6.3
4/19	905	372	14	7	8	153	7.6
4/25	905	372	14	6	10	117	5.2

Packed Bed Efficiency Correlation and Scale-Up:

Literature Study

Prior to the beginning of the packed bed experiments, a literature survey was completed in order to better understand the particulate collection theories in filter beds/packed beds.

A summary of the various dust and mist collection mechanisms and their dominant force fields is presented by K. E. Lunde and C. E. Lapple[6]. Basically, there are six different mechanisms:

1. Interception capture
2. Inertial capture
3. Diffusional capture
4. Gravitational settling
5. Electrostatic capture
6. Thermal precipitation

The authors of the above paper concluded that a systematic experimental work with the help of much improved measurement techniques should be pursued to better verify various theories. A qualitative summary of some of the other work on filtration is also listed in Table 38.

TABLE 38. LITERATURE ON FILTRATION

	Author	Reference	Mechanisms Studied
1.	Bragg, G.M. and Pearson, B.M.	Ind. Eng. Chem. Process Des. Dev., Vol. 18, No. 1, 1979 "A model for Aerosol Filtration by Fibrous Filters	·Inertial ·Diffusion ·Simultaneous inertial and diffusion (Aerosols on fibrous filters)
2.	Chen, C.Y.	Chem. Rev. V.55 (1956) "Filtration of Aerosols by Fibrous Media"	·Inertial ·Interception ·Brownian Diffusion ·Gravitational Settling ·Inertial and Interception (Aerosols on fibrous filters)

TABLE 36 (Continued)

	Author	Reference	Mechanisms Studied
3.	Gebhart, C.R. and Stahlhofen, W.	Journal of Aerosol Science, Vol. 4(Pergamon Press Gr. Britain "Filtration Properties of Glass Bead Media for Aerosol Particles in the 0.1-2 μm Size Range"	·Diffusion
4.	Jackson, S., and Calvert, S.	A.I.Ch.F.Journal Vol. 12, No. 6 "Entrained Particle Collection in Packed Beds"	·Inertial impaction (1 μm liquid droplets on Raschig rings, Bere Saddles and Interlox Saddles)
5.	Johnston, H. F. and Roberts, M. H.	Ind. & Eng. Chem. November, 1949 "Deposition of Aerosol Particles from Moving Gas Streams"	·Inertial impaction ·Diffusion (Aerosol particles on water droplets)
6.	Lunde, K.E., and Lapple, C.E.	Chem. Eng. Prog. Vol. 53, No. 8, Aug. 1957 "Dust and Mist Collection"	·Various collection mechanisms (no experimental work)
7.	Paretsky, L., Theodore, L., Pfeffer, R., and Squires, A.M.	Journal of the Air Pollution Control Assoc. V. 21, No. 4 (April, 1971) "Panel Bed Filters for Simultaneous Removal of Glyash and Sulfur Dioxide"	·Interception ·Inertial impaction ·Diffusion ·Gravitational settling (Aerosols on sand)
8.	Schmidt, E.W., Gieseke, J.A. Gelford, P., Lugar, T.W. and Furlong, D.A.	APCA Journal V.28, No. 2 (Feb. 1978) "Filtration Theory for Granular Beds"	·Interception ·Inertial ·Diffusion ·Gravitational settling (Aerosol on poly-ethylene beads)

Mathematical Modeling of Packed Bed Test Data:

The objective of the packed bed test program was to obtain capture efficiency data on a pilot size packed bed using actual container furnace exhaust gases. Because of time, cost, and process constraints, one did not obtain the benefits of conducting a set of elaborate and controlled experiments. This limitation precluded the development of a mathematical model which would fully characterize the various collection phenomena in packed beds. However, the use of actual system gases and a fairly large packed bed (approximately 1/3 to 1/4 scale) filled with real pellets did yield more conclusive data on the collection efficiences of packed beds. Thus, there was a trade off between a large number of laboratory based controlled experiments and a small number of "real" experiments.

Because of the high degree of accuracy and consistency of measured capture efficiency data from the packed bed experiments, a mathematical model based on these data is proposed below. It is a "gross" study of the collection mechanisms in the packed bed and it is believed that it is useful for scale-up purposes. This is assuming that static bed and almost the identical particle size distribution is valid.

In their paper, Schmidt, Gieseke, et. al.[5], presented a model for collection efficiency in granular beds for interception, inertial, diffusional and gravity settling mechanisms. For this study, an order of magnitude analysis was first performed to identify the most dominant mechanism.

Order of magnitude analysis:

$$\eta = 1 - \exp\left(-k\, E_{\beta i}\, L\, \beta / R\right)$$

Where η = overall filter efficiency

$E_{\beta i}$ = Single sphere collection efficiency with correction for interference effects from neighboring spheres packed with denisty β. The total single sphere collection efficiency may be noted as $E_{\beta T} = \Sigma E_{\beta i}$

k = Empirical constant

β = Packing density

L = Packed bed filter thickness (bed height)

R = Individual spherical collector radius

The expressions for individual collection efficiencies are:

$$E_\beta \text{ interception} = 1.45\ (r/R)^2$$

$$E_\beta \text{ inertial} = \frac{k_i\ 2\ P_\rho\ r^2\ UgC}{9\ \mu gR}$$

$$E_\beta \text{ diffusional} = 8\ Pe^{-1} + 2.308\ Pe^{-5/8} Re^{1/8}$$

and E_β gravity settling = Vs/Ug

Where r = radius of particulate
R = radius of filter media (pellet)
k_i = constant in inertial collection term = 3.97
ρ_P^i = particulate density
Ug = face or bulk velocity of gases
C = Cunningham correction factor
μg = gas viscosity
Pe = Peclet number

$$Pe = \frac{2\ R\ Ug}{D}$$

Where D is the diffusivity
Re = Reynolds number

$$Re = \frac{2\ R\ Ug\ \rho g}{\mu g}$$

When ρg = density of gas

The individual $E_{\beta i}$s were calculated for the packed bed conditions:

E_β interception = 1×10^{-9}
E_β inertial = 1×10^{-3}
E_β diffusional = 1×10^{-6}
and E_β gravity settling = 1×10^{-5}

It now became evident that the dominant collection mechanism for the packed bed under study is the inertial collection. Therefore, for the verification of our experimental data, a simplified capture model based on inertial collection alone was chosen. Some of the variables whose effect could not be studied, such as the particulate sizes, were grouped into one empirical constant since it was assumed that these will not vary significantly in the production runs.

Thus, the efficiency equation for inertial capture may be rewritten as:

$$\eta = 1 - C \exp.\ (k\ Stk\ \frac{L}{R})$$

Where η = total capture efficiency
C = empirical constant for the efficiency equation (determined experimentally)
k = grouped parameter coefficient for the capture mechanism (experimentally determined)
Stk = stoke's number signifying inertial capture

$$Stk = \frac{2 \rho_{\rho} r^2 C Ug}{9 R \mu g}$$

Where,
C = Cunningham's correction factor
r = particulate radius
L = bed height
R = radius of the pellets (filter medium)

The values for the experimental variables studied were:

ρ_p	= particulates' density	2.68 gm/cc
r	= mean particulate radius	0.08 μm
Ug	= gas velocity	0.58-2.8 m/sec.
R	= mean pellet radius	0.7 cm
μg	= gas viscosity	0.27-0.31 Pa
L	= bed height	0.61-1.52 meters

The efficiency equation may be rewritten as:

$$1-\eta = C \exp (K Stk. \frac{L}{R})$$

or

$$\ell n (1-\eta) = \ln C + k Stk. \frac{L}{R}$$

A linear regression was made using the experimental values of η at known Stk, L and R. The constants C and k were then determined. The linear regression graph is shown in Figure 31.

Based on the curve fit the efficiency can be expressed as:

$$\eta = 1-(0.88) \exp. [-118 (Stk) L/R]$$

Scale-Up

Capture efficiencies for larger scale packed beds utilizing identical particulate size characteristics, are plotted in Figure 31. Two bed depths and two gas temperatures were chosen for comparison purposes. As seen in the experiments, deeper bed and lower temperatures improve the capture efficiency. It should be noted that these efficiency calculations are based on static bed conditions with no dust entrainment (blow off) effects. If the pellet handling in the pelletizing and drying process is designed such that the pellets in the preheater are clean and have good dry strength, these predicted efficiencies should be applicable to the moving bed system as well.

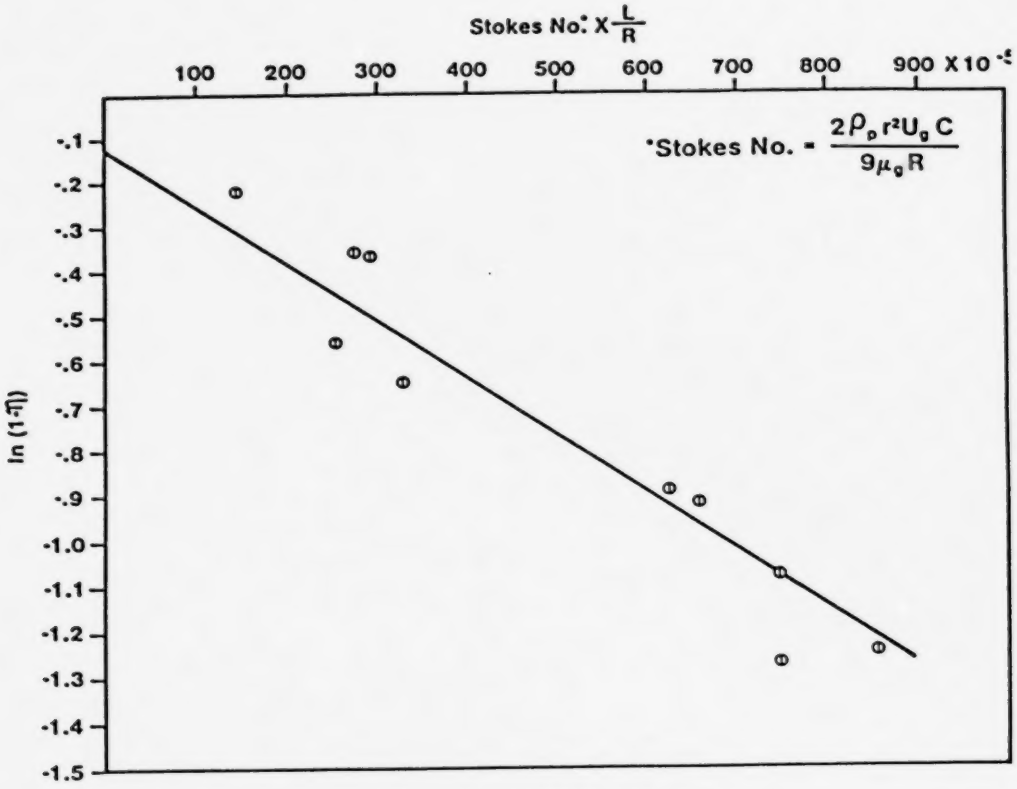

FIGURE 31. LINEAR REGRESSION OF PACKED BED EFFICIENCY DATA

SECTION 7

PROTOTYPE PROCESS

A process schematic showing the arrangement of equipment for pelletizing, drying, preheating and pollution capture will be discussed in this section. Based on the pelletizing and packed bed work done so far on this project, a process concept will be proposed which can efficiently manufacture pellets, preheat them using furnace waste heat, and capture furnace particulate emissions. This process should be applicable to all soda-lime glass manufacturing units.

The original concept developed during the Phase I work proposed that preheating and pollution capture take place in a shaft preheater. Thus, a moving bed preheater was designed for the melting demonstration pilot plant which would not only preheat the pellets but also satisfactorily capture particulate emissions. However, it was discovered, that while drying pellets in a moving bed shaft dryer, pellet abrasion in a moving bed will produce coarse particles (super micron) which escape the bed. Moreover, the pollution capture efficiency in the preheater can vary as a function of operating variables such as gas velocity, temperatures, and pellet feed rate, thus, in some instances the packed bed may not meet the plant emission specifications.

The idea of using pellets in an electrified bed was demonstrated at Corning Glass Works' Wellsboro Plant and was found to be successful (Section 4). Later, larger scale tests were made at Thatcher Glass Manufacturing Company's Elmira Plant which confirmed the good results at Wellsboro. It was concluded from these tests that pollution capture could also be done separately from the preheating, but still on pellets so that particulates could be recycled to the melter.

Thus, a system is proposed which includes a secondary collection device in the preheating process (Figure 32).

Pelletizing

A pan type pelletizer is recommended for the pelletizing part of the process.

Pelletizing has been done on a large enough scale in this project to confidently design a production size pelletizing operation. The key element in any such design is process control. If the water and batch are controlled precisely, the pelletizing

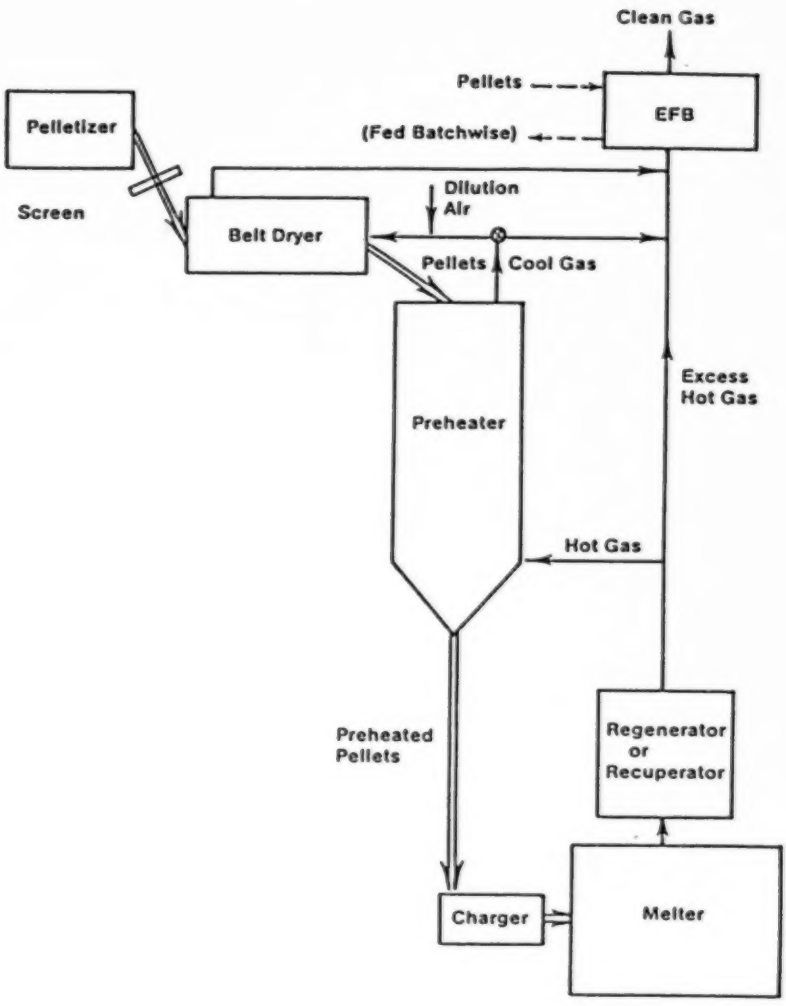

FIGURE 32. SCHEMATIC OF PROTOTYPE PROCESS

can continue uninterrupted and unsupervised for long periods of time. Thus, a gravimetric feeder is recommended for metering the batch and a good water flow meter/controller with pressure regulator for the water.

In normal operation, the pelletizer will produce some non-pelletized material as lumps or fines. Lumps of material which form on the plows occasionally break off and come over with the pellets. A screening step is required to remove both oversized and undersized products from the pelletizer before they reach the belt dryer. The pelletizer should be designed to operate at about 80% of its rated capacity. This is the point where maximum production of smooth spherical pellets takes place. At rates closer to maximum capacity, the pellets will be more grainy and less uniform in size.

Drying

A belt dryer is recommended for the drying part of the process.

As described in Section 5, drying pellets in a belt dryer was more difficult than anticipated, but the pellets were found to be subject to sticking and deformation when heated and the belt dryer tended to make the problem worse if the bed was more than two or three pellets deep. However, some low temperature drying is necessary before the pellets can enter the preheater. A belt dryer with a belt design wide enough to allow the pellet burden to be no more than two or three pellets deep should eliminate the sticking and provide more uniform drying at relatively low temperatures. The gas temperatures for the initial drying should not exceed 215°C for soda-lime batch.

There does not seem to be a need for both a shaft dryer and a shaft preheater, so the remainder of the drying can be combined with preheating in a dryer-preheater. It should be mentioned that the separate shaft dryer and preheater design for the pilot plant preheating and melting demonstration was intended to make the pelletizing and melting parts of the demonstration independent of each other for purposes of this study.

The amount of drying which must be done in the belt dryer depends on the strength required for the pellets to survive conveying into the preheater. The results of the pelletizing work confirmed that partially dried pellets are weaker than either wet or completely dry pellets. About 70% of the water must be removed before pellets are strong enough to survive extensive handling so the belt dryer should be at least capable of removing this much water. Good temperature control will be required to avoid sticking and deformation of the pellets in the belt dryer. It is anticipated that control of the temperature will be accomplished by using dilution air to lower the temperature of the flue gas leaving the preheater before the gases enter the belt dryer.

Preheating

The preheater is basically the same refractory-lined shaft as proposed in Phase I. However, the introduction of cooling air, as originally proposed, can be eliminated since pollution capture may not improve significantly enough to justify this cooling process. Thus, the preheater design can be based strictly on preheating the pellets. Please refer to a detailed discussion of the preheating equipment in the Phase I Design Manual[1].

In some applications only a part of the flue gas may be required to preheat the pellets. In this event, a side stream of the gas leaving the regenerator (or recuperator) will go to the preheater and the rest will go straight to the pollution capture device.

Pollution Capture

In the pelletizing, preheating and EFB process, the pollution capture takes place in two major steps. In the first step, the preheater captures most of the particulates and in the second step the EFB captures the remaining particulates.

Capture in the Preheater:

In Section 6, pollution capture efficiencies for large scale packed beds were calculated using a semi-empirical mathematical model. Based on this model, fairly high capture efficiencies (70%-90%) may be expected in the production size preheaters. As mentioned previously, the effects of the moving bed are not completely known although a moving bed is expected to result in lower capture efficiencies. In those applications where capture efficiencies in a preheating process do not meet standards, a second stage EFB pollutant-collection step is recommended.

Capture in the EFB:

An electrified filter bed using pellets has been shown to be a very effective device for pollution capture. If pollutant recovery for batching is important, a static bed EFB with pellets fed and emptied on a regular cycle (say once per week) may be used. A moving pellet bed may generate dust in the exiting gas due to abrasion. If a moving bed process is necessary in an EFB, it should be a gravel bed. Further studies are recommended in the pilot plant preheating and melting system to quantitatively evaluate the effects of dust carry-over in moving beds. These studies will be useful not only for proving the melting benefits of preheated glass batch pellets, but also useful for quantifying the need for second stage pollution collection devices.

REFERENCES

1. R. E. Miller, K. R. Jones, N. J. Camacho, J. H. Bruns, G. B. Boettner, B. Bansal, Batch Pretreatment Process Technology for Abatement of Emissions and Conservation of Energy in Glass Melting Furnaces: Phase I Process Design manual, Environmental Protection Agency, IERL Cincinnati, Ohio, EPA-600/57-81-038 May 1981.

2. New Source Performance Standards, Federal Register, 6-15-79, Vol. 44, No. 117: 34840-34854.

3. E. P. Spinosa, et al, Summary Report on Emissions from the Glass Manufacturing Industry, United States Environmental Protection Agency, EPA-600/2-79-101, April 1979.

4. H. W. Morelissen, A. H. Rikken and A. J. M. VanTienen, Pelletized Batch: Its Manufacture and Melting Behavior, The Glass Industry, March 1980, 16-20.

5. E. W. Schmidt, J. A. Gieseke, P. Gelford, T. W. Lugar and D. A. Furlong, Filtration Theory for Granular Beds, APCA 28, 2, Feb. 1978.

6. K. E. Lunde and c. E. Lapple, Dust and Mist Collection, Chemical Engineering 53, 8, August 1957.